Graduate Theses and Dissertations

Iowa State University Capstones, Theses and Dissertations

2014

A study of effectiveness of ground improvement for liquefaction mitigation

Bin Tong
Iowa State University

A study of effectiveness of ground improvement for liquefaction mitigation

by

Bin Tong

A dissertation submitted to the graduate faculty

in partial fulfillment of the requirements of the degree of

DOCTOR OF PHILOSOPHY

Major: Civil Engineering (Geotechnical)

Program of Study Committee:
Vernon Schaefer, Major Professor
Jeramy Ashlock
Jian Chu
Matthew Rouse
Thomas Rudolphi

Iowa State University

Ames, Iowa

2014

TABLE OF CONTENTS

LIST OF FIGURES

LIST OF TABLES

viii

ACKNOWLEDGEMENTS

ABSTRACT

Our ability to identify the existence of soil liquefaction potential is now better than our ability to know how to mitigate it economically and effectively. Based on a recent survey conducted by the Deep Foundation Institute (DFI) on liquefaction mitigation, remedial design methods and their effectiveness verification are regarded as "somewhat to highly non-uniform" by the majority of the geotechnical engineering community in the U.S.

Many recent reconnaissance reports also indicate that previous remediation design of ground improvement for liquefaction mitigation is not as reliable as expected. Hence, the lack of a uniform framework to evaluate and compare improvement effectiveness is an important factor leading to the insufficient or inefficient remedial design for liquefaction mitigation by ground improvement. An efficient, representative and comprehensive collection, evaluation and comparison of quantitative effectiveness data is a great challenge in liquefaction mitigation practice and the key issue is the establishment of a uniform evaluation framework. These expectations and objectives comply well with the requirements of an evolving evolutionary seismic design guideline termed Performance-Based Design (PBD). The process of establishing such an evaluation and comparison framework is also a process of re-evaluation of the improved performances and seismic design optimization, within the framework of PBD.

To establish the uniform framework, a comprehensive numerical study is conducted to identify the failure mechanisms of a well-documented case history; an unimproved caisson quay wall in liquefiable soil reported in the Kobe earthquake in 1995. After the calibration of numerical model based on the case study, in the second step, various remedial methods including the stone column method, vibro-compaction method and deep soil mixing method are evaluated to improve the performance of this specific quay wall. For each analyzed countermeasure, a

comprehensive parametric study is conducted to optimize the remedial design by determining the optimum design parameters. Eventually, all of the improved performance data or termed Engineering Demand Parameters (EDPs) in terms of quay wall seismic deformation and performance grades are plotted together to show the difference of improvement effectiveness achieved by various examined cases. These cases differ in the use of remedial methods and/or design parameters. The results are also used to rank the analyzed remedial methods and optimize their designs.

In addition, as a stand-alone product of this study, a simplified chart method is proposed to estimate the improved deformation of caisson quay walls placed in liquefiable soil. Based on the method, the improved deformation of the walls after an earthquake can be reasonably estimated with the input of peak ground acceleration (PGA) of ground motion, improvement zone dimensions and improved soil properties.

The results of this study show that failure of the examined caisson quay wall is induced by the deformation of the foundation and backfill soils. For all the analyzed remedial methods, improving the top 10 to 15 m of foundation soil under the wall and first 20 to 25 m of backfill soil behind the quay wall shows the best improvement efficiency. The improved performances of the quay wall are estimated to be acceptable, which only requires reasonable restoration effort to fully recover the damage under the earthquake motion with a probability of exceedance of 10 percent during its life-span. Different remedial designs using various methods are classified into three categories depending on their improved performance grades. Future research is recommended to include verification, implementation and updating of the proposed framework to advance the state-of-the-art of liquefaction mitigation using ground improvement.

CHAPTER 1.   INTRODUCTION

1.1   Background

Earthquake-induced liquefaction is a phenomenon where high excess pore water pressure develops in partially or fully saturated soil as a result of earthquake loading (Seed and Lee, 1966). When the ratio of excess pore water pressure to the total vertical stress is essentially unity, the soil is considered "liquefied" and loses a large portion of its shear resistance, as the effective stress of the soil goes to zero, causing a liquid-like response. Liquefaction triggering mechanisms, potential evaluation criteria, liquefaction-induced damage prediction, and mitigation has been extensively studied in the past 50 years (Seed and Idriss, 1967 and 1971).

"Our ability to identify the existence of soil liquefaction potential is now better than our ability to know what can be done to mitigate it economically and effectively" (Mitchell, 2013). Ground improvement methods used as countermeasures had been proved effective in reducing soil liquefaction potential using various improvement means (Mitchell et al., 1995). However, questions still remain. The lack of quantitative improved performance observations or improvement effectiveness data from previous earthquakes have led to weakness in (1) selection of appropriate remedial measures, (2) optimization (of a minimally adequate and efficient design) for liquefaction remediation by ground improvement, and (3) prediction of the improved performance based on pre-defined remedial design parameters (DFI, 2013). Hence, continued efforts are recommended to develop greater consensus within the field of liquefaction mitigation, especially on the collection, evaluation and verification of improvement effectiveness data.

1.2   Problem Statement

Based on the results of a comprehensive survey (DFI, 2013; Siegel, 2013) conducted on design, analysis and practical applications of ground improvement for liquefaction mitigation, it

was found that (1) remedial design and effectiveness verification process are still regarded as somewhat to highly non-uninform due to the lack of first-hand in-situ observations in the U.S.; (2) post-earthquake reconnaissance in recent years has provided results that contradict previously held beliefs on liquefaction and the effectiveness of some mitigation efforts. Therefore, it is difficult to establish a uniform and standardized effectiveness evaluation process for liquefaction mitigation using ground improvement.

In routine practice, pre-to-post field testing (e.g., standard penetration test, cone penetration test, shear-wave velocity test, etc.,) as part of a Quality Control/Quality Assurance (QC/QA) program is applied to verify improvement efficiency and ensure achievement of the designed ground improvement. This is the simplest, most direct and primary way of evaluating and comparing the remediation effectiveness among various ground improvement methods with a mechanism of densifying the liquefiable soil. However, the mechanisms of different geoconstruction methods are extremely diverse; it is difficult to conduct the verification and comparison of improvement effectiveness among all remedial methods (e.g., deep soil mixing and vibro-compaction) by simply using SPT blow count or CPT tip resistance measurements. Previous case histories involving ground improvement also indicate that unacceptable improved performances could be due to the lack of quantitative performance data that prohibited the development of an adequate and cost-efficient remedial design (Haulser et al., 2001&2002).

Therefore, both physical and numerical methods have been applied to compensate for this shortcoming (Adalier, 1996; Cooke and Mitchell, 1999; Cooke, 2000; Yang et al., 2003). It has been recognized that both qualitative and quantitative data of improvement effectiveness are important to compare and optimize the remedial design using ground improvement (Haulser, 2002; Kramer, 2008; Mitchell, 2008). In addition to the lack of in-situ improved performance

observations, a another important reason leading to the lack of quantitative performance or effectiveness data is that there is not a uniform method that is applicable to evaluate and compare the improvement effectiveness of these remedial methods for liquefaction mitigation.

There are numerous reasons leading the lack of quantitative effectiveness and performance data. The primary reason is that the techniques for evaluation and comparison of improvement effectiveness are always case-specific and the improved performance data is hard to extrapolate and compare to other cases in which different remedial methods were applied (Haulser and Sitar, 2001; Haulser, 2002). For instance, densification methods, as the most popular countermeasures for liquefaction mitigation, are always more attractive because the improvement can be verified and evaluated using the soil properties before and after improvement measured by a series of in-situ testing methods. On the other hand, drainage methods are less attractive than densification methods because drainage improvement effectiveness can only be verified or analyzed through fundamental mechanical principles and empirical observations, which can be more time-consuming and costly. Much like drainage for mitigation, the effectiveness of reinforcing methods also cannot be verified post-treatment based on standard penetration test (SPT) or cone penetration test (CPT) data. Therefore, for either drainage or reinforcement countermeasures, engineers must rely on theoretical or empirical analysis for the design and effectiveness verification. However, the methods to use to determine such effectiveness have not reached a consensus.

Therefore, to address this issue in this study, a uniform framework is proposed to evaluate and compare the effectiveness achieved by different geoconstruction methods associated with different working mechanisms. It is important to know that the objective of remedial design for ground improvement is to ensure the satisfaction of specified seismic

performance of improved structures after the designated earthquake motion instead of eliminating the liquefaction potential or maintaining the integrity of constructed remedial elements. The improved performance of structures are particularly emphasized in this study because case histories (Nishimura, 2012; DFI, 2013; Seigel, 2013) have indicated that even though the constructed remedial stiffer elements do not maintain integrity, or liquefaction may not be eliminated completely with the application of ground improvement, the applied remedial measures may still be effective in limiting the consequences or damages due to liquefaction.

1.3 Research Motivation and Scope

The primary objective of this dissertation is to first propose a uniform framework of evaluating and comparing the remedial effectiveness of ground improvement methods. Then, with the established framework, the following two tasks, which are not likely to be achieved using the conventional design method (Iai and Sugano, 2000), are undertaken:

1) The evaluation criteria are used to optimize the remedial design for each analyzed method based on the specified improved performances. In terms of the optimization process, the specific portion or area of the ground improvement and the effects of the remedial method on the performance of structures are appropriately evaluated.

2) The uniform evaluation criteria are used to compare the effectiveness of various ground improvement methods associated with different mechanisms.

Achieving the above two objectives is also a procedure of re-evaluation of the improved performances, and optimization of the liquefaction mitigation seismic designs using different ground improvement methods, following the principles of performance based design (PIANC, 2001). For comparison purposes, the improvement effectiveness data should be easily understandable and applicable to guide the remedial design. The improved performance of a

certain structure is expressed by a numerical value of Engineering Demand Parameters (EDPs) (PIANC, 2001; Kramer, 2008), improvement efficiency and/or the specified performance grades. Since geotechnical aspects of damage, especially for seismic design, are generally related to deformation magnitude, the optimal geotechnical EDPs likely consist of deformations or deformation-based criteria, such as the permanent deformation (horizontal and/or vertical) critical locations. For instance, for dam structures, the crest settlement is typically selected in new analyses as the parameter to represent seismic related deformation or damage.

The above is conducted within a well-calibrated analysis that can reasonably predict the unimproved performance and failure modes of a well-documented case history. This has also been regarded as one of the challenges in the practice of earthquake design and liquefaction mitigation design, where the opportunities for first-hand observations are rare and the time and cost for such a detailed model validation may be unacceptable. However, for research purposes, the prediction results should be validated using field performance data and/or previously published physical and numerical data. Finally, it is critical to obtain a reasonable prediction of the theoretically improved performances under various remedial programs (differing in both the analyzed remedial method or design features). To conduct any remediation work, there are some key factors should be taken into account, such as:

1) Influences due to the change of structure geometry when applicable;

2) Availability/restriction of construction area;

3) Time necessary for completing restoration work;

4) Environmental considerations (e.g., effective usage of debris from damaged region);

Considering the above, three commonly used remedial methods are analyzed in this study including (1) vibro-compaction, (2) deep soil mixing, and (3) combined stone column and deep

soil-mixing. The improvement effectiveness of each remedial method is discussed individually in the following chapters.

1.3.1 Performance-Based Design (PBD) method

All the above expectations and objectives comply well with the requirements and objectives of an evolving evolutionary seismic design guideline called Performance-Based Design "PBD" (PIANC, 2001). Simply speaking, the PBD is a deformation-based framework for seismic design. According to DFI (2013) and Siegel (2013), the PBD method based on tolerable ground movements and deformation reduction rate for liquefaction mitigation design is overwhelmingly preferred by the majority of the geotechnical engineering community in the U.S. However, it is not clear which level of design performance should be used, and there is not a well-accepted criteria addressing the issue at present, since the selection of the criteria is always structure- and project-specific. This also impedes the application of PBD in geotechnical engineering.

The proposed framework is not only to assess the relative effectiveness of remedial methods, but also to provide a uniform platform so that an "apples-to-apples" comparison can be made in terms of improvement effectiveness. Therefore, such a comparison is not likely to be conducted using the pre-to-post improvement testing measurements in the field (i.e., SPT blow count or CPT tip resistance). Also, for certain cases, the potentially applicable remedial methods should be compared, ranked and optimized in terms of improvement effectiveness based on case-specific information including availability of materials and cost estimations.

The principle of PBD has been developed over the last several decades (PIANC, 2001; Kramer, 2008). Even though there are different versions of performance-based design or performance-based earthquake engineering, the philosophy is to seek the seismic performance of

structures and facilities in ways that are useful in advancing the reliability and cost-efficiency of the seismic design. Evaluation of deformations and associated damages, which requires detailed evaluation of the seismic response of earth structures and water-soil-structure systems, are compared to the objectives of modern society. The primary difference among the different versions of PBD proposed by different research groups is the treatment and interpretation of the uncertainties and randomness associated with the input parameters in the design process, such as the uncertainties of input design earthquake motions, geotechnical conditions, material properties, system response and the damage loss prediction (Kramer, 2008). Therefore, PBD provides an more rigorous alternative way for determining the seismic performance of engineering structures. The result of PBD is the level of predicted damage with a design earthquake motion identified by the mean annual rate of exceedance, or corresponding return period. Therefore, the PBD method can overcome the primary limitation of conventional design, which is unable to provide the "damaged" but still acceptable performance when the limit of force-balance is exceeded. The objective of PBD is to ensure that the designed seismic performance satisfies the specified level of damage under the design earthquake, rather than focusing on the factor of safety in conventional design methods or complete elimination of liquefaction hazard, which can be impractical and costly in many situations.

1.3.2 Selection of a representative case history

It is important conduct such ground improvement effectiveness within a unimproved framework of comparing unimproved ground to improved ground using a representative and well-calibrated case study. A gravity caisson quay wall placed in liquefiable soil is selected and analyzed for this purpose. Hence, the seismic unimproved performance and "theoretically"

improved performance of gravity caisson quay wall are evaluated. There are five main reasons for using this case to verify the effectiveness of examined ground improvement methods:

1) Mitigating the seismic damage of port structures is a matter of worldwide interest and draws significant attention. A caisson quay wall placed in liquefiable soil is a "simple" but frequently encountered problem.

2) To comply with the topic (effectiveness of liquefaction mitigation) of this study seismic liquefaction of the backfill and foundation soils is the primary failure mechanism leading to the damage of the caisson quay wall. Hence, liquefaction mitigation of the backfill and foundation soil is effective for improving the seismic performance of the structure.

3) The utilized case history a damaged and unimproved caisson quay wall-has been well-documented in detail on the properties of the wall and native liquefiable soils in numerous publications primarily including Finn et al. (1996), Iai et al. (2000), Inagak et al. (1996), Alam et al. (2005) and Dakoulas and Gazetas (2008). Therefore, well-documented material properties can be applied in the numerical analysis in this study.

4) This case history has been successfully analyzed by numerous researchers using both physical and numerical methods to study the failure mechanisms of the unimproved gravity caisson quay wall placed in liquefiable soils. These previously published results can be used for modeling validation purposes in this study.

5) Widely seismic performance evaluation criteria for gravity caisson quay walls have been established by the port engineering community around the world (PIANC, 2001). The numerical criteria expressed using the wall's deformation, performance grades and even the restoration time and efforts can be used for comparison and classification of improved effectiveness and optimization of remedial design.

1.4   Dissertation Organization

The focus of this study is on prediction and comparison of improvement effectiveness and seismic design optimization of ground improvement for liquefaction mitigation of a caisson quay wall. This dissertation is organized into nine chapters as shown in Figure 1.

Chapter 1 introduces the deficiencies of current liquefaction mitigation strategies, the problem statement, research motivation, and proposed plan used in this study. Particularly, the principle of performance-based design (PBD), which is used as the guideline in this research, is described with the emphasis on its application in to liquefaction mitigation in seismic design. The value of this research is also highlighted within the big picture of liquefaction mitigation research in this chapter.

Chapter 2 provides a brief literature review on liquefaction triggering mechanisms, liquefaction potential assessment, and deformation prediction. The emphasis of literature review is on applications and design guidelines of ground improvement for liquefaction mitigation. In addition, by utilizing the information attained from literature review on applications of ground improvement for liquefaction mitigation, the author proposed an interactive, readily accessible web-based technology selection system for ground improvement methods for liquefaction mitigation.

Starting from Chapter 3, the improvement effectiveness of three ground improvement methods are studied within the calibrated case history. To ensure the accuracy of the numerical model, the unimproved performance/failure mechanisms of the damaged caisson quay wall are calibrated based on field observations and experimental data. The details of modeling and calibration processes and results are presented.

In Chapters 4, 5 and 6, remediation using different ground improvement methods is simulated to improve the quay wall in the case history. The improved performances from various remedial cases differing in both the utilized methods and remedial design parameters are calculated and compared to the unimproved performance simulated in Chapter 3. The details of modeling and improved performance results are presented individually for vibro-compaction, deep soil mixing method, and the combined stone column and deep soil mixing wall method.

Chapter 7 presents the author's proposed a simplified chart method to estimate the improved performance of caisson quay wall-liquefiable soil system remediated by vibro-compaction. The influences of soil liquefaction, ground improvement parameters and seismic excitation levels are involved in the development of the proposed method. Hence, such a method established using verified effective stress analysis can advance the routine remedial design for caisson quay wall structures.

In Chapter 8, formulation of the proposed uniform framework for effectiveness evaluation and comparison of ground improvement methods is presented. This framework is presented in Chapters 4, 5 and 6 to compare and rank the examined remedial cases for the reported caisson quay wall.

A summary of the findings and conclusions obtained from this study and possible future recommendations are presented in Chapter 9.

Research Topic: A Study of Effectiveness of Group Improvement for Liquefaction Mitigation

CHAPTER 1: Introduction and Research Motivation

Evaluation and Comparison of Effectiveness of Different Geoconstruction Methods

CHAPTER 2: Literature Review – An interactive geoconstruction technology selection system for liquefaction mitigation

Unimproved Framework

CHAPTER 3: Numerical Model Calibration of An Unimproved Case Study: A Damaged Caisson Quay Wall in Kobe Earthquake in 1995

Liquefaction Remediation

CHAPTER 4: Vibro-compaction

CHAPTER 5: Deep soil mixing

CHAPTER 6: The combined stone column and DMM wall

CHAPTER 7: A simplified improved displacement evaluation method

CHAPTER 8: A uniform framework for evaluation and comparison of improvement effectiveness

CHAPTER 9: General Conclusions

Figure 1. Dissertation organization

CHAPTER 2.   LITERATURE REVIEW

The evaluation of earthquake-induced liquefaction and need for remediation have become a routine part of geotechnical engineering design. PHRI (1997), Cooke and Mitchell (1999), Cook (2000), and Youd (1998) provide a complete process to assess the need of remediation for soil liquefaction. The process involves all key elements in soil liquefaction engineering: (1) assessment of liquefaction potential, (2) assessment of post-liquefaction strength and ground deformation, (3) evaluation of liquefaction-induced consequence and damage by comparing to the design specifications, (4) implementation (evaluation) of engineered mitigation if the consequence estimated in step (3) is unacceptable.

Mitigation efforts may consist of relocation of the construction site, removing native liquefiable soils, bypassing the liquefiable soils with deep foundations, structurally accommodating the deformations or strength loss caused by liquefaction, or preventing the onset of liquefaction through ground improvement. Within the scope of this study, ground improvement is assumed as the preferable remedial measure. For completeness, the literature review herein also briefly covers the other elements involved in the process, and the emphasis is placed on application and suitability issues of ground improvement for liquefaction mitigation.

2.1   Triggering Mechanism of Liquefaction

Saturated granular materials, such as sands and silts, subjected to cyclic loading will exhibit a tendency to contract (or densify), and thus will generate excess pore pressure if their drainage is too slow. Depending on their initial density and cyclic stress history, these soils may develop excess pore pressure high enough to cause complete loss of shear strength and stiffness at essentially zero effective stress (the historical definition of liquefaction), or cause excess deformations (defined as cyclic mobility or liquefaction with limited strain potential). Both

phenomena are particularly severe for native loose soil deposits such as those developed during conventional reclamation work (i.e., hydraulic placed fills). As shown in Figure 2, the reduction in strength (and stiffness) can result in permanent deformation ranging from a few meters (i.e., lateral spreading) to hundreds of meters (i.e., flow failure). In addition, loss of bearing capacity to shallow foundations and the floating or sinking of structures frequently occurs.
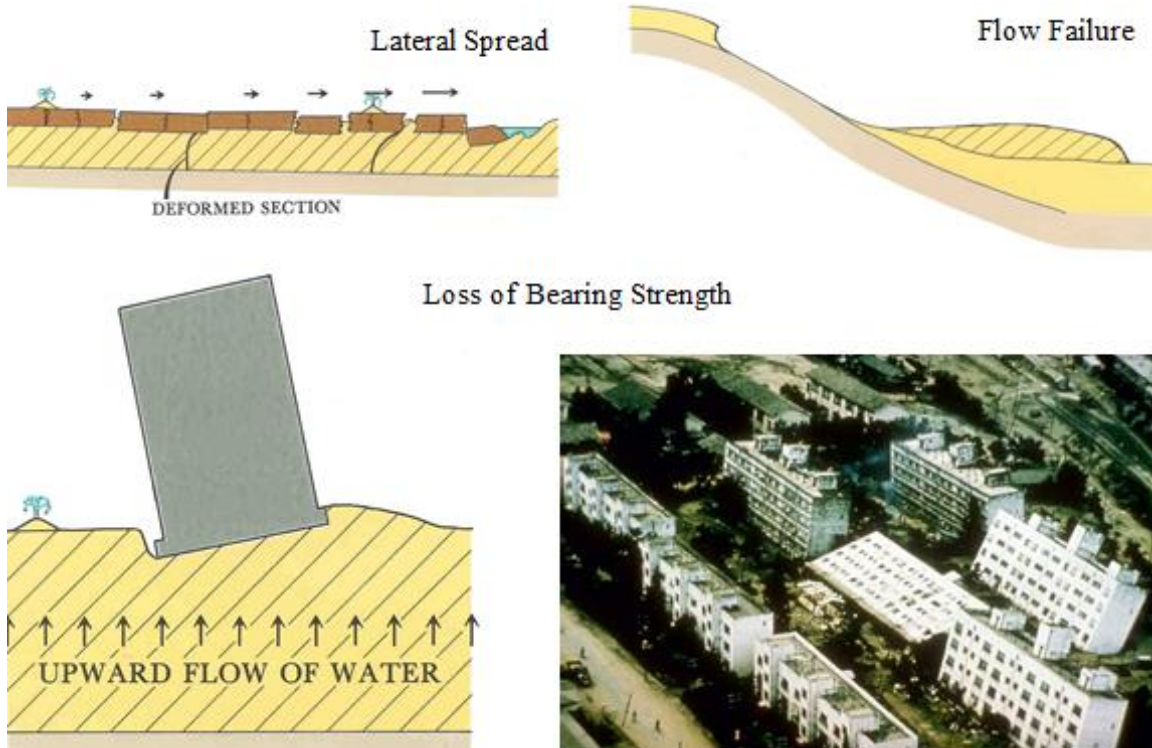
Figure 2. Liquefaction induced deformations and failure modes (After PHRI, 1997)

Modern studies of liquefaction with initial emphasis on liquefaction trigging mechanisms started in 1960s after the Niigata and Alaska earthquakes, such as Seed and Lee (1966), Seed and Idriss (1967, 1971), Martin et al. (1975) and Peck (1979). Experimental testing of liquefiable soils (especially on loose saturated granular soils) coupled with field observations provided the first understanding of the triggering mechanisms. The triggering mechanism has been studied extensively through both experimental testing and numerical methods. In brief, the triggering mechanisms of soil liquefaction or cyclic mobility have been well understood.

2.2   Assessment of Liquefaction Potential

The focus of liquefaction engineering research turned to the identification of liquefaction-prone sites after the underlying triggering mechanisms were understood. The soil liquefaction potential assessment has also been studied and various potential prediction approaches have been proposed since the phenomena was first observed in field in the 1960s (e.g., Seed, et al., 1966, 1967, 1971, 1977, 1983; Youd et al., 2001; Seed, R.B. et al., 2001, 2003; Idriss and Boulanger, 2008). Factors influencing the occurrence of liquefaction include soil properties, geological conditions, and earthquake motion.

The preliminary evaluation criteria proposed by PHRI (1997) for liquefaction potential evaluation are: (1) partially or fully saturated alluvial sand layers; (2) water table is less than 10m from the ground surface; (3) mean particle diameter (D_{50}) of native soil is between 0.02mm and 2.0mm.

The majority of the prediction approaches had many things in common and followed the basic framework of the "simplified procedure" that was initially developed by H.B. Seed and his colleagues (1966, 1971 and 1977). Among these prediction approaches, recommendations on empirical correlation factors, screening criteria, and interpretations of case history data and site responses are different; therefore the prediction results by each approach could differ significantly different. These differences cause difficulties when trying to select an appropriate approach for practical applications. Among these studies, Youd et al. (2001) received the most consensus among the liquefaction engineering committee in the U.S. The details on the prediction process are not expended herein.

In-situ test-based liquefaction susceptibility assessment techniques were developed based on empirical analysis of case histories. Seed et al. (1983) provided a relationship between soil

density (as inferred by "correlated" SPT blow count) and the liquefaction potential for a given level of cyclic loading. This method as incorporated into the "simplified procedure" has become the most widely used liquefaction potential assessment tool currently available. In addition, with the use of the Bayesin updating methodology and accumulated case histories, especially in past two decades, the initial correlations have been refined and updated by incorporating numerous modification parameters for account to earthquake magnitude, fines content, confining pressure, and topography. The increased use of SPT, CPT and shear-wave velocity (Vs) have also provided opportunities for development of similar liquefaction triggering tools based on such tests (Robertson, 1998; Seed et al., 2003; Moss et al., 2006; Andrus and Stokoe, 2000 and 2003).

A summary of in-situ techniques used for liquefaction potential assessment is provided in Table 1. The SPT-based method is regarded as the most reliable method due to the larger number of case histories in the database. SPT can be used in almost all the liquefiable soil types with proper corrections for site-specific characteristics. CPT has also been extensively used in the same manner as the SPT method. CPT is becoming more popular than SPT recently due to the advantages of measuring pore pressure generation and continuous measurements of soil profiles. Youd et al. (2001) recommended always using both methods if feasible. Shear-wave velocities from geophysical tests can be used on sites prone to seismic damage wherever penetration-type tests are not feasible. Further refining and updating the process of the "simplified procedure" based on cumulative case histories can further increase the prediction accuracy of liquefaction potential assessment using in-situ techniques.

Table 1. Comparisons of in-situ techniques for liquefaction potential evaluation (Youd et al., 2001)

Features	Test Type			
	SPT	CPT	Vs	BPT
Past measurements at liquefaction sites	Abundant	Abundant	Limited	Sparse
Type of stress-strain behavior influencing test	Partially drained, large strain	Drained, large strain	Small strain	Partially drained, large strain
Quality control and repeatability	Poor to good	Very good	Good	Poor
Detection of variability of soil deposits	Good for closely spaced tests	Very good	Fair	Fair
Recommended soil type	Non-gravel	Non-gravel	All	Primarily gravel
Obtained soil sample	Yes	No	No	No
Measures index or engineering property	Index	Index	Engineering property	Index

In addition to in-situ methods, a different method of liquefaction potential analysis was proposed by Seed et al. (1977) based on laboratory tests. These researchers found that a minimum shear strain must be achieved before excess pore pressure generation begins to occur. This strain was termed the "threshold strain" and was found to be approximately equal to 0.1%. Their results seem to suggest that this threshold strain does not depend on confining pressure, penetration technique, or failure mode. Namely, if the strain achieved exceeds the threshold strain, liquefaction is possible. Although this liquefaction potential prediction method based on shear strain can effectively determine if excess pore water pressure can or cannot begin to be developed, this tool has been much less used in routine practice than the "simplified procedure" due to the costs of sampling disturbance, and laboratory testing.

As a result of liquefaction potential assessment, if the predicted factor of safety against liquefaction is lower than unity, then the analysis is continued to assess the post-liquefaction conditions and consequences.

2.3   **Deformation Potential in Liquefiable Soils**

Once basic liquefaction theory and analysis tools were developed, researchers recognized the need to understand the performance implications. Tools were needed to assess the potential deformation behavior. Understanding the driving mechanisms of damage helps in developing mitigation measures against liquefaction. However, it is difficult to predict deformation by the methods used to identify liquefaction potential. In general, liquefaction-induced ground failures are normally caused by excess pore water pressure dissipation or ground softening under seismic loading. Depend on the surface slope or inclination, there are mainly four types: (1) lateral spread, (2) flow failure, (3) loss of bearing capacity, and (4) ground oscillation (PHRI, 1997; Bardet et al., 2002; Youd et al., 2002; Seed et al., 2003). Generally speaking, it is more convenient to consider liquefied sand as a liquid (PHRI, 1998). The research on prediction of deformation potential primarily emphasized lateral spreading displacement, because it is the most general failure type induced by soil liquefaction. The failure mechanisms of flow failure, vertical settlement and ground oscillation are not well understood and are not predicted with reasonable prediction.

In the past 30 years, research focused on developing deformation prediction tools for liquefaction-prone sites has taken two general paths: empirical relationships and numerical modeling. Semi-empirical methods based on residual strength of liquefied soils obtained from laboratory or in-situ SPT-N tests have also been proposed, but little information is available on these methods.

Since the deformation phenomenon involves numerous small irregularities and simultaneous mechanisms, the computation methods are usually empirically-developed. The analysis can only predict the average value at best. The most commonly-used deformation tool

has been a relationship developed by Youd et al. (1995, 2002 and 2009) based on a comprehensive statistical analysis of case histories (over 500 lateral spread locations in previous earthquakes), in which the liquefaction induced lateral spreading was caused by gravity-driven flows in fully liquefied, loose soils for both free-face conditions and ground-slope conditions. In brief, Multiple Linear Regression (MLR) analysis is utilized to derive the empirical expressions using seismological, topographical, geometrical, soil, and geotechnical parameters to ensure a minimum correlation (R-square), which indicates that the computed displacement magnitude most-closely matches with the recorded value induced by soil liquefaction.

Following similar strategies, various other studies (Hamada et al., 1987; Youd and Perkins, 1987; Tokimatsu and Asaka 1998; Zhang et al., 2004) also proposed different methods or expressions to compute lateral and vertical deformation induced by soil liquefaction. In addition to MLR, high-end programming such as artificial neural network (ANN) and genetic programming (GP) have been also used in the prediction process. However, the results of using more "advanced" prediction tools don't show a clearly improved accuracy, especially on the prediction of small to moderate deformation ranges (less than 1 m). Current studies indicate that the actual deformations induced by soil liquefaction are within 50% to 200% of the calculated values (Olsen, 2002), as shown in Figure 3. The dots with different colors in Figure 3 indicate the dates of recorded from different case histories. This could be attributed to the uncertainties associated with input parameters and bias of the utilized statistical model (Youd et al., 2002).

The dissipation of excess pore water pressure also induces vertical settlement of the ground. Similar to the prediction of lateral spread, an empirical chart for estimating volumetric strains due to soil liquefaction during an earthquake was proposed based on the in-situ SPT-N measurements and effective confining pressure (PHRI, 1998). The vertical settlement of loose

liquefiable soils under seismic loading can be computed by integrating the volumetric strains with depth. However, verification of the results of this semi-empirical method is needed, which may be based on data of case history or experimental testing.
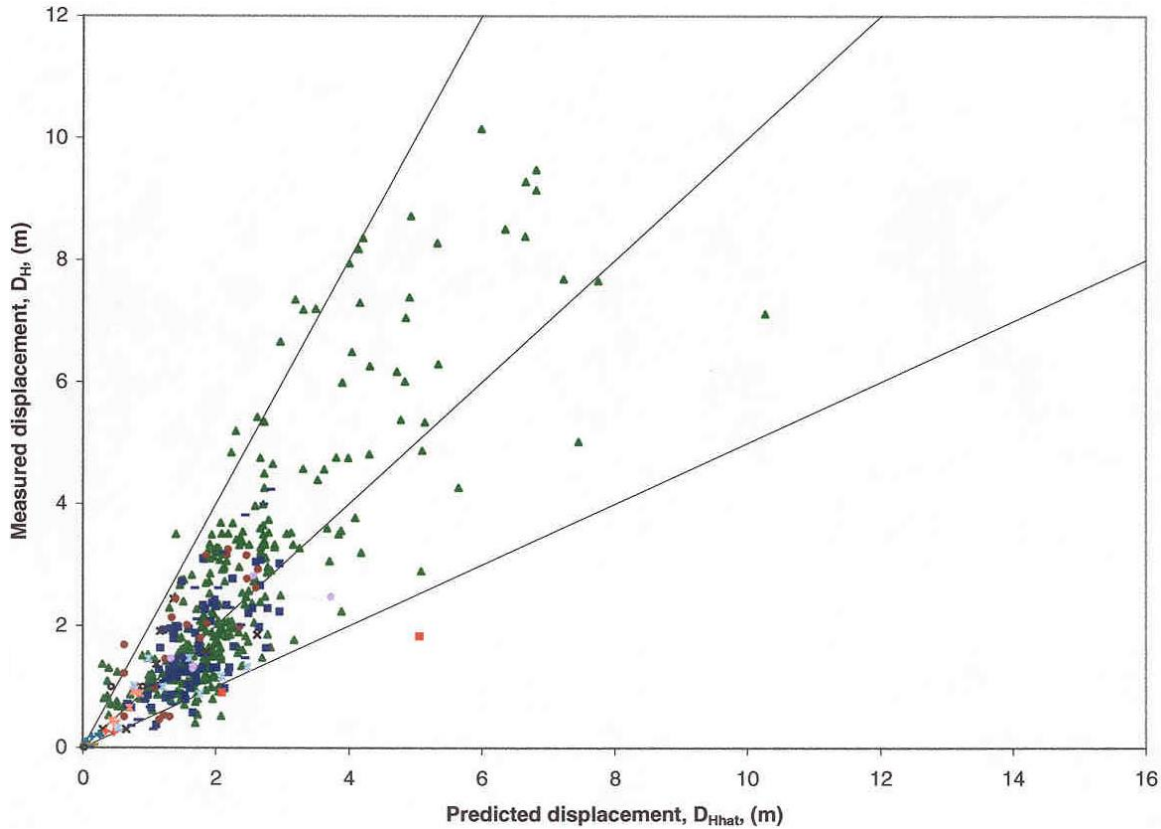
Figure 3. Measured versus predicted displacement from MLR analysis (Bardet et al., 2002)

Due to the emphasis on loose materials, accurate and reliable tools to predict small to moderate deformations for medium-dense soils do not currently exist. Based on laboratory testing of medium to dense materials (Bryne et al., 1991; Kammerer, 2002; Yang et al., 2003), dense materials would stiffer or "lock up" after some strain has occurred. Therefore, the greatest promise for simulating this behavior and, predicting deformations in medium to dense soils is numerical modeling. The need for such a tool is continually increasing due to the shift from stress-based design to the performance-based earthquake framework. Another drawback is that deformation of liquefiable soil is currently not properly accounted for in current seismic design

of structures, or is simplified by using conventional stress-based static or pseudo-static analyses. This drawback highlights the importance of experimental testing or fully-coupled numerical simulation in evaluating the influence of liquefiable soil deformation on adjacent structures.

Constitutive models implemented in numerical frameworks show particular promise as powerful predictive tools that are capable of dealing with even most complex sites. The benefits include the ability to: (a) compute excess pore pressures as they are generated, migrated and dissipated with time, (b) include the influence of the structure and foundations in analysis (partially or fully-coupled analysis), and (c) track a variety of quantities of interest over space and time. Some geotechnical researchers have developed promising models that are capable of capturing the limited available laboratory data or case history data fairly well. However, the accuracy and reliability required in predictive tools has not been reached. It is the objective of current study to apply the previous experimental data or observations from previous case histories to accurately predict the performance or deformation of soil liquefaction. Therefore, the importance of numerical methods to advance the current ability of predicting soil liquefaction-induced deformation and account for the influence of structures, generation of excess pore water pressure and soil strength degradation cannot be overstated. As a result, if the estimated hazard deformation exceeds the specified tolerable limits, remedial treatment would be required.

2.4   Previous Research on Liquefaction Mitigation by Ground Improvement

Efficient remediation of soils susceptible to liquefaction-induced damage is one of the most challenging problems in geotechnical earthquake engineering. The design guidance for liquefaction mitigation by ground improvement under certain earthquake conditions has been studied, and primarily developed semi-empirically based on the in-situ observations of case histories, and physical and numerical testing results. Based on these studies, the improved

performance is not always satisfactory but, in generally, fairly acceptable (Mitchell, 1991 and 1995; Haulser, 2002). However, in the majority of the analyzed case histories involving liquefaction mitigation by ground improvement, the design earthquake magnitudes were greater than the actual recorded magnitudes, such as the 1964 Niigata earthquake and the 1989 Loma Prieta earthquake. This may indicate that the seismic design could be unconservative. Therefore, verification of the design guidelines is needed.

2.4.1   Ground improvement methods used as remedial countermeasures

For earthquake-induced soil liquefaction, based on the sequences of following several phenomena or failure mechanisms, excessively large cyclic loading occurs to in-situ soils which could cause the collapse of the soil skeleton, by which excess pore water pressure is generated without rapid and sufficient drainage, and this could lead to the reduction of effective stress and occurrence of soil liquefaction. Ground improvement as remedial measures can be implemented to prevent the above failure mechanisms or reduce their influence on the stability of the soil skeleton. Theoretically, any ground improvement methods that can impede the failure mechanisms can be used for liquefaction mitigation.

According to NRC (1985), PHRI (1998), and DFI (2013), there are mainly three fundamental mitigation mechanisms usually involved: (1) densification, (2) reinforcement, and/or (3) drainage. The three methods are briefly discussed in the following sections, since these methods have been extensively presented in the literature on liquefaction mitigation.

2.4.1.1   Densification

As is well known, a soil's resistance to liquefaction is largely a function of relative density (D_r). Hence, improving soil relative density (increasing Cyclic Resistance Ratio "CRR" in the "simplified procedure") can be achieved by a substantial number of ground improvement

methods (e.g., vibro-compaction, vibro-stone columns, dynamic compaction, compaction grouting, etc.). Through densification, liquefaction will not occur or the induced deformation may be controlled during an earthquake. Densification is attractive because the methods are relatively simple and practical and improvement can be easily verified using in-situ penetration techniques (Mitchell and Solymar, 1984; Charlie et al, 1992; Elias et al., 2006). The design and constructions of densification primarily depends on fines content, elevation of ground water table and disturbance to adjacent structures.

2.4.1.2 Reinforcement

Inducing stiffer elements as shear reinforcement within a soil mass can reduce the cyclic shear stress ratio (CSR) applied to liquefiable soil and provide an improved axial stiffness. Soil reinforcement options include: full soil treatment (via permeation grouting, chemical grouting and bio-cementation), cellular or panel reinforcement (using jet grouting or slurry wall systems), or individual column elements (using jet grout columns, mechanically mixed columns, stone columns, aggregate piers, grout columns, etc.). Design of reinforcement is mainly based on the principle of strain compatibility between reinforcing elements and the enclosed soil even though its effectiveness could be significantly overestimated (Nguyen et al., 2012, Rayamajhi et al., 2012; Boulanger, 2012). Unlike densification methods for mitigation, the effectiveness of reinforcement cannot be verified based on post-treatment. Engineers must utilize theoretical analyses for their design and effectiveness verification (Baez, 1995; Hausler, 2002; Martin and Olgun, 2006; Nguyen et al., 2012, Rayamajhi et al., 2012; Boulanger, 2012). Comparing the individual columnar elements, underground wall panels or lattice shaped elements are more effective. In brief, numerical simulation in optimization of seismic design involving stiffer elements is more reliable than the semi-empirical methods.

2.4.1.3 Drainage

Generation of excess pore water pressure in liquefiable soil is the primary triggering mechanism leading to liquefaction. Hence, liquefaction can be mitigated and the reduction of effective stress in liquefiable soil under seismic excitation may be controlled if the development of high excess pore water pressure can be prevented through rapid drainage. The current design methods for drainage in practice are mainly semi-empirical or analytical (Seed and Booker, 1977; Pestana et al., 1997). The rule of thumb in most drainage designs for liquefaction is to find the installed drainage spacing to limit the excess pore water pressure ratio lower than 0.6 in soil to minimize deformation. Although drains can successfully mitigate liquefaction, the improvement of the ductility cannot be expected and the volume of water drained during seismic event is still approximately equal to the amount of deformation observed at the surface of drain treated ground (Iai, 1988). Therefore, the use of drainage is rarely relied on as the sole mechanism for mitigating liquefaction in the U.S. In addition, the effectiveness of an earthquake drain installation cannot be verified through conventional in-situ penetration techniques.

2.4.1.4 Overview of seismic design

Seismic designs of ground improvement remedial measures can be highly diverse and case-specific. As a rule of thumb, the area to be improved to reduce the effects of liquefaction is the part of the ground which significantly affects the stability of structures (PHRI, 1998) and enough to cover the influence (i.e., migration of excess pore water pressure; liquid-like response) of surrounding unimproved zone. According to Haulser (2002), the critical influencing factors on improved ground performance are the improved zone depth and lateral extent. The majority of design guidelines are developed semi-empirically based on case histories and experimental testing data.

Cooke and Mitchell (1999) and PHRI (1997) recommended that the improved depth should be equal to thickness of liquefiable soil depths determined by in-situ techniques by following the "simplified procedure". PHRI (1997) also recommended extending the improvement depth through the full liquefiable soil zone thickness with the maximum improvement depth up to 20 m. In terms of the specifications on lateral extent of improved zone, Iai et al. (1988&1990) and Mitchell et al. (1995) recommended extending the improvement distance in the lateral direction equal to the depth of the soil zone being improved. PHRI (1997) recommended an improved distance greater than or equal to two-thirds of the improvement depth. For light or small structures, the lateral extent of the treatment zone should be at least one half of the improvement depth. The improvement zone width to depth should always be greater than 1.5 to prevent the migration of excess pore water pressure from surrounding unimproved zones and also keep the maximum pore water pressure ratio in the treated zone less than 0.5 (DFI, 2013).

In brief, an adequate improvement zone should provide sufficient protection and resistance to the influence exposed from surrounding unimproved zones. The above mentioned rules of thumb are mainly for densification methods. However, the results of recent research and post-earthquake reconnaissance have challenged previously long-held beliefs about liquefaction and associated mitigation techniques. Therefore, in addition to the urgent need for verifying the previously held design guidelines, there is a great need to refine and develop the analytical seismic design of ground improvement for liquefaction mitigation (DFI, 2013; Seigel, 2013). Hence, the most ideal approach to determine the degree and configuration of soil improvement zones is a performance-or improved deformation-based approach (PHRI, 1997). This highlights the importance of design optimization of ground improvement based on displacement comparison.

2.4.2 Evaluation of improvement effectiveness evaluation

The effectiveness of ground improvement for liquefaction mitigation has been assessed and interpreted based on: (1) observations of the improved performances in case histories from previous earthquakes, or (2) implementation of physical modeling (i.e., shanking table and centrifuge testing), and (3) numerical modeling to compare the unimproved and improved performance of structures through measured engineering parameters. As indicated in PHRI (1997), if remedial measures are to be considered, the simplified method may not be sufficient and more advanced analytical or experimental methods are recommended.

2.4.2.1 Case histories

Mitchell et al. (1995), Hayden et al. (1994) and PHRI (1997) assessed the great effectiveness of implementing ground improvement for liquefaction mitigation based on field observations from previous earthquakes. Their results showed the improved areas normally performed better and suffered less damage than the surrounding unimproved areas or structures. The magnitudes of these seismic events were generally less than their ground improvement earthquake magnitudes, hence, the influence of shaking intensity and duration on improved performance remains uncertain. This drawback also highlights the importance of physical and numerical testing.

Based on case histories collected in Japan, PHRI (1997) indicated the SPT $(N_1)_{60}$ value, required as part of QA/QC process, was most frequently used as an index for evaluating the effectiveness of improvement for the densification method. The target N-values are normally taken to be at 14 to 16. The maximum pore water pressure ratio employed as a target value for drainage method is commonly set at 0.5. For solidification or grouting methods, the unconfined compressive strengths are usually taken to be from 0.9 to 6.0 kgf/cm^2 (14.2 psi) for the mixed

materials. All the above target values were determined based on the factor of safety against liquefaction occurrence. Therefore, the improvement effectiveness or design specifications of the improvement design are simply verified as part of QA/QC program in the field.

Yasuda et al. (1996) analyzed the effectiveness of several ground improvement methods based on the post-earthquake ground settlements observed in Kobe earthquake in 1995. Based on their results, sand compaction piles were regarded as the most effective, followed by densification methods which were more effective than drainage methods. The other evaluation criteria also included the in-situ SPT blow count measured before and after earthquake occurred. The main conclusions include:

1) The average unacceptable performance rate for buildings with shallow foundations and piles was about 15% to 20%, which was slightly higher than tanks with shallow foundations and embankments.

2) Using sand compaction piles as the remedial measure, the unacceptable performance rate was 20%, which was slightly higher than the cases involving other remedial measures.

3) The unacceptable performance rate using vibro-compaction in this earthquake was surprisingly about 50%, which may indicate the seismic design method of the vibro-compaction method for liquefaction mitigation in Japan may be unconservative.

4) No clear trend between the building settlement and improved thickness was found based on the data obtained from this case history.

2.4.2.2 Experimental testing

Another data source on improvement effectiveness evaluation is based on experimental testing, which include laboratory tests (i.e., cyclic triaxial tests, hollow cylinder torsional test, or cyclic simple shear test) on "undisturbed improved samples" to obtain the improved strength

under cyclic loading or full scale tests such as shaking table and centrifuge test. The emphasis herein is on the full scale experiment tests because they can predict the improved performance in greater details and accuracy.

For the full scale experimental tests, extensive measurements (i.e., acceleration, excess pore water pressure generation within the soil mass, structure deformation, etc.) to discover the insights of the failure model and improvement mechanisms from physical testing can be collected and future used to optimize the seismic design of ground improvement to ensure satisfactory improved performance under the design earthquake. In general, centrifuge test can generally provide more accurate results than the shaking table test (Adalier, 1996; Haulser, 2002).

Adalier (1996) performed a series of centrifuge tests and shaking table tests to evaluate the effectiveness of various ground improvement methods in liquefiable soil. The primary measurements included: (1) time histories of acceleration response, (2) time histories of excess PWP ratio, (3) time histories of deformation, and (4) shear stress and strain distribution within the soil mass. These data can be measured at numerous selected critical locations within the modeled structure-soil system without and with the implementation of ground improvement. Based on their results, the following conclusions were drawn:

1) Increasing over consolidation ratio of liquefiable soils can reduce excess pore water pressure generation and densification efforts.

2) The effectiveness of vacuum-suction for liquefaction mitigation was proved and although a reliable design has not yet been developed.

3) Densification methods were effective in mitigating liquefaction risk, and the island soil effects should be accounted in remediation design. Reinforcing effects of stiff grid shape metallic as stiffer elements may not be effective in eliminating the liquefaction potential.

4) For earth embankments, compaction and sheet piles can minimize excessive deformation and prevent catastrophic failure from occurring without completely eliminating the risk of liquefaction.

2.4.2.3 Numerical modeling

Like the experimental testing, well calibrated and verified numerical modeling also has great benefits in evaluating the improved performance and optimizing the remedial design. Three reasons explain why using numerical modeling for improvement effectiveness evaluation:

First, numerical modeling can account for influences of complex and simultaneous phenomena in seismic design. For instance, the improved part of the ground will be affected by migration of excess pore water pressure and liquid-like response of the liquefied part of ground surrounding the improved part. However, to evaluate this change and the effects on the stability of structures, which cannot be captured using simplified procedures, requires detailed and advanced investigation. Hence, well-calibrated numerical analyses can provide valuable insights on this issue.

Second, numerical modeling can capture multiple types of improved response data. Cooke and Mitchell (2000) conducted a comprehensive numerical study to determine the effectiveness of grouting methods on an existing highway bridge stub abutment supported on soil embankment underlying by liquefiable zone. Using an effective stress analysis technique in FLAC (Itasca, 2007), the effectiveness of three remedial measures (chemical grouting, jet grouting and compaction grouting) were examined quantitatively based on a series of improved numerical engineering parameters (reduction of excess pore water pressure within the liquefiable zone, the reduced displacement of the sub abutment and deformation of the soil embankment) under seismic excitation. Similar to physical modeling, the effectiveness evaluation and

comparison based on numerical testing was based on the time histories of soil or structure deformations and/or responses under seismic excitation.

Third, numerical modeling can be used to examine different remedial measures, regardless of the improvement mechanisms. For instance, in-situ penetration techniques are unable to be used to verify the improvement effectiveness of soil mixing method, such as lattice or wall shaped mixed elements by grouting methods within liquefiable soil. Rourke et al. (1997), Namikawa et al. (2007) and Nguyen et al. (2012) evaluated the effectiveness of deep soil mixed elements in liquefiable soil under seismic loading. In these studies, the primary performance evaluation parameters and comparison criteria were: (1) unimproved and improved cyclic stress ratio "CSR", (2) dynamic performance (i.e., stress-strain correlations, failure models) of the induced stiffer elements, (3) unimproved and improved shear strain ratio distribution, (4) reduction of the peak shear stress and (5) excess pore water pressure ratio distribution in the enclosed soil. Similar studies on columnar type remedial measures are also conducted by Green et al. (2008) and Olgun and Martin (2008).

As indicated by Mitchell (2008), with the increasing development and application of numerical modeling and computational power, implementation of appropriate and calibrated constitutive models should be encouraged in effectiveness evaluation and optimization of the liquefaction mitigation design. Beyond the effectiveness evaluation, there is still considerable room for future developments in perusing an accurate and efficient design framework for liquefaction mitigation by ground improvement. This is also the primary objective of this research.

2.5   Development of Ground Improvement Technology Selection System

2.5.1   Introduction

Beyond a summary of the previous important studies, an interactive web-based ground improvement technology selection system for liquefaction mitigation is developed. Proper selection and design considerations of ground improvement methods are important to ensure the satisfactory performance of the improved structure. The proper selection of ground improvement technolog(s) under site and project-specific conditions is an important first step to ensure an adequate, sufficient and cost-efficient mitigation treatment plan. Inappropriate selection and application of a remedial technology may lead to unacceptable, structure damage, and/or high cost.

Liquefaction mitigation using ground improvement technologies has been widely applied and has proven to be effective in reducing liquefaction induced damage. Design and remedial practice is normally different from country to country due to local engineering practice. However, before developing an adequate, economical, and effective remedial design using ground improvement technologies, engineers always encounter the first key step, which is to select the proper technology(s) based on site or project-specific characteristics. Previous studies, including Youd (1998) and Mitchell et al. (1995) indicated that the inappropriate use of ground improvement technologies could result in an unexpected high construction cost and unsatisfactory improved ground performance. To assist engineers in selecting suitable ground improvement technologies for liquefaction mitigation, a web-based interactive technology selection system focusing on liquefaction mitigation has been developed.

On any given project, the factors leading to the use of ground improvement technologies are diverse, reflecting both a number of "hard" concerns (including geotechnical, logistical,

accessibility, environmental, cost, schedule, and performance factors) as well as a number of less tangible issues (including national issues, the degree of logistical, accessibility, environmental, cost, schedule and performance factors) as well as a number of less tangible issues. The selection of suitable technology(s) to mitigate liquefaction potential is also based on integration of available engineering knowledge, experiences, technology related features, and site or project-specific features. Moreover, several of these factors, such as experience and site characteristics, cannot be evaluated and described quantitatively. Application of ground improvement is often a combination of engineering and art (Chu et al., 2009). Therefore, the primary challenge in development of the proposed selection system is to take those influencing factors into consideration in the selection process.

To address this challenge, lessons learned from previous case histories are summarized and presented in a readily accessible way. The suitability of ground improvement technology subjected to various site- and project-specific characteristics are first evaluated based on information from case histories; then, an interactive web-based technology selection system is established to present an evaluation of suitability in a fast, readily accessible, convenient, and dynamic manner.

The proposed system is planned to be accessible under a comprehensive information and guidance web-based system, called GeoTechTools, hosted at www.geotechtools.org. The GeoTechTools System was developed as part of a Strategic Highway Research Program (SHRP) 2 project entitled Geotechnical Solutions for Transportation Infrastructure, with the goal of making geotechnical solutions more accessible to public agencies in the United States. More details about this information and guidance system can be found by accessing the website, or in Douglas et al. (2012a and 2012b).

Herein, the development process of the proposed system is presented along with a brief description of the critical screening criteria. The goal is to provide an informative reference and summary of well-accepted rules from the literature for liquefaction mitigation using ground improvement technologies. Moreover, the product of this study, the interactive selection system, can assist engineers with the desk study when encountering liquefaction remediation problems.

The ground improvement technology candidates involved in this system are all commonly used for liquefaction mitigation in practice, and are shown in Figure 4. Figure 4 is also the user interface of the proposed system. The primary supplementary information supporting this technology selection system is the elimination process of ground improvement technologies. For the elimination process, the focus is on various key technical factors involved in the initial selection process. These factors include depth of liquefiable zone, type of soil to be treated, foundation type, ground water table and potential failure type.

The technology elimination process can be best described as a heuristic process (Douglas et al., 2012a), and the development of reasonable heuristic rules is the core of a reliable selection system. The heuristic rules developed in the proposed selection system are site- and project-specific characteristics, general limitations and functionality of the ground improvement technologies, and other technical related issues. When evaluating the suitability of technologies subjected to certain heuristic rules, the selection system could miss the most optimized solution, but the apparently less-attractive and less-applicable solutions would be eliminated. Therefore, the proposed selection system is best used for screening, filtering, or pruning to reduce the number of alternatives. The selected critical factors of the heuristic rules considered in the proposed selection are presented in Table 2.

Liquefaction Mitigation Selection System

The Liquefaction Mitigation Selection System is in the development stage and is shown for informational purposes only.

The following geoconstruction technologies involved in this interactive system are commonly used for liquefaction mitigation purpose in practice.

- Stone columns
- Blasting densification
- Permeation grouting
- Compaction grouting
- Deep dynamic compaction
- Deep soil mixing
- Excavation and replacement
- Jet grouting
- High-energy impact rollers
- Rapid impact compaction
- Sand compaction piles
- Vibro-compaction

Help icons ❷ are found throughout the interactive selection system to provide additional information regarding each selection.

❷ **Which of the following options best describes the site characteristics?**

  - select - ▼

❷ **What primary type of failure are you trying to protect against?**

Select at least one.

☐ Lateral spreading
☐ Flow failures
☐ Vertical settlement

❷ **Project constraints (e.g., construction influences/damage to the adjacent structures, site access, traffic patterns, mobilization, sensitive equipment):**

You may leave all checkboxes blank if none of the listed constraints apply.

☐ Low overhead clearance
☐ Adjacent structures
☐ Existing utilities

❷ **Depth to ground water table:**

  - select - ▼

❷ **Select the liquefiable soil conditions of the in-situ liquefiable profile:**

  - select - ▼

❷ **Which of the following descriptions can best describe the treated soil?**

  - select - ▼

Figure 4. User interface of the proposed technology selection system

Table 2. Site and project-specific and non-technical related evaluation criteria

Category	Factors
Site	Site topography, depth to ground water table, initial liquefiable soil condition, fines content in treated soils, drainage conditions.
Project	Project constraints, specified minimum treatment depth, specified minimum improved area, specified minimum improved properties, primary improvement category.
Non-Technical	Schedule, cost, environmental controls, availability of construction material.

The evaluation rating criteria are presented below. As seen, different ratings are applied to describe the suitability of a certain technology subjected to different conditions:

1) Not Applicable ("NA"): not applicable under the specified condition.

2) Low Suitability ("L"): can be used but practically difficult, costly and time consuming.

3) Moderate Suitability ("M"): can be used but may not be the best option.

4) Applicable ("A"): applicable under the specified condition.

5) High Suitability ("H"): application recommended.

In Figure 4, users can input the site and project characteristics by answering questions using a drop-down menu; Non-applicable technologies are removed from the list based on the user's input. Users can select the unit system for the parameter input and results output. The suitability of a technology subjected to different evaluation criteria or an "elimination engine" is discussed in following sections. Descriptions of several factors (the treated project type, potential ground failure type, soil type to be treated, and depth of liquefiable soil) and their influences on the suitability of technologies are discussed herein.

2.5.2 Technology screening criteria

2.5.2.1 Foundation type

Different foundation types require different remedial plans in terms of the applied improvement method, improved zone geometry, and improved degree. However, no well-accepted guidelines have been established on this issue. Out of 256 case histories of liquefaction mitigation by technologies that were reviewed (Mitchell et al., 1995; Haulser, 2002). Based on considerations of the effectiveness of improvement for different foundations types, the suitability evaluation of ground improvement technologies for different foundation types is summarized in Table 3. The technologies ID are assigned as:

Tech ID	Tech	Tech ID	Tech
1	Stone column	7	Excavation and replacement
2	Blasting densification	8	Jet grouting
3	Permeation grouting	9	High energy impact rollers
4	Compaction grouting	10	Rapid impact compactions
5	Deep dynamic compaction	11	Sand compaction piles
6	Deep soil mixing	12	Vibro-compaction

Table 3. Ground improvement technologies for different foundation types

Tech ID	Shallow	Deep	Tech ID	Shallow	Deep
1	L to M	M to H	7	M to H	L
2	M	M to H	8	L	M to H
3	L to M	M to H	9	H	L
4	L to M	M to H	10	H	L
5	H	L to M	11	L to M	M to H
6	L	M to H	12	M	M to H

2.5.2.2 Failure type

Table 4 shows the suitability evaluation of different ground improvement technologies for different failure types. In most cases, more than one type of failure can occur; therefore, the primary failure type is defined as the one with largest magnitude. The applied remedial technology is also not unique; the successful liquefaction mitigation can be achieved using a different mechanism provided by different types of remedial methods.

Table 4. Ground improvement technologies for different failure types

Tech ID	Lateral Disp.	Flow Failures	Vertical Settlement	Tech ID	Lateral Disp.	Flow Failures	Vertical Settlement
1	M to H	M to H	M to H	7	L to M	L to M	M to H
2	L	L	M to H	8	H	H	M
3	M	M	M to H	9	L to M	L to M	M to H
4	L to M	M	M to H	10	L	L	M to H
5	L to M	L	M to H	11	H	H	M to H
6	H	H	M	12	H	H	M to H

2.5.2.3 Soil type

Fully or partially saturated loose cohesionless and slightly cohesive soils are susceptible to liquefaction in earthquake events. Table 5 summarizes the liquefaction potential of various types of soil subjected to earthquake loading. In general, any ground improvement technologies that can effectively improve the shear and compression resistance of liquefiable soil can be used for liquefaction mitigation, but each remedial technology has its own suitable soil type to which it should be applied. Based on well-proven guidelines about the applications of ground improvement technologies in liquefiable soils (e.g. Mitchell et al., 1995; Mitchell, 2008; Chu et al., 2009; Mitchell, 2013), the suitability of ground improvement technologies subjected to various types of liquefiable soils is evaluated and presented in Table 6.

Table 5. Liquefaction risk for various soil types

Soil Type	Liquefaction Risk	Soil Type	Liquefaction Risk
GW	L to M	SP	M to H
GP	L	SW	H
GM	M	SM	M to H
GC	L	SC	L to M
		ML	L to M

Table 6. Ground improvement technology for liquefaction mitigation for various soil types

Tech ID	Suitable Soil Type	Symbol (USCS)
1	Silty sands, clayey silts, or combined with vertical drains	S-,ML
2	Saturated clean sands and gravels, granular soils	G-,S-
3	Loose sands and coarser material with fines < 10-15%	G-,S-
4	Any rapidly consolidating, compressible soils	G-,S-
5	Saturated sands; silty sands; partly saturated materials	S-
6	Most soils susceptible to liquefaction	G-, S-
7	Most soils susceptible to liquefaction	G-, S-
8	Most soils susceptible to liquefaction	G-, S-
9	Clean loose granular soils	G-, S-
10	Clean loose granular materials	G-, S-
11	Most soil types susceptible to liquefaction	G-, S-, ML
12	Sands, silty sands, clayey silts, gravelly sands with fines < 20%, or combined with vertical drains	G-,S-

2.5.2.4 Depth to liquefaction zone

Youd et al. (2001) indicated that liquefaction is not likely to occur when soil depth exceeds up to 25 m (80 ft) based on extensive review on past earthquakes. Several studies have empirically specified the minimum improved depth: (1) Mitchell et al. (1995) recommend improving the full thickness of liquefiable materials beneath the structures; (2) PHRI (1997) recommends a minimum improved depth of 15 m (50 ft) or up to the bottom of liquefiable layer encountered. Therefore, the specified improved depth is primarily governed by the maximum value of (1) foundation depth, (2) the critical soil depth influencing foundation seismic performance, or (3) the depth of liquefiable layer.

Table 7. Effective improved depth of ground improvement technologies in selection system

Tech ID	Effective Depth, Unit: ft (m)	Depth to Liquefiable Soil Profile Bottom, Unit: ft (m)				
		< 10 (3)	10 - 20 (3 - 6)	20 - 40 (6 - 12)	40 - 60 (12 - 25)	> 60 (25)
1	33 - 50 (10 -16)	M	H	H	H	H
2	110 (30 - 35)	L	L	M	M	M
3	Unlimited	M	M to H	M to H	M to H	M to H
4	Unlimited	L	M to H	M to H	M to H	M to H
5	20 - 30 (6 - 9)	H	M	L	NA	NA
6	125 (20 - 65)	L	M to H	M to H	M to H	M to H
7	10 - 12 (3 - 4)	M to H	L	NA	NA	NA
8	Unlimited	L to H	M to H	M to H	M to H	M to H
9	7 - 10 (1.5 - 2.5)	H	L	NA	NA	NA
10	10 (4)	H	L	NA	NA	NA
11	25 - 30 (8 - 10)	L	M to H	H	H	H
12	80 - 100 (25 - 35)	L	H	H	H	H

A summary of effective improved depths of the ground improvement technologies in Table 7 can be used as a screening criterion to eliminate the technologies if their effective treatment depths are less than the specified depth of liquefiable soil depth based on user's input. Since the effective improved depth could vary significantly under different cases, the lower

bound values based on literature review are used for conservative purposes. Finally, the suitability of ground improvement technologies subjected to various liquefiable soil depths is determined.

2.5.2.5 Depth to ground water table

Fully or partially loose saturated soils in shallow depth (less than 12 to 15 m or 40 to 50 ft) are always an important indication of liquefaction in a seismic region. Also, a high ground water table can critically influence the improvement effectiveness of ground improvement technologies. The records on depth of the ground water table in case histories are insufficient to make a general conclusion on the influence of the water table on technologies selection. Based on well-accepted rules found in the literature (e.g., PHRI, 1998; Towhata, 2006; Mitchell, 2013), the suitability evaluation of ground improvement technologies subjected to various depths of ground water table is presented in Table 8.

Table 8. Suitability evaluation of technologies subjected to various ground water depths

Depth to Depth of Ground Water Table, Unit: ft (m)								
Tech ID	< 5 (2)	5-10 (2-3)	10-20 (3-6)	20-40 (6-12)	Tech ID	< 5 (2)	5-10 (2-3)	10-20 (3-6)	20-40 (6-12)
1	T	T	T	T	7	F	F	T	T
2	T	T	T	T	8	T	T	T	T
3	T	T	T	T	9	F	F	T	T
4	T	T	T	T	10	F	F	T	T
5	F	F	T	T	11	T	T	T	T
6	T	T	T	T	12	F	F	F	T

(T: True. F: False)

2.5.3 Discussion

In this section, two case histories involving liquefaction mitigation work using ground improvement technologies are provided to illustrate the usefulness of the proposed selection system. For each presented case history, a brief introduction to site, project and other critical factors that potentially influence the on technology selection is presented; then, the input phase

and results phase of the system is presented. The limitations of the proposed selection system are also discussed in this section.

2.5.3.1   Case history 1: Improvement using aggregate column

In this case history (Wijewickreme and Atukorala, 2005), the liquefaction mitigation was proposed for a gas station with buried natural gas pipeline, which could only be accept low risk of liquefaction. The gate station was rectangular in plan (100 m by 75 m) and located on the bank of Fraser River in Vancouver, BC, Canada. The river bank sloped down toward the south at slopes up to 12 degrees, which indicated a high risk of flow slides toward the river under dynamic loading.

Field investigation indicated the upper soils within the gate station consist of 2 to 3 m of loose to medium dense sandy soil. Below the upper sandy soil, a layer of very soft silt extended to depths of 6 to 8 m below the ground surface. The soft silt zone is underlain by a dense to very dense sand and gravel stratum at a depth of 9 to 14 m. The ground water table across the gate station area is about 2 to 3 m below the ground surface. Engineers found the liquefaction zone was primarily located within the depth of 10 to 12 m below the ground surface.

The post-earthquake performance of the unimproved ground was evaluated by using numerical analysis. The results indicated a downslope lateral displacement of about 3 m would influence an area extending to about 40 m from the crest of the river bank. The gate station and buried pipeline were located within this area. Therefore, the risk of damage to these utilities under earthquake loading was well above the owner's acceptance criteria. Based on CPT results, improvement was needed to increase the cone tip resistance (q_t) values to the specified performance q_t criteria between 100 to 125 bar for the soil in liquefaction zone. Based on the numerical analysis, an improved zone, with width of 20 m, length of 100 m, and depth of 12 to

14 m located next to the gate station in the downslope direction was designed to act as an in-ground densified barrier to reduce the earthquake deformation below the structural deformation capacity of the pipelines. Eventually, the engineers decided aggregate columns were the most suitable technique for establishing the densification zone at the gate station site.

THIS MODULE IS ONLY OFFERED AS A SELECTION GUIDE AND SHOULD NOT BE USED FOR DESIGN.

Your Selections

The selections you made on the previous page are listed below:

Site characteristics:	Large, open undeveloped sites, rural areas
Primary failure types to protect against:	Lateral spreading, Flow failures
Project constraints:	None selected
Depth to ground water table:	10 to 20 ft
Liquefiable soil conditions:	Liquefiable soils and stable soils are interlayered
Treated soil type:	S-
Peat layer:	No sufficiently thick peat layer present
Shear strength of unstable soils less than 500 psf:	Not applicable
Subsurface obstructions:	No surface obstructions
Depth of treatment/remediation zone:	20 to 40 ft
Size of area to be improved:	10 to 50 ft
Improved foundation type:	Not applicable
Project/structure type:	Not applicable
Environmental regulations:	No environmental regulatory issues

Return to your selections

Results

The results of your selections are provided in the following table.

Candidate technology	Degree of Establishment	Rapid Renewal	Minimal Disruption	Long Lived Facilities
Aggregate Columns	4	3	1	4
Compaction Grouting	4	3	3	3
Deep Mixing Methods	3	4	1	4
Sand Compaction Piles	2	4	1	3

Figure 5. Selection results of case history 1

Inputting the above site and project information into the proposed system, a list of suitable technologies including aggregate columns, compaction grouting, deep mixing methods, and sand compaction piles is shown in Figure 5. For each of these technologies, the results also include the ratings that indicate the degree of technology establishment and a technology's potential

contribution to the Strategic Highway Research Program 2 (SHRP 2) Renewal objectives. More details regarding the SHRP 2 project and interpretations of the ratings can be found in Douglas et al. (2012a).

2.5.3.2   Case history 2: Improvement using compaction grouting

Ground improvement was implemented to improve an existing foundation on a liquefied natural gas plant in Delta, British Columbia, Canada. The foundation was a shallow reinforced concrete raft foundation about 6 m to 8 m in plan area and 0.75 m in thickness. Ground improvement was applied to densify the foundation soil and to minimize the liquefaction-induced settlement in soils below the foundation.

Field investigation results indicated the site was underlain by 1 m of granular fill over 6 m of silty sand over more than 20 m of river sand. Under the river sand, a thick layer of marine silt extended to a depth of about 75 m. The ground water table was 1 to 2 m below the ground surface. Both SPT and CPT results indicated that there was a high risk of liquefaction of soils underlying the existing foundation to a depth of about 22 m. A remedial plan was proposed by the engineers to improve the liquefiable soil within a footprint of about 12 m by 12 m and 24 m in depth below the ground surface. However, there were several critical project constraints to consider including: (1) 2 m of headroom clearance available for construction; (2) potential damage to the existing vibration and settlement-sensitive utilities near the construction site; and (3) an accelerated construction schedule. Engineers eventually decided to use compaction grouting as the remedial countermeasure. The ground surface and adjacent utilities were carefully monitored to prevent the damage to the existing utilities.

Based on the available information, the selection result of this proposed system is shown in Figure 6. As can be seen, only the method of chemical grouting/injection systems is

recommended. In the system, the selection of adjacent existing utilities that are sensitive to ground movement and disturbance is the primary reason of removing compaction grouting and other technology candidates from the list. However, as mentioned in the case history, engineers monitored the utilities during the implementation process. Therefore, compaction grouting with careful monitoring work was implemented in this case history.

THIS MODULE IS ONLY OFFERED AS A SELECTION GUIDE AND SHOULD NOT BE USED FOR DESIGN.

Your Selections

The selections you made on the previous page are listed below:

Site characteristics:	Constrained, developed sites, urban areas
Primary failure type to protect against:	Vertical settlement
Project constraints:	Existing utilities
Depth to ground water table:	5 to 10 ft
Liquefiable soil conditions:	Liquefiable soils and stable soils are interlayered
Treated soil type:	S-
Peat layer:	No sufficiently thick peat layer present
Shear strength of unstable soils less than 500 psf:	Shear strength 500 psf or greater
Subsurface obstructions:	No surface obstructions
Depth of treatment/remediation zone:	40 to 60 ft
Size of area to be improved:	Less than 10 ft
Improved foundation type:	Shallow foundations
Project/structure type:	Not applicable
Environmental regulations:	No environmental regulatory issues

Return to your selections

Results

The results of your selections are provided in the following table.

Candidate technology	Degree of Establishment	Rapid Renewal	Minimal Disruption	Long Lived Facilities
Chemical Grouting/Injection Systems	3	3	4	4

Figure 6. Selection results for case history 2

2.5.4 System limitations

Within the theme of this study, only technical related issues are discussed and involved in the proposed selection system. An effective and economical hazard mitigation program requires both technical matters and non-technical matters, as shown in Table 1. The use and application of the results of this interactive system are the responsibility of the users. It is imperative that the

user understand the potential limitations of the program results, independently cross checks those results, and examines the reasonableness of the results with engineering knowledge and experience. In addition, previous studies (e.g. PHRI, 1998; Mitchell, 2008) indicated the combination of more than one method was found to be more effective than the adoption of single method. Also, as illustrated by case history 2, the proposed system can only covers the basic and general technical issues that are normally considered in all liquefaction mitigation projects. Other site and project-specific characteristics are likely to be involved. Therefore, it is the users 'responsibility to make the final choice.

2.5.5 Conclusion

The suitability and constraints associated with commonly-used ground improvement technologies for liquefaction mitigation are summarized from previous studies and presented in this chapter. As discussed above, a proper selection of ground improvement technologies based on site and project-specific characteristics is the first and critical step to achieve an adequate, economical and effective liquefaction mitigation design. Herein, a readily accessible ground improvement technology selection system is proposed. Based on a comprehensive review of case histories of liquefaction mitigation using ground improvement technologies, the screening criteria or reasoning of a technology elimination process in the system is developed based on a suitability evaluation of ground improvement technology subjected to various conditions. This study discusses the influence of selected factors on the technology selection process, primarily from technical aspect. However, several other case-specific issues may be important, such as structural tolerable deformation, specified performance criteria, and use of a combination of ground improvement technologies. The case histories indicate the usefulness, and also show the limitations of the proposed system. In summary, the proposed system can assist engineers in

identifying the important factors and properly evaluating their influence on the selection of ground improvement technologies for liquefaction mitigation in a quicker and more efficient way. The proposed interactive system is designed to be easily updated to incorporate new knowledge and findings for future applications.

2.6 Important Findings from Literature Review

The state-of-practice of assessment of liquefaction potential, liquefaction-induced consequence and remediation design of ground improvement for liquefaction mitigation are regarded as non-uniform in the U.S. (DFI, 2013; Siegel, 2013).

1) The SPT and CPT are the primary in-situ techniques for evaluating the site conditions for the design and verification for densification methods for liquefaction mitigation.

2) Deformation potential in liquefiable soils under seismic loading is predicted empirically based on large number of case histories through the MLR analysis for routine practice. However, reliable prediction method on the cyclic mobility induced deformation in medium to dense soils is not currently available.

3) Densification is the most implemented mechanism for liquefaction mitigation followed by reinforcement. Drainage is not effective in reducing excessive ground deformation induced by soil liquefaction. The application of reinforcement for liquefaction mitigation relies on precedence, judgment and results of numerical modeling. Research is in progress to better define the efficacy of reinforcement and drainage methods and to develop simplified design methods.

4) Current design guidelines of ground improvement for liquefaction mitigation were mainly empirically developed based on case histories, and could be unconservative.

Verification on the design guidelines is recommended using experimental and numerical studies.

5) Development and application of performance-based design and well-calibrated numerical method in the seismic design of liquefaction mitigation by ground improvement is encouraged due to various benefits over the conventional methods.

CHAPTER 3. CALIBRATION OF AN UNIMPROVED CAISSON QUAY WALL CASE HISTORY IN 1995 KOBE EARTHQUAKE

3.1   Introduction

Gravity caisson wall is a widely used port structure around the world. The durability, ease of construction, and capacity of reaching deep seabed levels are the primary benefits of caisson walls. Significant damages occur to this type of structure when subjected to large earthquake motions (e.g., Kobe earthquake in 1995). Through the field observations, physical testing and numerical testing, the three major failure modes for caisson quay wall structure have been identified as the large seaward displacement, vertical deformation and seaward tilting. The primary reasons of inducing these failure modes are the liquefaction of backfill and/or foundation soil under earthquake loading (Hazarika et al., 2008; Moghadam et al., 2009; Andresen et al., 2011; Arablouei et al., 2011; Taiyab et al., 2012).

Understanding the failure mechanisms through numerical modeling analysis provides the basis for applying the effective mitigation efforts through various improvement means. Since the conventional stress-based or force-equilibrium method is difficult to take soil-water-structure interaction into analysis and not likely to reasonably predict the structure response when the force-equilibrium state is exceeded. Thus, since the late 1980s, increased attention has been directed towards a full seismic analysis of port structures using finite element or finite difference technique, because the effective-stress analysis can access all the possible failure modes without pre-defined constraints.

Studies on mitigation of liquefaction-induced damage to caisson quay wall structure have been conducted, yet question remains (PIANC, 2001; Alam et al., 2005). Different improvement mechanisms have been proposed and studied, and valuable insights on the improved

performances of caisson quay wall have been obtained, including densification of foundation and backfill soils (Alyami et al., 2007&2009; Taiyab et al., 2012); installation of a sheet pile or deformable deep soil mixed panels in foundation soil front of the caisson wall or backfill soil behind the caisson wall (Moghadam et al., 2009); utilization of low density but high strength of Expanded Polystyrene (EPS) as compressible buffer to replace a small volume of backfill soil immediately adjacent to the quay wall (Hazarika et al., 2008). However, most of these studies do not provide an easily-executable methodology with sufficient guidelines specifying the improved zone dimensions, improved performance and acceptable level of damages to be followed for practical construction. Most of the studies have shown that mitigation is effective, but rarely provided implementation details for routine practice.

Hence, as mentioned in Chapter 1, an important objective of this study is to propose numerous easily executable remediation programs of using three ground improvement methods with the practical design features by following the philosophy of seismic performance-based design as specified in details in PIANC (2001). Then, based on their improved performances of the caisson quay wall, these three different remedial ground improvement methods are evaluated and compared in terms of the improvement effectiveness, which is the other primary objective in this study. Additionally, additional new insights on the optimization of liquefaction remediation design are provided to further advance the current understanding and conventional design process for liquefaction mitigation.

In this chapter, the numerical modeling, which is further used as the unimproved framework for the hypothetical application of ground improvement in following chapters, is established to capture the failure mechanisms and deformation magnitude of the specific caisson quay wall example. Especially for performance-based design, reasonably estimating the large

deformation induced by the seismic liquefaction is one of the important issues. Therefore, the conducted modeling, verification process and investigation of failure mechanisms of caisson quay wall placed in liquefiable soils under seismic loading are presented in great details, which are skipped in following chapters.

3.2   Finite Difference Analysis

As the first step, the employed soil constitutive model for simulating the soil liquefaction phenomena is verified, through an elementary testing, by estimating the response of a low to medium dense granular sand specimen in undrained simple cyclic shear testing. In the second step, after the soil constitutive model is verified, the case history simulation, which is used as the unimproved framework, is verified based on two criteria: (1) the simulated caisson wall-soil system deformation pattern is compared to field observations recorded by Inagak et al. (1996); (2) the computed distribution of excess pore water pressure (EPWP) is compared to the experimental results measured from s shaking table test conducted on the identical case history (Iai and Sugano, 2000).

For detailed numerical method for liquefaction analysis, dissipation and redistribution of generated EPWP is considered in the effectiveness stress analysis. The interactive behavior of three components (pore water, soil skeleton and soil particle) are considered simultaneously. The dynamic response of soil skeleton and adjacent structure is obtained by solving the equation of motion, whereas the coupled behaviors between pore water pressure and soil skeleton are solved by using the consolidation and seepage equation. The dynamic response analysis and consolidation analysis are conducted repeatedly in every time increment of the analysis. In addition to these analyses, the generation, dissipation and redistribution of EPWP are also computed simultaneously.

Within the verified framework of this unimproved caisson quay wall, different ground improvement methods as remedial measures can be hypothetically applied to improve it. In this study, the numerical modeling is conducted using FLAC^{3D} (Itasca, 2007) in Figure 7. The FLAC^{3D} technique is an explicit finite difference scheme for the continua and it is suitable for the solution of large deformation problem.
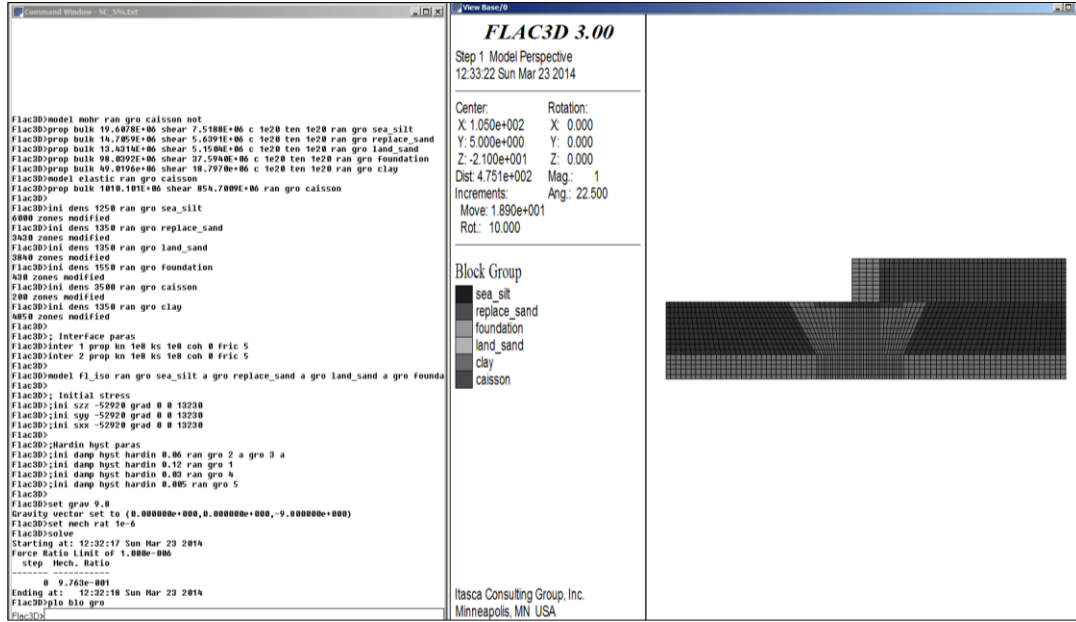
Figure 7. User interface of FLAC^{3D} (Itasca, 2007)

3.3   Soil Constitutive Model for Liquefaction Simulation

According to Yang et al. (2003), as the "common rules" of constitutive models to simulate soil liquefaction, the typical characteristics of liquefiable soil behavior should include the following phenomena: (1) gradual EPWP generation during the cyclic loading process, (2) smaller cycle-by-cycle degradation in cyclic shear stiffness, (3) shear strain accumulation under cyclic loading, (4) phase transformation behaviors from solid to liquid in terms of a sudden shear strain increase, (5) residual strength regain at large strain excursion. However, one single constitutive model may not always reasonably capture all of these coupled failure mechanisms (Yang et al., 2003). Developing one single constitutive model to describe all above coupled

correlations still remains a primary challenge to the geotechnical committee. The previous analyses have indicated that there was a non-linear response of the clay and gravel layers during Kobe earthquake in 1995, however the attention is primarily devoted to the detailed modeling to the liquefiable backfill and foundation soil, which predominately control the seismic behavior of quay wall.

This study utilizes the finite difference formulation of FLAC^{3D} (Itasca, 2007), together with a comprehensive elasto-plastic effective constitutive model, termed as the "post-liquefaction-Finn or PL-Finn" model developed by Chen and Xu (2007) to describe the soil stiffness and strength degradation at large excess pore water pressure generation for effects of nonlinear behavior and liquefaction.

The Finn-model, as one of the "built-in" models in FLAC package (Itasca, 2007), to predict the nonlinear dynamic response while considering dynamic EPWP generation, was developed by incorporating the empirical estimation of volumetric strain into the standard Mohr-Coulomb plasticity model (Martin et al., 1975). The Finn-model can capture the basic mechanisms that lead to liquefaction in sand or granular material. In Finn-model as mathematically presented in Equation 1 to 5, the volume change that leads to dynamic pore pressure build-up in sand is a function of the material-dependent parameter C_1, C_2, C_3 and C_4, which can be determined based on relative density D_r% or SPT blow count SPT $(N_1)_{60}$ of the soil in simulation. The detailed description and the parameters determination procedure of Finn-model, which can be found in Martin et al. (1975), Bryne et al. (1991, 2004) or FLAC^{3D} User's Manual (Itasca, 2007), are not expanded herein. However, the effect of regain in soil strength at large strain induced by compaction is not incorporated in Finn model. The Finn-model is utilized to describe the soil stress-strain response and dynamic EPWP generation at small strain range or

when EPWP ratio is less than 0.6. Following equations 1 to 5 describe the Finn-model mathematically:

$$\Delta\varepsilon_{vd} = C_1(\gamma - C_2\varepsilon_{vd}) + \frac{C_3 \times \varepsilon_{vd}^2}{\gamma + C_4\varepsilon_{vd}}$$ Equation 1

$$\frac{\Delta\varepsilon_{vd}}{\gamma} = C_1\exp(-C_2 \times \frac{\varepsilon_{vd}}{\gamma})$$ Equation 2

$$C_2 = \frac{0.4}{C_1}$$ Equation 3

$$C_1 = 7600 \times (15 \times (N_1)_{60}^{0.5})^{-2.5}$$ Equation 4

$$C_1 = 8.7 \times (N_1)_{60}^{-1.25}$$ Equation 5

C_1 = 0.8, C_2 = 0.79, C_3 = 0.45, and C_4 = 0.73 are material-specific fitting parameters and primarily depended on relative density of the soil; $\Delta\varepsilon_{vd}$ is plastic volumetric strain change; γ is shear strain; $(N_1)_{60}$ the corrected Standard penetration resistance blow count. C_1 mainly controls the amount of volume strain increment and C_2 mainly controls the shape of volumetric strain curve, and both two parameters can be obtained from simple shear tests for particular granular materials (Arablouei et al., 2011).

Finn-model in this study is utilized to describe the soil stress-strain response and dynamic EPWP generation at small strain range or when EPWP ratio "r_u" is less than 0.6, because the compressibility or deformability of granular material increase dramatically once the "r_u" value exceeds 0.6 (Seed and Booker, 1977; DFI, 2013). Therefore, the soil and the stress-strain behavior differs significantly with great excess pore water pressure generation especially when "r_u" value becomes from less than 0.6 to greater than 0.6. Hence, Chen and Xu (2007) proposed the "Post-Liquefaction-Finn" PL-model based on theory of fluid mechanics to capture the stress-strain behavior at large shear strain when the large reduction in effective shear stress occurs or "r_u" value is greater than 0.6. Based on the experimental testing results, the stress-strain

correlation of deformed liquefied soil can be simplified using a power function, as presented in Equation 6 and 7. The experimental PL-model concentrates on the zero effective stress state in the soil liquefaction process, and can be used to capture the large shear strain and stress-regain response when the effective stress of soil is approaching to zero or equal to zero by establishing a correlation between cyclic shear stress and strain increment, which involves a series of material-dependent fitting parameters (k_0, k_1, n_0, n_1) using the following correlations.

$$\tau = k_0(\gamma')^{n_0} \qquad (when\ r_u > 0.6\ at\ large\ shear\ strain) \qquad \text{Equation 6}$$

$$\log\left(\frac{\tau}{\gamma'}\right) = k_1(1 - r_u)^{n_1} \quad (when\ r_u < 0.6) \qquad \text{Equation 7}$$

τ and γ' are cyclic shear stress and shear strain rate and "r_u" is the EPWP ratio. These parameters have been verified and calibrated for the low to medium dense granular soils based on the shaking table test and hollow torsional shear test results (Chen and Xu, 2007), which can be applied in this study. In brief, There are two steps in the analysis: (1) to view the material of soil as an elastic continua, and set initial stress, calculate the initial stress distribution in the pre-liquefaction state when computed "r_u" value is less than 0.6; (2) to view the liquefied layer soil as liquefied state, and perform liquefied solution for a certain time to get the result of deformation in the liquefied state when computed "r_u" value is greater than 0.6.

To ensure a reasonable prediction on the liquefaction triggering mechanism and the post-liquefaction deformation, the Finn-model and PL-model are used together based on the value of "r_u". In FLAC^{3D}, users can define or revise any of its "built-in" soil constitutive models by following the regulations specified by FLAC^{3D} even though this process is sophisticated for most users. In this case, Finn-model and PL-model are "combined" using C++ for operation in FLAC^{3D} (Itasca, 2007), and complied as a DLL (dynamic link library) that can be loaded during computation. Therefore, for calculation of every time step of each liquefiable soil element, if the

calculated "r_u" value is less than 0.6, then the employed constitutive model for this specific soil element is Finn-model, which is regarded as pre-liquefaction. Otherwise, the employed soil constitutive model switches to PL-model in the next time step calculation for this soil element, or vice versa. A "transfer-function" is established between two constitutive models based on the determination of "r_u" value for estimating the stress-strain behavior and generation of EPWP of the potentially liquefiable soil. The "r_u" value is defined as equation

$$r_u = \frac{\Delta_u}{\sigma'_{0m}}$$ Equation 8

where Δ_u is excess pore water pressure and σ'_{0m} is the initial mean effective stress.

To verify the suitability of proposed model to capture the characteristics of soil liquefaction behavior, an element test simulation (an undrained cyclic shear testing) is simulated on a cubic sand specimen. The tested soil specimen is assumed to be low to medium dense granular soils with density corresponding to SPT $(N_1)_{60} = 10$, which can be used to determine the Finn-model parameters (Martin et al., 1975; PHRI, 1998). The dimension of the soil element is a cube with side length of 0.1 m. The initial effective stress is equal to 100 kPa, and the initial horizontal effective confining stress is equal to 100 * 0.5 = 50 kPa, since K = 0.5; A cyclic shear stress of 10 kPa is applied on the top of soil specimen. A total of 6 cycles of shear loading is applied after the soil liquefies.

The simulated results presented in Figure 8 include: 8-(a) effective vertical stress vs. effective shear stress; 8-(b) effective shear stress vs. shear strain; 8-(c) EPWP vs. shear strain; 8-(d) shear stiffness degradation vs. shear strain. As shown in Figure 8-(b), the sudden and significant increase in shear strain indicates the soil element starts to fully liquefy after 4th cycles, and the soil phase changes from solid to liquid due to the large EPWP generation shown in Figure 8-(c). In 5th and 6th cycles, the EPWP reaches 100 kPa, and the vertical effective stress

reduced dramatically shown in Figure 8-(a). The shear stiffness degradation with gradual increase of cyclic shear strain is shown in Figure 8-(d). By comparing the estimated responses (in Figure 8) to the results presented in Bryne et al. (1991, 2004), the Finn-model parameters ($D_r\%$ or SPT $(N_1)_{60}$, C_1, C_2, C_3, and C_4) and PL-model parameters (f and n) are adjusted and calibrated. Above observations in Figure 8 indicate the typical liquefaction failure characteristics can be well captured by simulating a loose granular soils element with the initial vertical effective stress of 100 kPa and cyclic shear stress of 10 kPa. Hence, the capability of the utilized "combined" model for simulating soil liquefaction failure mechanisms is verified.

(a) Effective stress response

(b) Cyclic stress-train response

(c) Excess pore water pressure generation

(d) Degradation of shear modulus
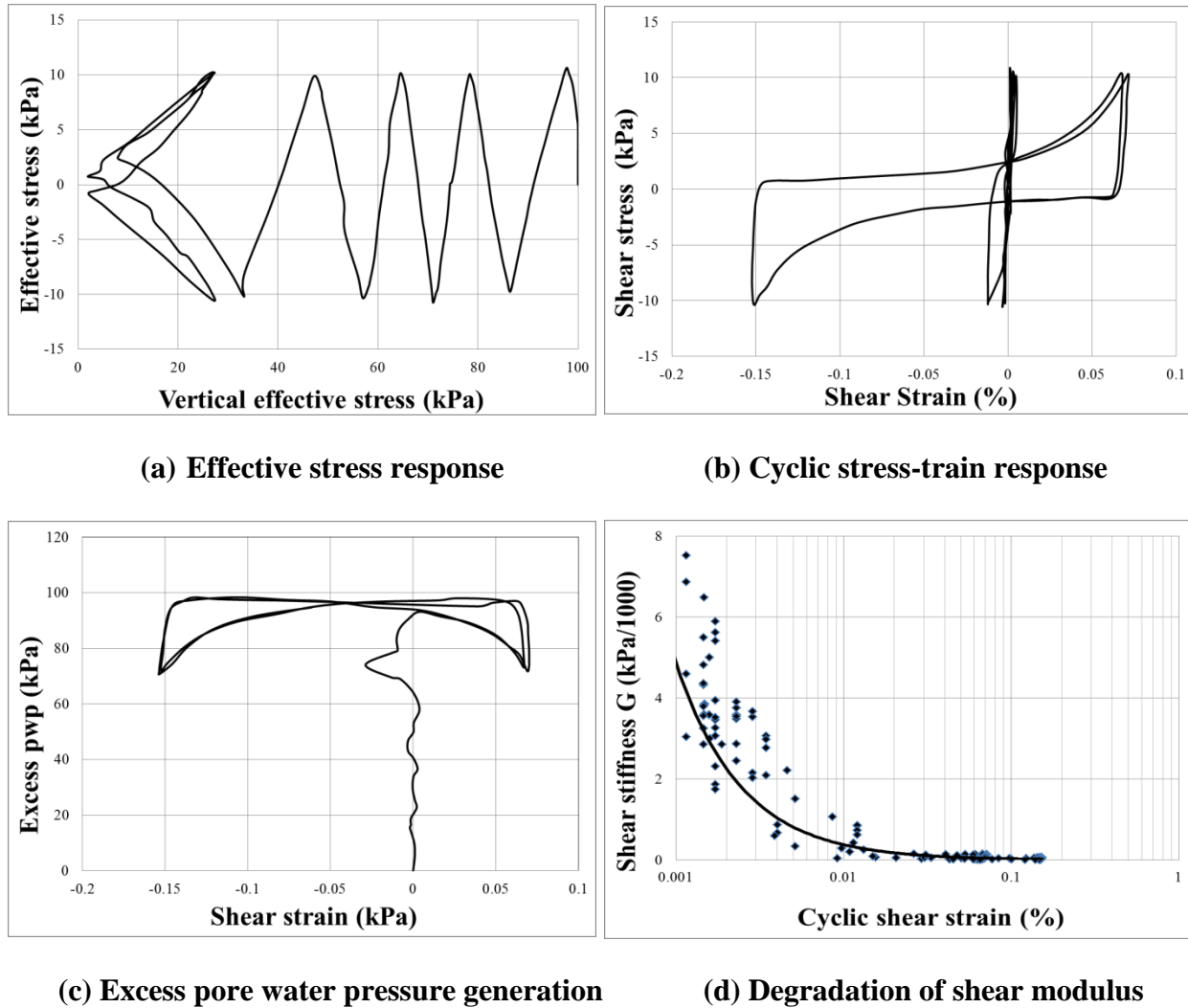
Figure 8. Estimated soil response subjected to undrained cyclic simple shear stress

3.4   Case History Simulation Results Verification

According to PIANC (2001), Mitchell (2008) and Seigel (2013), numerical modeling has been regarded the most important engineering tools for liquefaction mitigation designs. A verified case history simulation is important to provide an unimproved benchmark and framework to shown the initial mechanism and the unimproved performance for comparing to the unimproved performance if ground improvement methods are applied. However, the biggest challenge is the lack of first-hand observations for verification of numerical modeling. The numerical modeling without calibration and validation can provide misleading results. The objective of this chapter is to address this issue for the modeling in this study.

3.4.1   Field observations of the quay wall-soil system post-earthquake

The analyzed case history corresponds to the typical gravity caisson quay wall section in Rokko Island in Kobe earthquake in 1995, in which both foundation soil and backfill soil were liquefiable (Inagak et al., 1996; Finn et al., 1996) during the earthquake. The numerous case histories offer a valuable source of field data against which to check new methods of analysis, and which to discover phenomena that are not well understood at present. The details of this case history can be referred to Dakoulas and Gazetas (2008), and are not repeated herein.

As recorded in Inagak et al. (1996), the displacement seaward at the top of quay wall was approximate 4.5 m (exceeding 5 m in a few locations) during the earthquake. It settled about 1 to 2 m and tiled around 4.5 degree seaward. However, no structural damage or crack was observed on the deformed caisson walls along the coastline. Based on the field observations, the majority of quay walls were damaged due to excessive deformations, rather than the structural damage. Based on the observations, most caisson quay walls were damaged due to excessive deformation, rather than the catastrophic structural damage. Significant deformations were observed within a

zone of extending about 25 to 30 m behind the wall. Very limited deformations were observed in the free-field approximate 80 to 100 m away from the caisson quay wall even though some traces of liquefaction was observed such as sand boiling at this distance. Investigation by divers reported in Inagaki et al. (1996) revealed a substantial heaving of foundation layer at a distance of 2 to 5 m in front of the bottom seaward toe of the caisson. The in-situ observation of the quay wall also suggested that there were generally lack of sand boils in the backfill soils in the vicinity of the caisson walls whereas in the landfills further in land there was extensive evidence of liquefaction.

3.4.2   Numerical modeling and analyses

In the present model, the length, height and width of the model are 170 m, 38 m and 10 m, in X, Z and Y-direction, respectively, based on actual dimensions (Inagak et al., 1996). The caisson wall is 18 m high, and 10 m width and 12 m long. The ocean level is 2 meter below the top of the caisson wall. The model is shown in Figure 9.
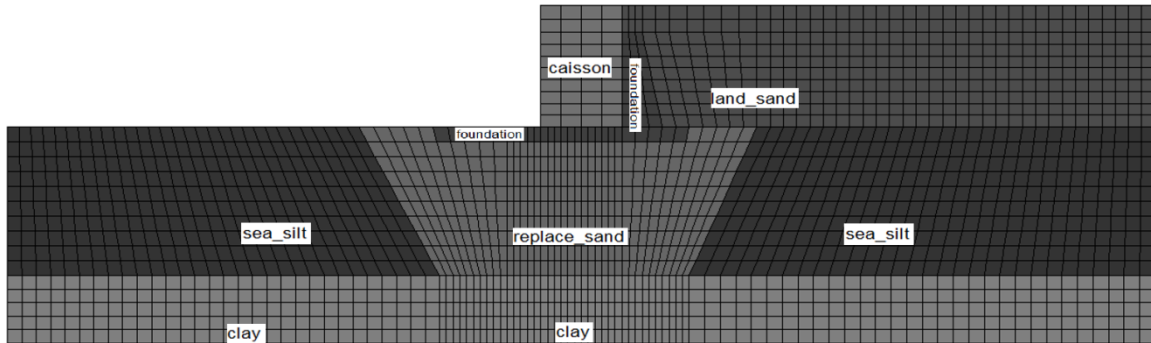
Figure 9. Established model for the simulated case history

For the constitute model, the caisson quay wall is modeled as an elastic body, having an interface that allows slippage and separation at the base and the back of the caisson wall. The potentially liquefiable soils are foundation soil and backfill soil, which are both modeled by using Mohr-Coulomb failure criteria for static for static analysis and the "combined" model for

dynamic analysis. The other non-liquefiable zones (seabed clay and sea silt zone) are modeled by using Mohr-Coulomb failure criteria in both static and dynamic analysis.

The static analysis is first conducted to ensure the model's stability under gravity condition. After the system stability is achieved, the model deformations are "initialized to zero" for dynamic analysis in the next step. For dynamic input the two time histories of vertical and horizontal acceleration, recorded at a depth of 32 m in the Port Island array (Iwasaki and Tai, 1996), whose peak acceleration values reached 0.60 g and 0.20 g, respectively, are shown in Figure 10. The magnitude of this earthquake motion is recorded as 7.2, which can be regarded as the earthquake motion type with probability of exceedance of 10 percent during life-span (PIANC, 2001). These two time histories of accelerations are applied as the seismic input at the bottom nodes of the model. Instead of using the complete 38 seconds of recorded excitation period, the first 20 seconds of intensive excitation is applied in the calculation. To verify the results, a comparison between the calculated quay wall's deformations of using 20 and 38 seconds is conducted. It is found that even though the computation time is much shorter, the calculated quay wall's deformation using 20 seconds is only 5% less than the result calculated by using 38 seconds of excitation record. Therefore, 20 seconds of time histories of accelerations in two directions are applied as the seismic input at the bottom modes of the model.

The geotechnical problems can be idealized by assuming that regions far from the area of interest extend to infinity. Therefore, the boundary condition at the sides of the model was achieved by using the Free-Field Boundary "FFB" condition to minimize wave reflections (Itasca, 2007) and allow an "unconstrained" response. The details on FFB condition can be found in the FLAC^{3D} User's Manual (Itasca, 2007). During the static analysis, the bottom boundary is fixed in both the horizontal and the vertical direction and the lateral boundaries only in the

horizontal direction. In dynamic analysis, when the model is subjected to earthquake motion, lateral boundaries are changed into FFB to eliminate the wave reflections from the truncated boundaries.
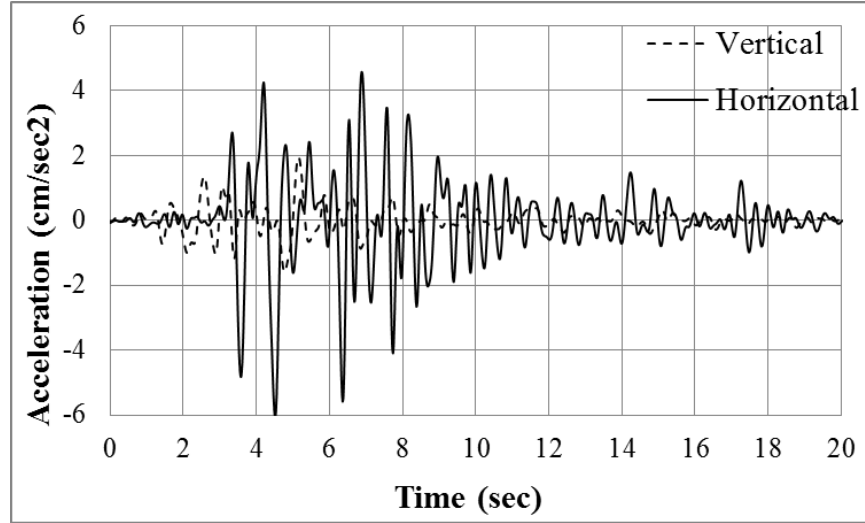
Figure 10. Seismic input: horizontal and vertical time history of acceleration (cm/sec²)

Contact condition between the caisson quay wall and the surrounding soil is such that the wall is connected to the foundation soil both horizontally and vertically. Properties of the interface between the caisson wall and adjacent soil include the normal and shear stiffness, friction angle and cohesion, which can be determined based on the two attached material properties (Itasca, 2007) in Table 9. A sensitivity study was performed to determine the influence of interface parameters on the overall wall-soil system performance, and the results indicated that the influence by changing the values of interface parameters is insignificant. The friction between the quay wall and backfill soil is not modeled in this research.

Table 9. Interface parameters

Interface mesh length (m)	Normal stiffness (Pa/m)	Shear stiffness (Pa/m)	Cohesion (kPa)	Friction angle (Deg)
1.5	1.00E8	1.00E8	0	5

3.4.3   Material properties

Referring to Inagak et al. (1996), Finn et al. (1996) and Dakoulas and Gazetas (2008), the backfill soil is 16 m thick of loose hydraulic sand fill over dense clay. Loose granular material used for backfill soil ground was also used as the foundation soil under the quay wall. The ground water table is 3 m below the backfill ground surface, and the reported SPT resistance for the backfill soil and foundation soil is 10 to 15 on Rooko Island. Accordingly, the estimated relative density and SPT $(N_1)_{60}$ for both foundation soil and backfill soil are close, which are 35% to 40% and 15, respectively, based on the in-situ measurements reported in Inagak et al. (1996), Finn et al. (1996), and used in Alyami et al. (2007 and 2009). The friction angle for the foundation and backfill soil is 37 degree, as used by Dakoulas and Gazetas (2008). In addition, to account for the degradation effect of the strength properties of liquefiable soil under cyclic loading, the friction angle of backfill and foundation soil approximately equals to 10 and 11 degrees, respectively, based on the measurements in Inagaki et al. (1996).

As described in Inagak et al. (1996), both seabed clay and sea silt zone are regarded non-liquefiable, dense and relative stiff. However, no field measurements are available on the properties of clay and sea silt in this case history. The relative density $D_r(\%)$ of both clay and sea silt was assumed to be 80 to 85 percent by Alam et al. (2005). By following previous studies such as Dakoulas and Gazetas (2008), Mohr-Coulomb model is used as constitutive model for the sea silt and clay in both static and dynamic analysis. Based on the estimated properties of clay and silt, it is found that the influences of clay and sea silt under seismic loading on the seismic deformation of quay wall-liquefiable soils are relatively minor compared with the liquefiable foundation and backfill soil. All zones except for caisson wall are assumed to be isotropic, and the permeability values are empirically estimated based on their relative density

$D_r(\%)$ (Look, 2007). The other properties such as density, permeability, bulk and shear modulus, porosity, cohesion, Poisson's ratio can be estimated based on SPT $(N_1)_{60}$ by using the empirical correlations as provided by Look (2007) or directly from the published data (Taiyab et al., 2012; Alyami et al., 2009; Dakoulas and Gazetas, 2008; Alam et al., 2005). As recommended by Look (2007), the geological material damping commonly falls in the range of 2 to 5 percent of the critical damping ratio. For many non-linear dynamic analyses that involve large strain, only a minimal percentage of damping ratio (e.q., 5%) may be required. Therefore, the local damping of 0.157 is used for all soil zones (Itasca, 2007) based on calibration of the case history presented as below. A summary of the soil parameters used in this study is presented in Table 9.

Table 10. Material properties and model parameters utilized in this study

Static Analysis						
Material	Model	Density (kg/m3)	Elastic Modulus (Mpa)	Poisson's ratio	Cohesion (Kpa)	Friction angle (Deg)
Seabed Clay	MC	1550	20	0.33	20	20
Sea silt	MC	1550	20	0.33	0	20
Foundation soil	MC	1350	15	0.33	0	30
Backfill soil	MC	1350	13.7	0.33	0	30
Foundation layer	MC	1550	100	0.33	0	40
Caisson	Elastic	2500	1300	0.17	-	-
Dynamic Analysis						
Material	Model	Permeability (cm/s)	Porosity	Damping ratio	Finn-model Parameters	PL-model parameters
Clay	FL-isotropic	1.0e-6	0.45	0.05	-	-
Sea silt	FL-isotropic	1.0e-5	0.45	0.05	-	-
Foundation soil	FL-isotropic	1.0e-3	0.45	0.05	$D_r = 40\%$; $C_1 = 0.751$; $C_2 = 0.533$; $C_3 = 0$	$k_0 = 3105.4$ $n_0 = 0.3225$
Backfill soil	FL-isotropic	1.0e-3	0.45	0.05	$D_r = 35\%$; $C_1 = 0.432$; $C_2 = 0.164$; $C_3 = 0$	$k_1 = 5503.1$ $n_1 = 0.1739$
Foundation layer	FL-isotropic	1.0e-1	0.45	0.05	-	-
Caisson	Fl-null	-	-	-	-	-

3.4.4   Computed caisson quay wall – soil deformations

The computed caisson wall–soil deformations with contours of deformation labeled are shown in Figure 11. Figures 11-(a) and 11-(b) show the calculated seaward and vertical displacement at the seaward top corner of the caisson wall is approximately 4.4 m and 2.5 m, respectively. The calculated residual seaward rotation is about 4.3 degree. Based on the field measurements on the deformation of the quay wall post-earthquake in this case history, the seaward lateral deformation and vertical deformation at the top seaward corner of the quay wall was 4.5 m and 2.2 m, respectively, as reported by Ishihara (1997).

The displacement counters show that both surface horizontal and vertical deformation in backfill soil propagate with the increasing distance from the caisson wall. Approaching the left boundary of the model, at approximate 80 meter from the caisson wall in the backfill soil, the calculated seaward and vertical displacement are less than 0.1 m. This is consistent with the observation over a distance of 100 to 200 m from the back of quay walls (Ishihara, 1997). Also, the retained soil immediately behind the caisson wall settled significantly (with the maximum settlement of 2 m). The model quay wall tilted into the foundation soil and pushed the rubble mound out. The large shear deformation can be observed in foundation soil in front of quay wall starting from toe. This model of deformation is also consistent with that investigated in the field by diving in Iai and Sugano (2000).

Figure 11-(c) show the two time histories of total displacements at the top seaward corner of the caisson wall computed by using the "combined" model and just Finn-model, respectively. As shown, both curves are relative close up to 5 seconds, when the large EPWP build up and the soil constitutive model for calculating the large seismic deformation switches to PL-model. In this study, the computed displacement by using Finn-model is 45% less than the value using the

combined model utilized in this study, which is consistent with the results by Arablouei et al. (2011).
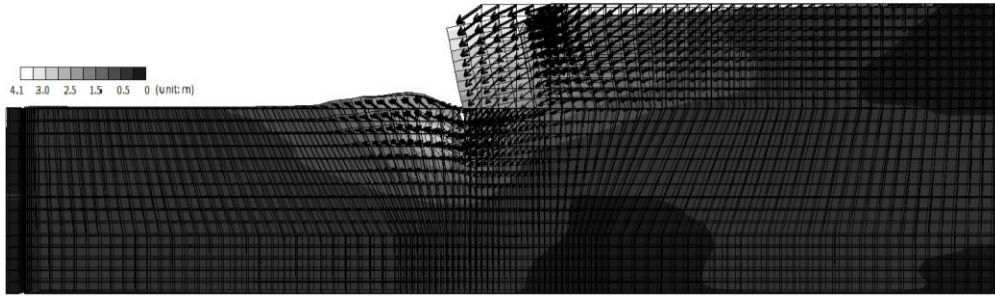
(a) Horizontal deformation contour
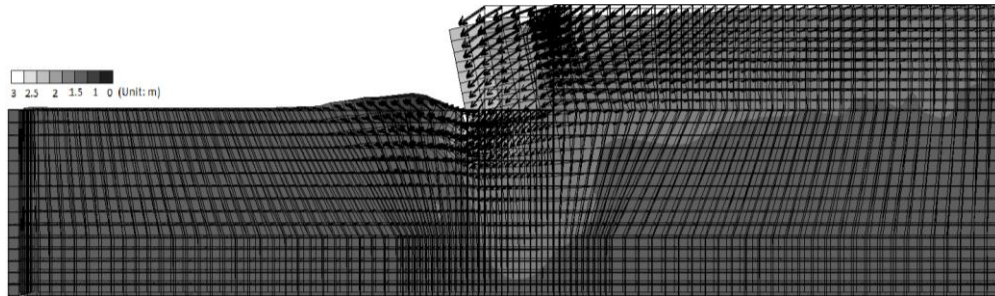
(b) Vertical deformation contour
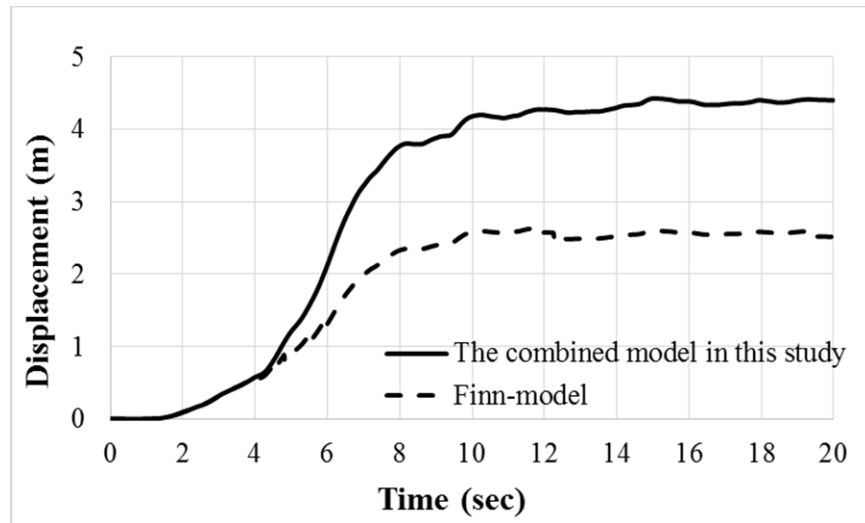
(c) Time history of displacement at the top seaward corner of the quay wall

Figure 11. Horizontal and vertical displacements of the caisson wall-soil system

In conclusion, the computed and observed results in terms of quay wall's seismic deformation match fairly well. In addition to the calibration on deformation, verifications on excess pore water pressure generation within the foundation and backfill soil are also presented below.

3.4.5 Computed excess pore water pressure generations

In addition to the good agreement between computed and measured deformations of the quay wall-soil system, the computed distribution of EPWP generation in backfill and foundation soils also show the consistency with the previous studies, such as the numerical results by Dakoulas and Gazetas (2008) or the shaking table test measurement by Iai and Sugano (2000). As shown in Figure 12 (adopted from Iai and Sugano, 2000), extensive EPWP was generated in both foundation soil and backfill soil, which explained the significant deformations.

The computed distribution of maximum EPWP in the foundation soil and backfill soil were also compared to the results (Figure 12) from a shaking table test on this identical case history, as performed by Iai and Sugano (2000). Points A, B, C, and D (Figure 12) are located in backfill soil with a horizontal distance of 20 to 25 m away from the caisson quay wall. The depth of A, B, C, and D from the backfill land surface is approximately 4 m, 8 m, 13 m and 16 m based on the scaled dimensions. In the foundation soils, points E and F, G and H were located near the front of the seaward bottom corner and immediately behind the inward corner of the caisson wall, respectively. The depth of points E and G, and F and H is the same, which are 4 and 8 m respectively, below the caisson wall bottom. The maximum EPWP at these points by using different soil densities in various cases were measured and plotted.

Accordingly, the locations in the simulated model corresponding to the above points were highlighted, and the EPWP values at these locations were calculated and compared to the

measured results. The maximum EPWP value was back calculated based on the difference between the initial PWP prior to dynamic analysis and the maximum PWP ratio from the computation. The calculated initial PWP value and maximum PWP values at point A to H are shown in Table 11, which are compared to the average measured values from cases 2, 6 and 7 from Iai and Sugano (2000), as presented in Figure 12. The comparisons are shown in Figure 13 and general good agreements are received, except for point G and H, where the calculated max EPWP are approximate 20 kPa less than the measurements. As shown, the backfill soil and the foundation soil in front of the bottom corner of caisson wall suffer more severe liquefaction.

Based on above results, the overall estimated responses in terms of deformations, EPWP distributions are consistent with the observed behavior (Inagak et al., 1996). Therefore, the simulated case history, as the framework for the application of ground improvement methods in next phase, is verified.

Table 11. Computed maximum EPWP at the highlighted locations

ID	Improved zone	Initial PP (kPa)	Max PP (kPa)	Max Ex. PP (kPa)	EPWP ratio
A	Backfill	8.8	29.4	20.6	0.71
B	Backfill	61.3	107	45.7	0.87
C	Backfill	131	262	131	0.79
D	Backfill	173	181	8	0.30
E	Foundation	217	254	37	1.12
F	Foundation	261	329	68	0.76
G	Foundation	195	284	92	0.58
H	Foundation	261	403	142	0.44
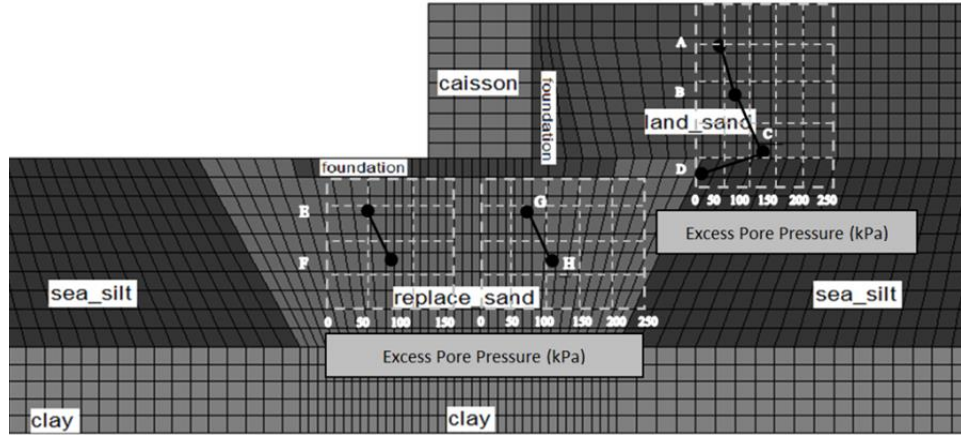
Figure 12. Distribution of maximum EPWP obtained from the shaking table test based on Iai and Sugano (2000).
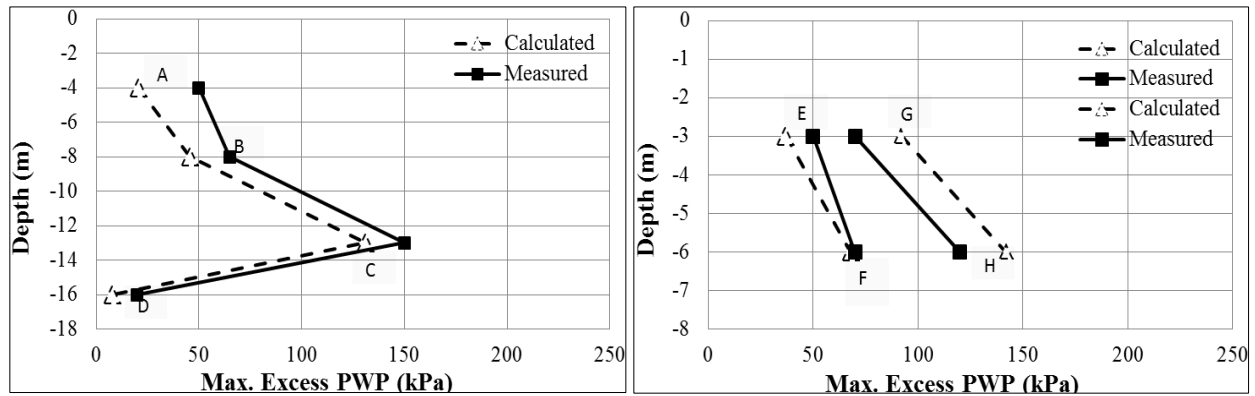
(a) Backfill soil   **(b) Foundation soil**

Figure 13. Computed vs. Measured EPWP distributions at the highlighted locations

3.5   Summary and conclusions of the numerical model calibration results

The verification process, based on field observations and experimentally measured EPWP, shows that the simulation is reliable. Also, the computed deformations of the caisson quay wall-soil system show good agreement with the field observations. The validated case history is used as an unimproved framework for remediation effectiveness evaluation and comparison conducted in Chapters 4, 5 and 6.

CHAPTER 4. APPLICATION OF VIBRO-COMPACTION

4.1   Introduction

Extensive studies on mitigation of liquefaction induced damage to caisson quay wall structure have been conducted, yet questions remain (Alam et al., 2005). Different improving mechanisms have been proposed and studied, and some valuable insights on the improved seismic performances of caisson quay wall have been obtained. The improving mechanisms include densification of foundation and backfill soils (Alyami et al., 2007&2009; Taiyab et al., 2012), installation of a sheet pile in front of the caisson wall (Alam et al., 2005), or installation of a deformable panels behind the caisson wall (Moghadam et al., 2009). However, most of these studies do not provide an easily-executable methodology with sufficient guidelines by specifying the improved zone dimensions, improved seismic performance, and acceptable level of damage, to be followed for practical contraction. Most of the studies have shown their mitigation mechanisms are effective but rarely provided the implementation details for routine practice. Herein the primary objective of this chapter is to (1) numerically evaluate the effectiveness of vibro-compaction as a remedial method to mitigate liquefaction-induced damage of a well-calibrated quay wall-soil system, and (2) to provide an easy-implemented remediation program with the design features using the vibro-compaction method.

By following the philosophy of PBD method (PIANC, 2001), as previously discussed in Section 1.3.1, the vibro-compaction program parameters such as the improved soil zone length in backfill soil behind the quay wall and improved soil zone depth in foundation soil under the quay wall are optimized based on the residual improved performance of the quay wall subjected a specified earthquake loading through a comprehensive parametric study.

4.2   Liquefaction Remediation Using Vibro-Compaction

The vibro-compaction method is one of the most economical remedial countermeasures for liquefaction mitigation purpose (Mitchell, 2008). With the application of vibro-compaction, the liquefaction risk of in-situ soil can be reduced by increasing the soil density and shear rigidity to resist to collapse of soil skeleton and reduce the volumetric contraction under dynamic loading, which can limit the EPWP generation and reduction in effective stress (Chu et al., 2009). In general, the practical effective depth of vibro-compaction is 30 m (Chu et al., 2009), and the maximum relative density can reach up to 80% (Elias et al., 2006), and the improved SPT $(N_1)_{60}$ can reach up to 20 or 25 depend on improved soil characteristics (PIANC, 2001; Elias et al., 2006; Mitchell, 2008). For granular materials, the angle of internal friction can increase 5 to 10 degrees depending on the initial state (Elias et al., 2006).

For the improved scenario, the vibro-compaction program is hypothetically applied to the described port site in this case history (Inagak et al., 1996) prior to the placement of the caisson wall; then the improved performance is investigated and compared to the unimproved scenario described previously. To obtain a better understanding on the influence of using different vibro-compaction programs, a comprehensive parametric study was conducted to evaluate the influence of the design parameters on the improved performance of caisson wall-soil system. The parametric study results provide some initial insights to optimize the remedial plan in terms of the improvement effectiveness and efficiency (PIANC, 2011).

4.2.1   Remedial design features

According to Elias et al. (2006), relative density $(D_r\%)$ is the most important design parameters for the vibro-compaction design. As numerous site-specific parameters may influence the compaction effectiveness, the design of a typical vibro-compaction program is always

established based on experience or trail. In this study, a preliminary design process, as

recommended in Elias et al. (2006), is applied to determine the probe spacing and patterns of the

remedial program (Figure 14). Different from conventional liquefaction mitigation design, which

requires the improved factor of safety against liquefaction is greater than one, the PBD method

(PIANC, 2001) is followed based on the performance of the improved structure. Accordingly,

the typical assumptions of the design features are made and listed as below:

- A commonly used high-powered, probe-type vibrator should be utilized.

- The specified minimum average relative density (Dr %) is assumed to be 65% (a typical

  value for vibro-compacted granular soils), which requires minimal probe distance of

  approximate 2.2 m (Figure 14).

- An equivalent triangular pattern of the probe location, which is the most efficient pattern

  for large improved area, is followed (Elias et al., 2006).

- A QA/QC program using in-situ testing methods (e.g., SPT) is required to ensure a

  minimum average SPT $(N_1)_{60}$ of 20 to achieve the above specified design features.

The other two parameters, improved lateral extent in backfill soil (defined as "L") and

vertical depth in foundation soil (defined as "D"), are evaluated by conducting a comprehensive

parametric study (Table 12). An example of the remedial option in the mesh is shown in Figure

15. The improved thickness in the backfill soil is equal to the full thickness of the backfill soil

profile. The conducted parametric study consists of three categories: (1) improving the

foundation soil only (D ≠ 0 and L = 0); (2) improving the backfill soil only (D = 0 and L ≠ 0); (3)

improving both foundation and backfill soil (D ≠ 0 and L ≠ 0). To limit the number of

computational runs, the incremental magnitudes, ΔL and ΔD, are assumed to be 5 m and 3 m,

respectively. This resolution satisfies the practical limits of using the vibro-compaction method

in defining the improved zone, and provides an adequately accurate range in terms of D and L to optimize the remedial design.

Figure 14. Relative density vs. probe spacing distance for granular soil (Elias et al., 2006)

The other two parameters, improved lateral extent in backfill soil (defined as "L") and vertical depth in foundation soil (defined as "D"), are evaluated by conducting a comprehensive parametric study (in Table 12). An example of the remedial option in the mesh is shown in Figure 13. The improved thickness in the backfill soil is equal to the full thickness of the backfill soil profile. The conducted parametric study consists of three categories: (1) improving the foundation soil only ($D \neq 0$ and $L = 0$); (2) improving the backfill soil only ($D = 0$ and $L \neq 0$); (3) improving both foundation and backfill soil ($D \neq 0$ and $L \neq 0$). To limit the number of computational runs, the incremental magnitudes, ΔL and ΔD, are assumed to be 5 m and 3 m, respectively. This resolution satisfies the practical limits of using the vibro-compaction method in defining the improved zone, and provides an adequately accurate range in terms of D and L to optimize the remedial design.

Table 12. Parametric study metrics for the vibro-compaction method

		Vibro-Compaction											
		Vibro-compacted soil zone configurations											
Remedial Option ID		**"L" in backfill soil (m)**											
		0	5	10	15	20	25	30	40	50	60	70	80
"D" in foundation soil (m)	0	1	2	3	4	5	6	7	8	9	10	11	12
	3	13	14	15	16	17	18	19	20	21	22	23	24
	6	25	26	27	28	29	30	31	32	33	34	35	36
	9	37	38	39	40	41	42	43	44	45	46	47	48
	12	49	50	51	52	53	54	55	56	57	58	59	60
	15	61	62	63	64	65	66	67	68	69	70	71	72
	18	73	74	75	76	77	78	79	80	81	82	83	84
	21	85	86	87	88	89	90	91	92	93	94	95	96
	24	97	98	99	100	101	102	103	104	105	106	107	108

Figure 15. Mesh for remedial option 54

4.2.2 Improved material properties

It is assumed that the specified improvement is satisfied by achieving the minimum average improved relative density $D_r\%$, of 65% in the improved zone. Therefore, the other parameters (Table 13) of the improved zone can be approximately estimated based on Elias et al. (2006) and Look (2007). These parameters are assumed based on the published typical range or empirically correlated based on the SPT $(N_1)_{60}$ of 20 in this study. It is important to note again that the QA/QC process in actual construction should be carefully conducted to ensure the satisfactory achievement of the average of improved density specification. The "combined"

model as described earlier is used for the improved soil zone to investigate the development and migration of EPWP and deformation in the improved soil zone. The parameters for the other zones in this model remain unchanged as used in unimproved scenario.

Table 13. Vibro-compacted zone properties

	$D_r\%$	SPT $(N_1)_{60}$	Density (kg/m^3)	Friction (Deg.)	Young E (Mpa)	Poisson	Permeability (cm/sec)	Damping
Densified Zone	65%	20	1600	33	45	0.33	1.0E-3	0.05

4.3   Simulation Results and Discussions

With the hypothetical application of the vibro-compaction method to improve the backfill and foundation soil prior to the placement of caisson wall, the liquefaction risk of foundation and backfill soil are reduced by different extents depending on the improved zone configurations. The quantitative evaluations of improvement effectiveness by various remedial programs (Table 12) are discussed by comparing the improved caisson wall deformation to that from the unimproved scenario. The deformations of the top outward corner of the caisson quay wall is determined and compared among the various remedial options through the parametric study.

4.3.1   Caisson wall-soil system deformations

The influences of "D" and "L" in various remedial options on lateral deformation and vertical deformation are presented in Figures 16 and 17, respectively. Since the difference among some of the curves is very small and these curves may be too close to distinguish by showing in one figure, the total of 9 curves (D = 0 m to D = 24 m with $_\Delta$D of 3 m) are shown in two figures (a) and (b) for each type of the analyzed deformations. Curve "D = 12 m" is shown in both figures for reference. Overlap of the curves can be found in Figure 16-(b) and 17-(b), and this clearly indicates that the additional lateral deformation reduction with increasing in L or the improved lateral extent in backfill soil is fairly insignificant.

As shown in Figure 16 and 17, all of the curves with different "D" become fairly flat when "L" value becomes equal to exceeds 25 m, which may indicate that when the improved length in backfill exceeds 25 m from the inward edge of the caisson wall, additional improvement may not result in any further reduction of the lateral deformation for this specific case history. The improved lateral deformation at the top seaward corner of the caisson wall is 0.7 to 2 m (50% to 80% of reduction) depends on the improved depth "D" value in the foundation soil. These observations may indicate that densifying the first 20 to 25 m of backfill soil immediately behind the caisson wall may be important in reducing the lateral deformation of the caisson wall. As the improved length extends over this range, the improvement efficiency may decrease in terms of the smaller impact on deformation reduction.

Considering the influence of "D" values on lateral deformation, as shown in Figure 16-(b), when improved depth in foundation soil exceeds 12 m, the difference in improved lateral deformation becomes insignificant. This observation indicates that improving the foundation soil deeper than 12 m may not significantly contribute to the reduction of lateral deformation. However, improving the top 12 m of foundation soil can be effective and recommended as shown in Figure 16-(a). A continuous reduction in lateral deformation can be found among the curves with "D" values increasing from 0 to 12 m. When D is equal to or exceeds 12 m, the lateral deformation remains approximately 0.7 m. The influences of "D" and "L" on tilting angle are also found similarly as described above for lateral deformation and lateral deformation. When D = 12 m and L = 25 m, the permanent tilting angle is around 0.6 degree, and the reduction is up to 90% compared to the unimproved case.
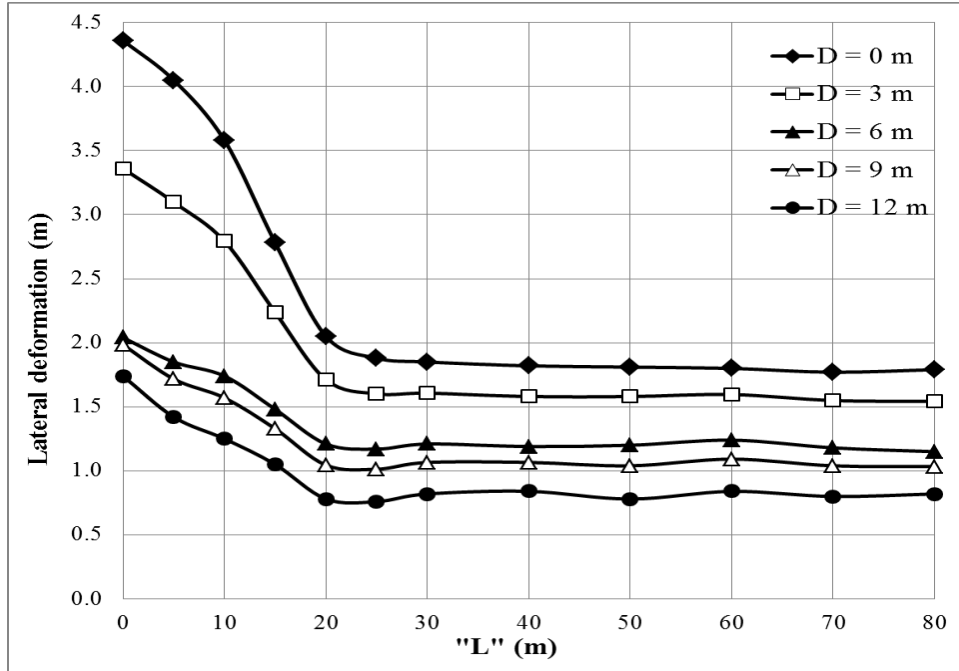
(a) **Lateral deformation achieved by the remedial options with D = 0, 3, 6, 9, 12 m**
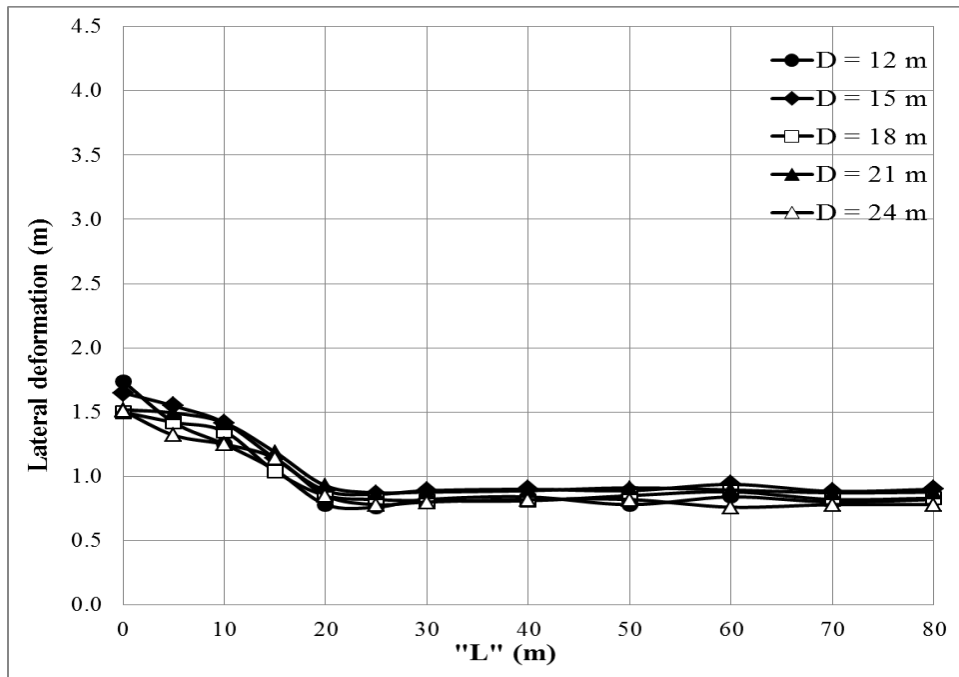
(b) **Lateral deformation achieved by the options with D = 12, 15, 18, 21, 24 m**

Figure 16. Calculated lateral deformation of the top outward corner of caisson wall
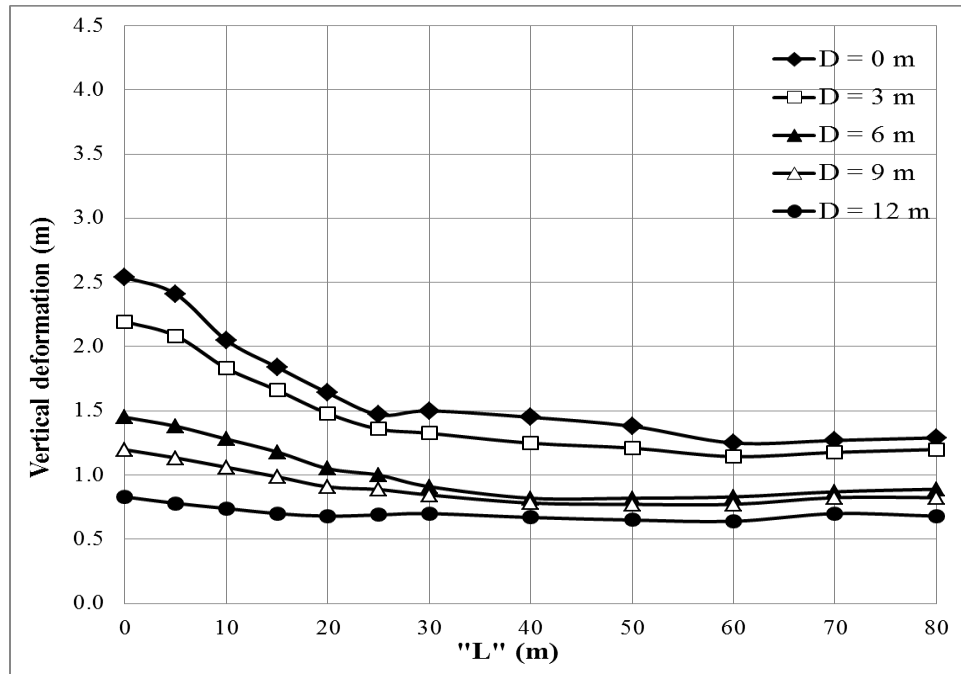
(a) Vertical deformation achieved by the remedial options with D = 0, 3, 6, 9, 12 m
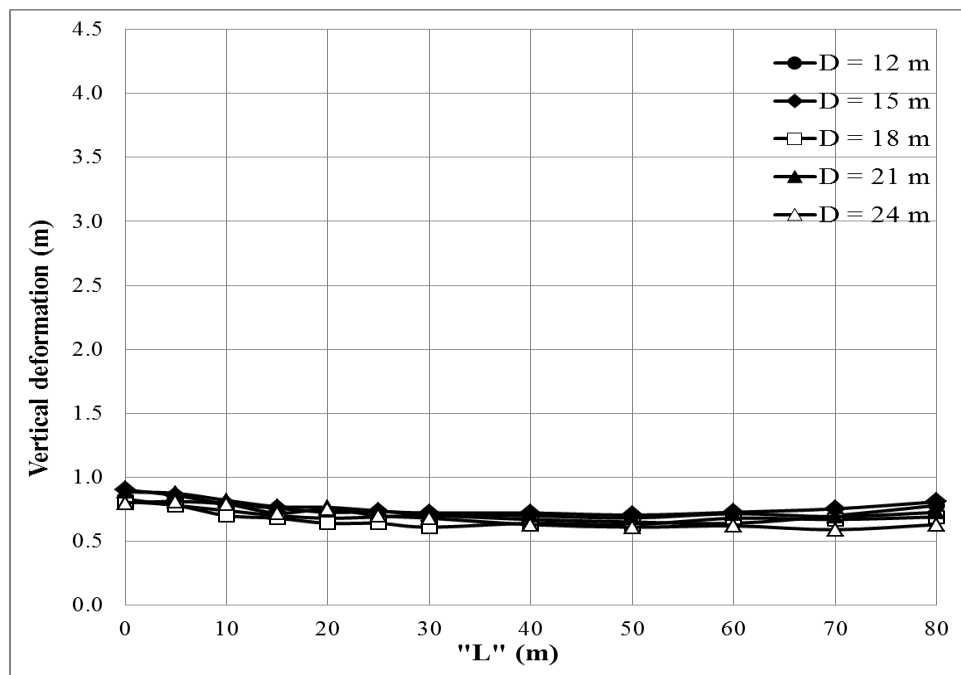
(b) Vertical deformation by the remedial options with D = 12, 15, 18, 21, 24 m

Figure 17. Calculated vertical deformation of the top seaward corner of caisson

Therefore, based on this specific simulated case history, improving the top 12 m of foundation soil and the first 25 m of backfill soil can be effective in reducing the lateral deformation of caisson wall. Additional improvement beyond this range may lead to low improvement efficiency or simply "a waste of dollars". By following this design process, the reduction of lateral deformation can reach 80%, and the residual improved lateral deformation is about 0.7 m.

A similar observation can be made in Figure 17 for vertical deformation as made in Figure 16 for lateral deformation. It appears that the critical value of D = 12 m and L = 25 m is also applicable to reduce the seismic vertical deformation of the caisson wall, and by following this plan, the improved vertical deformation at the top seaward corner of the caisson wall is approximately 0.6 m (75 % reduction).

Therefore, the vibro-compaction program is utilized to density the soil into a denser state of minimal average D_r% of 65%. The probe spacing is about 2.2 m by following an equivalent triangular pattern. By hypothetically vibro-compacting a specific port site prior to the placement of caisson wall described in Inagak et al. (1996), an important insight may be concluded that improving the first 25 m of backfill soil and the top 12 m of foundation soil (option no. 54) is the most effective remedial options in terms of the smallest improved zone, which can lead to a residual lateral deformation of 0.8 m, vertical deformation of 0.7 m, and tilting angle of 0.6 degree. Therefore, the improved performance can satisfy the specified performance of less than 1 m of deformation and 1 degree of tilting angle (PIANC, 2001).

Table 14. Improved deformations summary result by the vibro-compaction method

(a) Horizontal deformation

Remedial Option ID_Horizontal		"L" in backfill soil (m)											
		0	5	10	15	20	25	30	40	50	60	70	80
"D" in foundation soil (m)	0	4.4	4.1	3.6	2.8	2.1	1.9	1.9	1.8	1.8	1.8	1.8	1.8
	3	3.4	3.1	2.8	2.2	1.7	1.6	1.6	1.6	1.6	1.6	1.5	1.5
	6	2.0	1.9	1.7	1.5	1.2	1.2	1.2	1.2	1.2	1.2	1.2	1.2
	9	2.0	1.7	1.6	1.3	1.0	1.0	1.1	1.1	1.0	1.1	1.0	1.0
	12	1.7	1.4	1.3	1.1	0.8	0.8	0.8	0.8	0.8	0.8	0.8	0.8
	15	1.7	1.5	1.4	1.1	0.9	0.9	0.9	0.9	0.9	0.9	0.9	0.9
	18	1.5	1.4	1.4	1.0	0.9	0.8	0.8	0.8	0.9	0.9	0.8	0.8
	21	1.5	1.5	1.4	1.2	0.9	0.9	0.9	0.9	0.9	0.9	0.9	0.9
	24	1.5	1.3	1.3	1.1	0.9	0.8	0.8	0.8	0.8	0.8	0.8	0.8

(b) Vertical deformation

Remedial Option ID_Vertical		"L" in backfill soil (m)											
		0	5	10	15	20	25	30	40	50	60	70	80
"D" in foundation soil (m)	0	2.5	2.4	2.1	1.8	1.6	1.5	1.5	1.5	1.4	1.3	1.3	1.3
	3	2.2	2.1	1.8	1.7	1.5	1.4	1.3	1.3	1.2	1.1	1.2	1.2
	6	1.5	1.4	1.3	1.2	1.1	1.1	0.9	0.8	0.8	0.8	0.9	0.9
	9	1.2	1.1	1.1	1.0	0.9	0.9	0.8	0.8	0.8	0.8	0.8	0.9
	12	0.8	0.8	0.7	0.7	0.7	0.7	0.7	0.7	0.7	0.6	0.7	0.8
	15	0.9	0.9	0.8	0.8	0.7	0.7	0.7	0.7	0.7	0.7	0.8	0.8
	18	0.8	0.8	0.7	0.7	0.6	0.6	0.6	0.6	0.6	0.7	0.7	0.7
	21	0.9	0.9	0.8	0.8	0.8	0.7	0.7	0.7	0.7	0.7	0.7	0.7
	24	0.8	0.8	0.8	0.7	0.8	0.7	0.7	0.6	0.6	0.6	0.6	0.6

A summary of improved vertical deformation and lateral deformation is presented in Table 14. For the further study, utilizing the increased computational capacity, a chart (Figure 16 and 17) or table (Table 14) method of determining the improved seismic performance (horizontal Table 14-(a) and vertical deformation Table 14-(b)) of caisson wall structure can be approximately established by correlating the densification program design features including the improved soil zone dimension parameters "D" and "L", and improved soil properties such as

relative density D_r% or other design features based on a specific utilized improvement method. By establishing such a method, numerous case histories could be analyzed to cover a wide range of soil parameters, earthquake motions, various ground improvement methods and the improved soil characteristics.

4.3.2   Excess pore water pressure generation

A comparison of excess pore water pressure generation at the highlighted locations (Figure 18 and 19) is made between the unimproved and improved scenario. Since the remedial option no. 54 is found to be the most efficient option based on the parametric study in terms of the best efficiency, the improved "r_u" values at the highlighted locations in the soil from no. 54 are compared to the unimproved scenario.

A comparison of "r_u" contours from the unimproved scenario and improved option no. 54 is presented in Figure 18. As seen from the unimproved scenario, both foundation soil and backfill soil are heavily liquefied, especially at the greater depth of backfill soil, and in front and behind the caisson wall in foundation soil. The highest "r_u" value can reach as high as 0.8 to 0.9 in backfill soil and 0.5 to 0.6 in foundation soil. However, the foundation soil vertically underneath the caisson wall receives the lower "r_u" value of about 0.2 to 0.3 due to the heavy vertical loading of caisson height. The "r_u" distribution in backfill soil immediately behind caisson wall within a distance of 15 - 20 m remains low; this is because of the large seaward deformation occurring to this area due to the caisson wall movement, which does not allow the accumulation of EPWP. The similar observation was also observed in field observations (Inagak et al., 1996) and confirmed in the analytical study by Dakoulas and Gazetas (2008). Also, a trend of EPWP migration between foundation soil and backfill soil can be found. However, it is difficult to identify the direction of migration. Regardless of the migration direction, it is

important to cut the migration path between the foundation soil and backfill soil to prevent the migration of high EPWP and distribution and propagation of liquefaction.

By improving both foundation soil and backfill soil in option no. 54, the soil volume of high "r_u" value decreases dramatically in both foundation and backfill soil. The highest "r_u" value is about 0.1 to 0.2 in foundation soil, and still 0.7 to 0.8 in backfill soil, but this area about 40 to 50 m away inward from the caisson wall, which may not impact on the deformation of caisson wall largely. The first 30 to 40 m backfill soil is stable due to the small "r_u" value after improvement, due to the vibro-compaction improvement.

Time histories of "r_u" value at these locations are presented in Figure 19. The improved zone is the first 25 m in backfill soil immediately behind the caisson quay wall and top 12 m in foundation soil under the caisson quay wall. Therefore, all these points are located inside the densified zone. As seen, with densification, most locations suffer much less generation of EPWP comparing to that of unimproved scenario. The peak improved "r_u" values are typically within 0.2 to 0.4 depends on the locations. Also, the residual EPWP exist in the improved zone at point B, E, G, and H, which could lead to small potential deformation in the longer period. The reduction in peak "r_u" value indicates the improvement effectiveness of densification in soil liquefaction by restraining the soil structure.

Above results indicate improving both backfill and foundation soil can establish a stronger "composite" retaining structure, which consists of the caisson quay wall and a certain range of densified foundation and backfill soil.
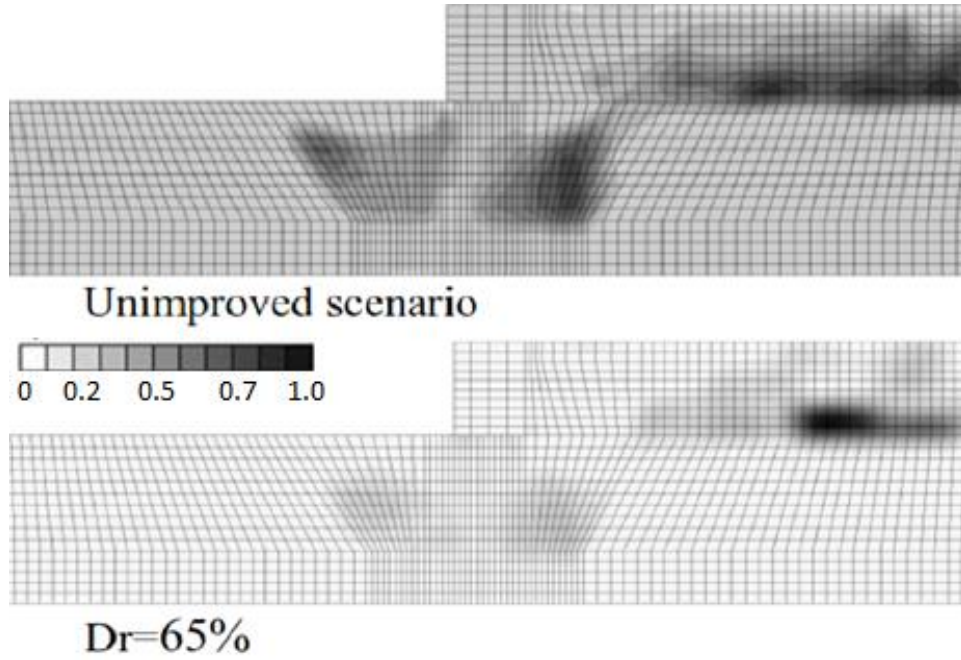
Figure 18. EPWP comparison: Unimproved vs. Improved scenario (remedial case No. 54).
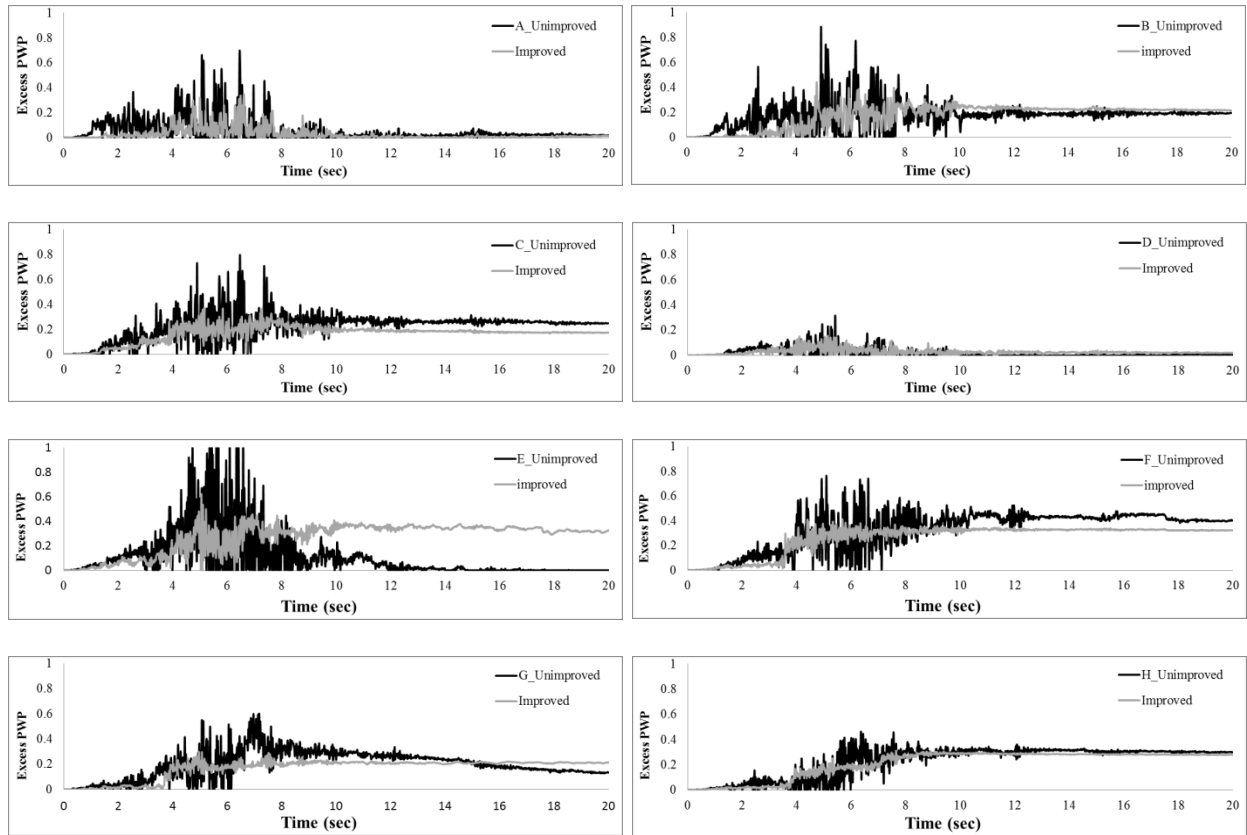
Figure 19. The time histories of "r_u" values at highlighted locations from point A to H

Therefore, soil densification can restrain liquefaction by increasing the soil rigidity and stiffness. However, the size and capacity of this stronger "composite" retaining structure to resist the earthquake loading can only be accessed through a comprehensive parametric study by performing a verified fully coupled numerical analysis. In this specific study, the improved zone dimension in terms of "D" and "L", and the capacity in terms of specified D_r% of the improved soil are verified.

4.4   Conclusions

Through the conducted parametric study, an executable liquefaction remedial vibro-compaction program (a recommended probing distance of 2.2 m) is proposed by optimizing the improved zone dimension in both foundation and backfill soils based on the specified improved soil properties (D_r% = 65%) and acceptable performance grade (PIANC, 2001). Within the framework of the case history, it is recommended to improve the first 25 m of backfill soil and top 12 m of foundation soil to achieve about 0.8 m of deformation and 0.6 degree of tilting angle. This satisfies the specified performance grade "Repairable" (PIANC, 2001) of less than 1 m of deformation and 1 degree of rotation angle, which would only require acceptable restoration effort to fully recover the damage. Observed reductions on EPWP ratios at the highlighted locations indicate the improvement effectiveness. Further study is recommended to establish a more chart or table method for estimating the improved deformation of caisson quay wall structure with liquefiable foundation and backfill soils. By using this method, the estimation of seismic performance of improved deformation of the caisson wall can be accessed by correlating the improved soil zone dimensions, improved soil properties and earthquake motions for certain utilized improvement technologies.

CHAPTER 5. APPLICATION OF DEEP SOIL MIXING METHOD

5.1   Introduction

Wet deep soil mixing method (DMM) is extensively used for seismic stabilization of waterfront developments (Elias et al., 2006; Bruce et al., 2013). Based on principle of the PBD method (PIANC, 2001), the important design DMM parameters such as the improved zone location and geometry are optimized based on the objective of satisfying the specified performance grades while achieving acceptable improvement efficiency. In addition, through numerical testing, Namikawa et al. (2007) indicated that partially damaged DMM mixed elements in unimproved soil can still ensure an acceptable improved performance of the improved structure under strong earthquake events. This also well highlights the importance of the PBD and remedial design optimization in liquefaction mitigation by DMM. Therefore, such a consideration involves a balance between an improved seismic performance, and increased cost associated with a larger volume of grout injection and associated borehole drilling.

A comprehensive parametric study involving over 100 analyses is conducted to demonstrate the influences of various DMM mixed elements locations and geometries on seismic deformation of the improved caisson quay wall. Similar to Chapter 4, the hypothetical application of DMM is conducted within a framework of a well-calibrated case history (Chapter 3) using a three dimensional finite technique FLAC^{3D} (Itasca, 2007). A comparison of the seismic deformation of the caisson wall between unimproved and improved conditions is made, and the improvement effectiveness is highlighted using various evaluation parameters.

This chapter aims to achieve two objectives. First, various remedial options of differing in the locations and dimensions of the DMM mixed element are proposed based on different specified performance grade S (Serviceable) and A (Repairable) as pre-defined in PIANC (2001),

respectively. Second, additional new insights on the optimization of liquefaction remediation design are provided to further advance the current understanding and conventional design process for liquefaction mitigation.

5.2   Liquefaction Remediation Using Deep Soil Mixing Method

The DMM method, an in-situ admixture stabilization technique with cement and/or lime as binder or mixing agent, has been widely used for liquefaction mitigation in practice (Mitchell, 2008; Chu et al., 2009; Nguyen et al., 2012, Rayamajhi et al., 2013; Bruce, et al., 2013). By constructing column shapes of DMM mixed soil, any arbitrary shape of mixed elements can be formed, such as block, wall and lattice types. Lattice- and wall-shape DMM elements are widely used for liquefaction mitigation (Namikawa et al., 2007; Nguyen et al., 2012). The applicability, improvement mechanisms and effectiveness of DMM to remediate against liquefaction have been studied by mainly qualitative studies including Nguyen et al. (2012); Takahashi and Hayano (2009); Namikawa et al. (2007).

The applications of numerical simulation techniques can further advance the design and understanding of the improvement mechanisms and effectiveness of DMM in liquefaction mitigation. However, questions still remain concerning the: (1) development of the uniform, efficient and adequate DMM configurations for liquefaction mitigation; (2) balance between the seismic performance and integrity of the DMM mixed elements and the performance of its improved structures; (3) adoption of principles of the PBD (PIANC, 2001).

The focus herein is to optimize the configuration of the DMM improved zone based on improved deformation and associated damage by demonstrating the influence of various DMM improved zone locations and geometries on residual deformation of caisson wall-soil system. By studying the seismic behaviors of DMM mixed elements in unimproved soil under strong

earthquake loading through numerical analyses in Namikawa et al. (2007), the results indicate that the partially damaged DMM mixed elements can still ensure that the improved performance of structure is still acceptable under the designated earthquake loading. Therefore, the optimum DMM improved zone configuration is demonstrated in terms the two evaluation parameters – improvement effectiveness and improvement efficiency, rather than the seismic performance or damage of the stiffer elements of DMM-mixed elements. In this section, the DMM design features, materials' properties in the parametric study, and other simulation features in terms of application of the DMM are presented.

5.2.1   Properties of DMM mixed material

Some idealizations and simplifications on the properties of DMM mixed materials are incorporated into the numerical analysis without scarifying the accuracy of simulation results. For example, grouted materials produced by grouting are normally modeled as elastic-perfectly plastic materials, and Mohr-Coulomb failure envelop is always used as failure criteria based on Cooke (2000), Nguyen et al. (2012) and Bruce et al. (2013). The most important parameter used for design and construction quality control and assurance for DMM project is the unconfined compressive strength of the DMM mixed material (Elias et al., 2006; Filz, 2012; Bruce et al., 2013). However, the properties of DMM mixed material can be highly variable and depend on site and project-specific characteristics. It is also difficult to predict within a reasonable level of accuracy the strength that will results from adding a particular amount of binder to a given soil based on the in-situ characteristics of the native soil (Bruce et al., 2013). Therefore, the materials' properties applied in this study are primarily estimated to be the typical values in practice based on the published data.

As reported in Navin (2005) and Bruce et al. (2013), the typical range of unconfined compressive strength (q_u) of laboratory-mixed material specimens is from 20 to 4,000 psi (0.1 to 28 MPa) for the wet DMM with a high variability depending on the properties of mixed soil, utilized binder characteristics and construction variables, operational parameters, curing time and loading conditions. In the U.S, a common expectation is that the strength of field-mixed materials can consistently achieve at least 50 to 60 percent of the strength of laboratory-mixed specimens (Bruce et al., 2013). Also, the q_u value typically equals to two times of the undrained shear strength (s_u) for DMM improved material (Adams, 2011; Elias et al., 2006; Bruce et al., 2013). The ratio between the elastic modulus (E_{50}) to q_u is normally between 75 and 1000 for wet DMM mixed material (Namikawa et al., 2007). Reported Poisson ratio ranges from 0.2 to 0.5 for small strain behavior of wet DMM mixed soils (Elias et al., 2006; Terashi, 2003; Porbaha et al., 2005). No significant difference in density was found between the unimproved soil and the improved soil (Broms, 2003). Since the construction quality of DMM project can be highly variable, a QA/QC program must be conducted to ensure the mixed material satisfy the specifications. The above general rules based on the published data and relationships for soil-binder mixtures (e.g., Filz, 2009; Adams, 2011; Bruce et al., 2013) provide the basis for assuming the properties of wet-DMM mixed material used in this study, as below:

- 56-day q_u (psi) = 300 (Elias et al., 2006; Bruce et al., 2013)

- Elastic modulus (E_{50}) (psi) = 300 * q_u = 90,000 (Adams, 2011; Bruce et al.,2013)

- Improved density (kg/m^3) = same as unimproved soil density (Terashi, 2003)

- Poisson ratio = 0.3 (Bruce et al., 2013)

- Cohesion (kPa) = 1500 (Namikawa et al., 2007)

- Tensile strength (psi) = 15% of q_u = 45 (Elias et al., 2006)

- Friction angle (degree) = 30 (Namikawa et al., 2007)

- Permeability (cm/sec) = 1.0E-7 (Namikawa et al., 2007; Elias et al., 2006)

5.2.2 DMM design and representative improved zone characteristics

There are various types of DMM mixed elements, such as wall-shape, lattice-shape and block. However, few studies have quantitatively evaluated their effectiveness, optimization of remedial design and improved performance based on a well pre-defined performance grade for caisson quay walls by following PBD (PIANC, 2001). Although the shape of the DMM mixed elements may be different, their improvement mechanisms are similar, which is to reinforce, stabilize or enclose the native loose soil to increase its liquefaction resistance. The optimization process and insights on the locations and geometries of DMM improved zone are also similar. Therefore, within this study, the wall-shape DMM mixed elements are utilized in the examined remedial case (Figure 20). The optimization process and insights in terms of the influence of different configurations of DMM improved zone on the deformation of caisson quay wall are also valuable to other cases utilizing different shape of DMM elements. These DMM-mixed walls, which are oriented perpendicular to the caisson quay wall alignment and parallel to the direction of lateral spreading of backfill soil, can be constructed using the deep mixing method by overlapping wet-mixed, triple-axis columns (Bruce et al., 2013). As indicated by PHRI (1997), the wall type, with walls parallel to the excitation direction have a larger resistance against horizontal forces, comparing to the case that the wall perpendicular to the excitation direction.
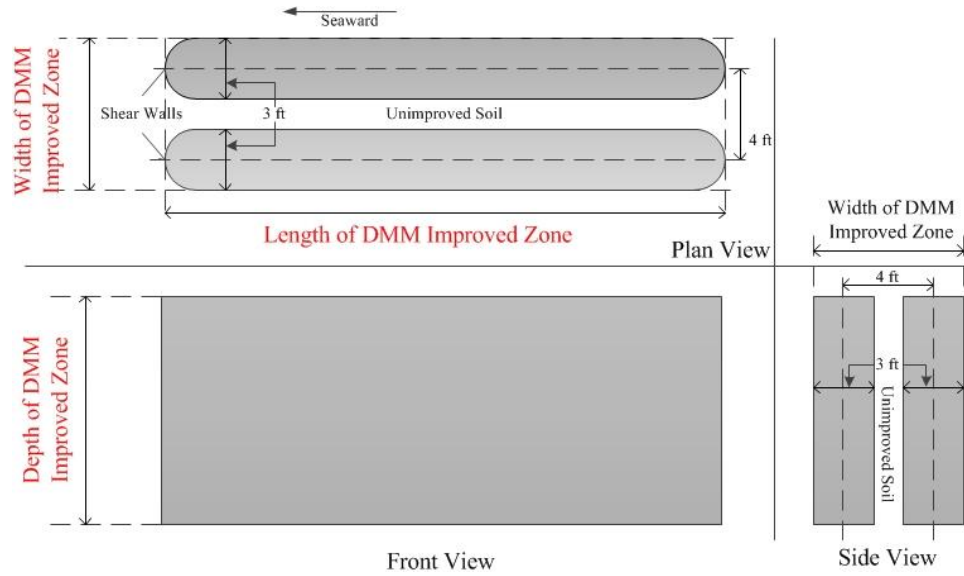
Figure 20. Three dimensional view of the DMM mixed wall and DMM improved zone

According to Bruce et al. (2013), there are differences of opinion regarding the most appropriate strength envelope for DMM mixed soils for use in numerical analysis, and it is acceptable to use an effective friction angle of 30 to 35 and cohesion intercept of c = 1/2 unconfined compressive strength for DMM mixed materials. Nguyen et al. (2012) used a linear elastic model to describe the DMM mixed lattice element in unimproved liquefiable soil. As used by Adams (2012), the representative DMM improved zone is modeled using elasto-perfectly plastic Mohr-coulomb model with additional properties as described above.

For the dimensions of the DMM mixed walls, Figure 20 shows a three-dimensional view of the DMM improved zone consisting of the DMM mixed walls and the surrounding unimproved soil between the walls. The center to center spacing between the DMM mixed walls is 4 ft, and the diameter of the overlapped DMM mixed column or regarded as the wall thickness is 3 ft. The representative properties of DMM improved zone are calculated based on the properties and dimensions of DMM mixed wall and unimproved soils enclosed.

The determination method to estimate the properties of DMM improved zone is called homogenization method proposed by Adams (2011). The DMM improved zone can be characterized as a zone of DMM improved ground with representative material properties (stiffness and shear strength) that considers the relative contribution of the DMM mixed walls and the enclosed unimproved soil. The shearing through the DMM improved zone along any other orientations can be represented by the representative shear strength of DMM improved zone. The DMM improved zone is reasonably assumed to be non-liquefiable and impermeable (Nguyen et al., 2012; Namikawa et al., 2007). For simplification, the influence of vertical joints in the DMM mixed walls can be neglected. The overlapped column diameter is 3 ft and the center to center spacing is 4 ft. the area replacement ratio, as defined as the ratio of area of treated material to area of DMM improved zone, is 20%. The layout details of the DMM mixed element and DMM improved zone are shown in Figure. Therefore, the replacement ratio, effective width of the shear wall, representative stiffness and representative shear strength are determined based on equations recommended by Navin (2005), Adams (2011), and Filz (2009) below:

- $E_{dmz} = E_{wall}a_s + E_{soil}(1 + a_s) = (3E + 4) * 0.2 + 15 * 145 * (1 + 0.2) = 86 \, Mpa$

- $\alpha = acrcos(1 - \frac{e}{d}) = 1.04$

- $a_s = \frac{\pi d(1 - a_e)}{4 \times S \times cos(\alpha)} = \frac{\pi * 3 * (1 - 0.65)}{4 \times 4 \times cos(0.65)} = 0.20$ or 20%

- $a_e = \frac{2\alpha - sin(2\alpha)}{\pi} = \frac{2 * 1.04 - sin(2 * 1.04)}{\pi} = 0.65$

- E_{dmz} = a representative stiffness of the DMM improved zone

- E_{dm} = the stiffness of DMM material in the walls

- E_{soil} = stiffness of the unimproved soil between shear walls

- a_s = area replacement ratio

- d = column diameter = *3 ft* ≈ DMM mixed wall thickness

- e = overlap distance between columns = *0.5*d = 1.5 ft*

- S = center-to-center spacing of shear walls = *4 ft*

- a_e = overlap area ratio (ratio of area of overlap to area of individual column)

The parametric study is divided into three scenarios, which are: (1) placing a single DMM improved zone in foundation soil; (2) placing a single DMM improved zone in backfill soil; (3) placing DMM improved zones in both foundation and backfill soil based on the results of scenarios 1 and 2. The process is first to determine the efficient DMM improved zones for improving foundation soil in scenario 1, and then repeat the same process for backfill soil in scenario 2. Finally, the efficient DMM improved zones for foundation and backfill soils are applied together in scenario 3, and their combinations are evaluated and compared in terms of the improvement effectiveness and efficiency. The optimum configurations of DMM improved zone for the entire quay wall-soil system are recommended based on two criteria - (1) satisfaction of the specified performance grade, and (2) good improvement efficiency.

5.3   Improved Seismic Performance Results and Discussions

Two results interpretation parameters, improvement effectiveness and efficiency, are used to evaluate and compare the improved results from various remedial cases. Improvement effectiveness is defined as the deformation reduction magnitude (unit: m) between the unimproved and improved deformation of the caisson wall.

Since the cost of DMM largely depends on the volume of grout injection or the volume of native soil requiring improvement, it is important to define a parameter to evaluate the efficiency. The definition of improvement efficiency utilized herein follows the principle of the "improved ratio" defined in Bradley et al. (2013) and the "efficiency" defined in Adams (2011). In Adams

(2011), the efficiency of DMM improved zone is calculated "by dividing the increase in factor of safety by the volume of DMM improved ground." Hence, in this study, the improvement efficiency is defined as the ratio of deformation reduction percentage to the volume of DMM improved zone. The volume of DMM improved zone is defined as the product of width, length and depth of DMM improved zone (Figure 20).

Specifically, the width of DMM improved zone in all examined cases remains at 10 m equal to the width of constructed quay wall-soil system model. Using these parameters, the DMM improved zone configuration in terms of location and geometry can be optimized, while the dimensions of DMM mixed walls remain the same through the study. The improved response of the simulated case history with various DMM improved zones differing in locations and geometries also can be established for routine practice.

5.3.1   Scenario 1 – a single DMM improved zone in foundation soil

The improved results for the three categories in scenario 1 are shown in Figure 21 and 22. Especially in Figure 21, it is important to note that only the front view of the DMM improved zoon together with the quay wall-soil system is shown. The front view of DMM improved zone is also shown in Figure 20. In Figure 21, all DMM improved zones start at Point O highlighted, which is the point of around 0.5 m vertically under the seaward bottom corner of the quay wall.

For each specific applied DMM improved zone, the improved deformation at the top seaward corner of the quay wall and improvement efficiency are plotted in the parenthesis at the lower left corner (for category 1 and 3 in Figure 21-(a) and 21-(c), respectively) and the lower right corner (for category 2 in Figure 21-(b)) of each specific DMM improved zone applied in its corresponding case.

Liquefaction extent of the foundation soil is critical to the residual deformation of the supported quay wall. Particularly, results from shaking table test (Iai and Sugano, 2000) indicated that deformation of quay wall induced by foundation soil is more significant than that of backfill soil. However, the influences of improved zone extent and improvement degree on the performance of quay wall are rarely quantified in previous studies. Accordingly, the improvement of foundation soil is divided into three categories: (1) improving the soil before the seaward bottom corner of the quay wall; (2) improving the soil behind the seaward bottom corner of the quay wall; (3) placing a continuous DMM improved zone centered underneath the seaward bottom corner the caisson wall. To get a reasonable resolution with the computational capacity limit, for category 1 and 2, the length increment of the DMM improved zone is 5 m, and the depth increment of the DMM improved zone is 7 m or 1/3 of the total thickness of foundation soil of 21 m (Figures 21-(a) and 21-(b)). For category 3 in Figure 21-(c), the length increment is 5 m on both sides (in front of and behind the seaward bottom corner of the quay wall) is used with the depth increment in vertical direction is still remaining 7 m. The specified edge of the DMM improved zones in different scenarios do not always allow for the edge of DMM improved zone to be located exactly at the edge of the mesh. The influence is relatively minor on the final results.
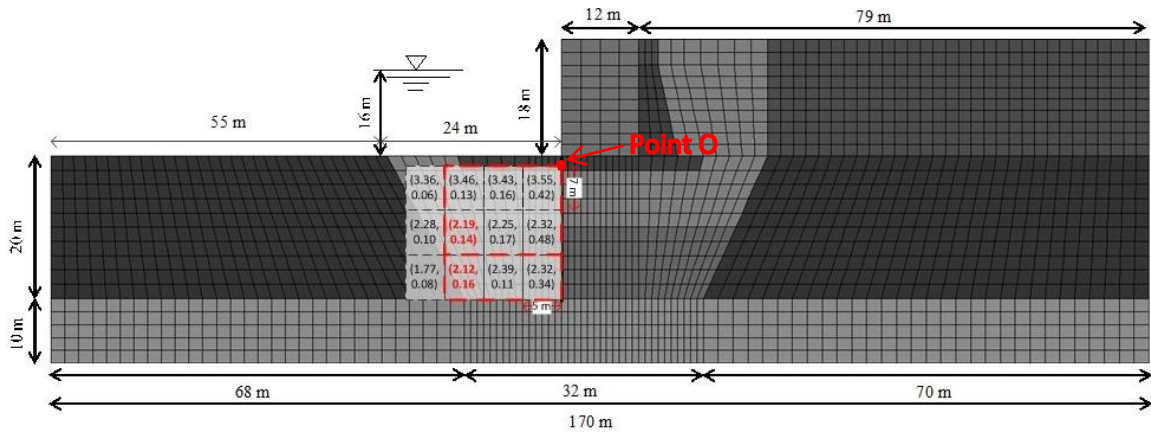
(a) Category 1 of Scenario 1
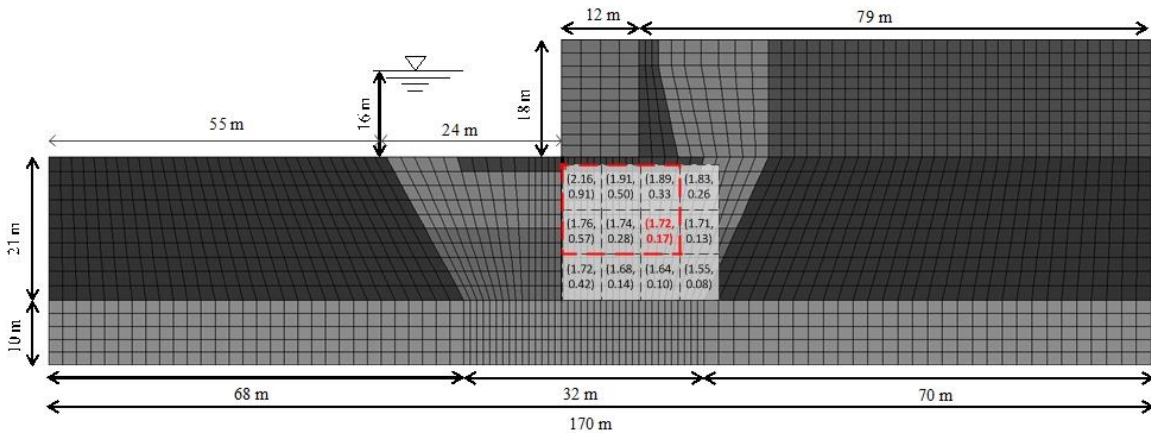
(b) Category 2 of Scenario 1
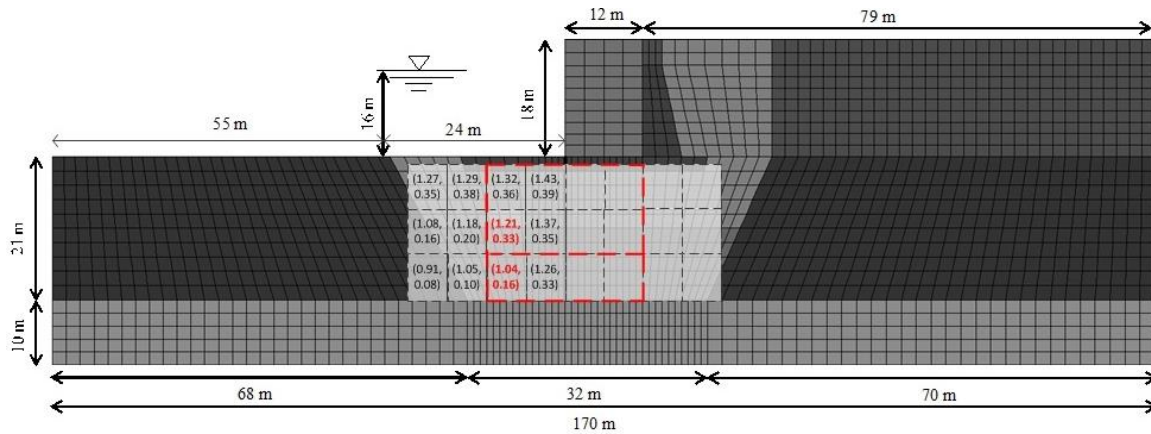
(c) Category 3 of Scenario 1

**Figure 21. Computed deformation and efficiency for multiple DMM improved dimensions in foundation soil**

Also, to optimize the dimension of DMM improved zone, the improved deformations (horizontal, vertical and tilting angle) of quay wall with the corresponding DMM improved zone geometries (depth and length) are plotted for all three categories in scenario 1. As shown in Figure 22, for all three categories, the improved seismic deformation and efficiency both decrease with the increasing volume of DMM improved zone, which indicates that balance between the improved deformation and improvement efficiency that should be analyzed depending on the specified performance grade and cost. Also, based on the deformation reductions in Figures 22-(b) and 22-(c), improving foundation soil can be more effective in reducing the vertical deformation than reducing the seaward deformation of the caisson quay wall.

For all three failure modes, a continuous DMM improved zone centered under the seaward bottom corner of the quay wall can provide the maximum deformation reduction. As shown in Figure 22, at the same DMM improved zone length, placing a DMM improved zone before (category 1) or behind the bottom seaward corner (category 2) of the quay wall shows the larger improved deformation than placing it centered under the quay wall (category 3). This indicates the better improvement effectiveness. When the length of DMM improved zone distance exceeds 20 m in Figure 22-(c), additional deformation reduction becomes insignificant. Also, the improved deformation of the quay wall decreases with DMM improved zone depth, but the improvement efficiency decreases with the depth of DMM improved zone for each scenario.
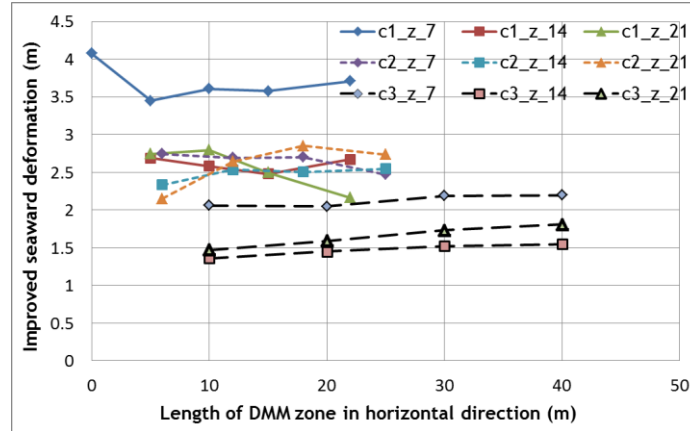
(a) Influence of DMM improved zone length on lateral displacement of the quay wall
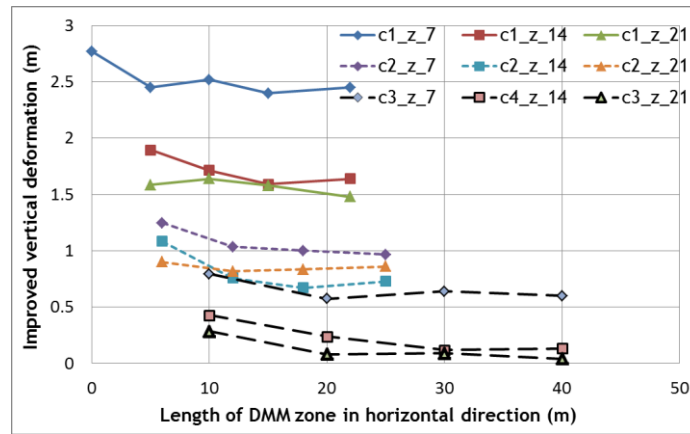
(b) Influence of DMM zone length on vertical displacement of the quay wall
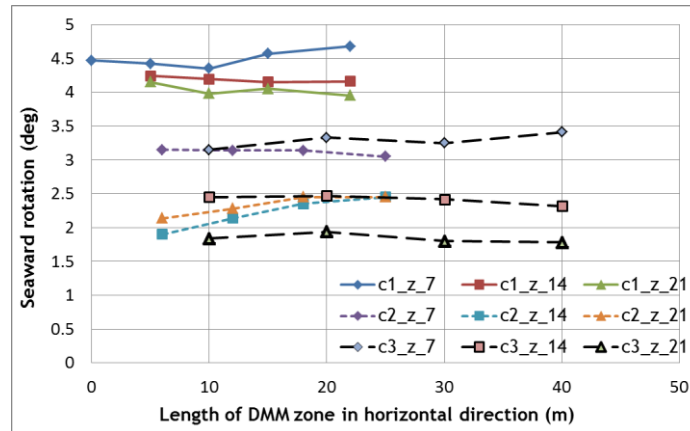
(c) Influence of DMM zone length of tilting angle of the quay wall

Figure 22. Computed deformations versus with multiple DMM improved zone length in foundation soil (e.g., c1_z_7: the result from category 1 with improved zone depth = 7 m)

Accordingly, the possible efficient DMM improved zone layouts for each category are highlighted on Figure 21 in red. Among these highlighted remedial cases, the geometries of DMM improved zone with length of 20 m and depth of 14 m to 21 m (Figure 21-(c)) in category 3 shows the maximum deformation reduction and good efficiency. Placing a continuous DMM improved zone in foundation soil centered under the quay wall can reduce all three failure modes (Figure 21-(c)). Therefore, these two DMM improved zone geometries are further analyzed in scenario 3.

5.3.2   Scenario 2 – a single DMM improved zone in backfill soil

To investigate the influence of backfill improvement on the seismic deformation of the quay wall, a single DMM improved zone with various lengths is evaluated. With a minimal clearance distance of 3 m behind the quay wall, the analyzed DMM improved zone extends inward in the backfill soil with an increment of 5 m in horizontal direction and 6 m (one third of the backfill thickness) in vertical direction. Three meter of clearance distance is to prevent excess passive pressure applied on the quay wall during the construction (Namikawa et al., 2007).

In Figure 23, the improved deformation and efficiency results (following the same format as in Figure 21) is plotted at the lower right corner of each corresponding DMM improved zone. The improved seaward and vertical deformation and tilting angle at the top seaward corner of the quay wall are shown in Figure 24.

As shown in Figure 23, similar to the results from scenario 1, the improved seismic deformation and improvement efficiency also decrease with the increase of DMM improved zone length. Figure 24 indicates that when the length exceeds 20 to 25 m, the improvement efficiency becomes consistently low (less than 0.1) and the seismic improved deformation remains unchanged with the additional length increment of the DMM improved zone.

Comparing the general curve trend shown in Figure 24-(a), 24-(b) and 24-(c), it can be seen that improving the backfill soil can be more effective in reducing the seaward displacement than in reducing the vertical deformation and tilting angle of the quay wall. This observation matches well with the results obtained by Iai and Sugan (2000) that reducing the EPWP in foundation soil is more beneficial than in backfill soil in terms of the deformation reduction of the quay wall. In Figure 24-(a), a sudden reduction in improved lateral deformation occurs when the DMM improved zone in about 20 m, likely due to the heavy liquefaction occurred within this area that is at the backfill 20 to 25 m away from caisson wall (Dakoulas et al., 2008). In Figures 24-(b) and 24-(c) also show the similar trend for the reduction of vertical settlement and tilting computed at the top seaward corner of the quay wall. Therefore, the efficient DMM improved zones (highlighted in red) for backfill soil improvement may be determined as highlighted in Figure 23.
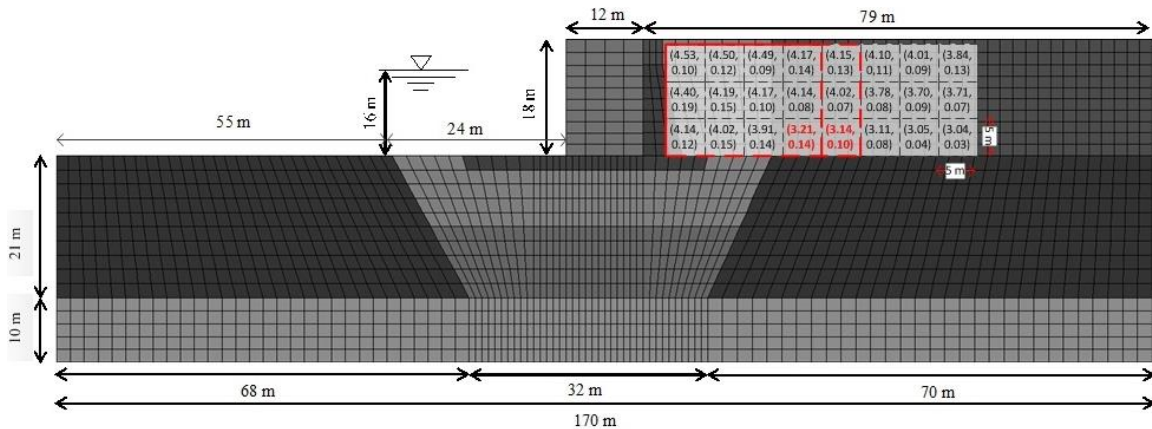
Figure 23. Computed deformation and efficiency for multiple length and depths of DMM improved zone dimensions
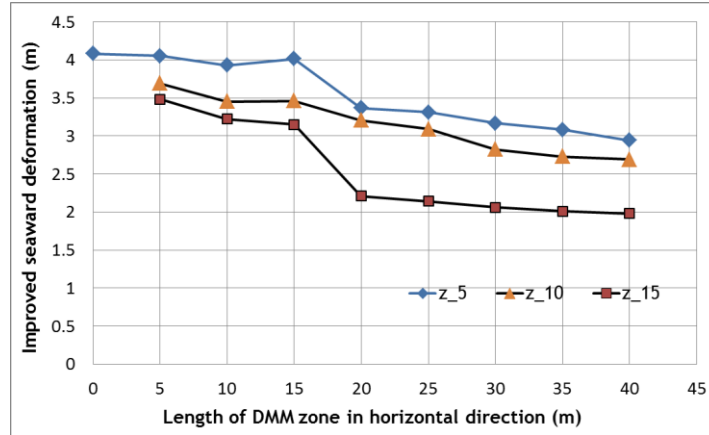
(a) **Quay wall's lateral disp. by differing DMM improved zone length in backfill soil**
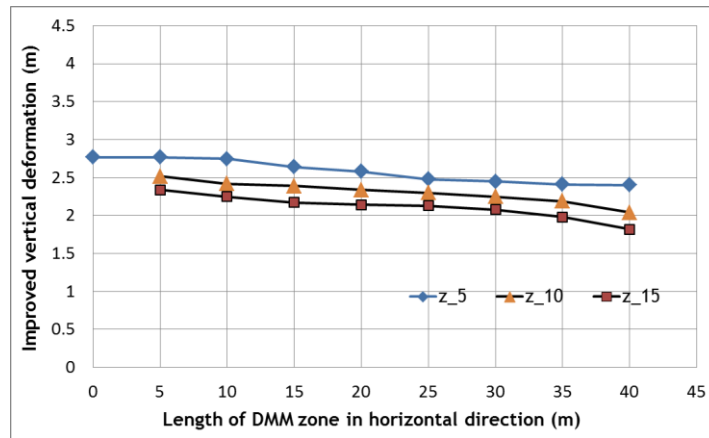
(b) **Quay wall's vertical disp. by DMM differing improved zone length in backfill soil**
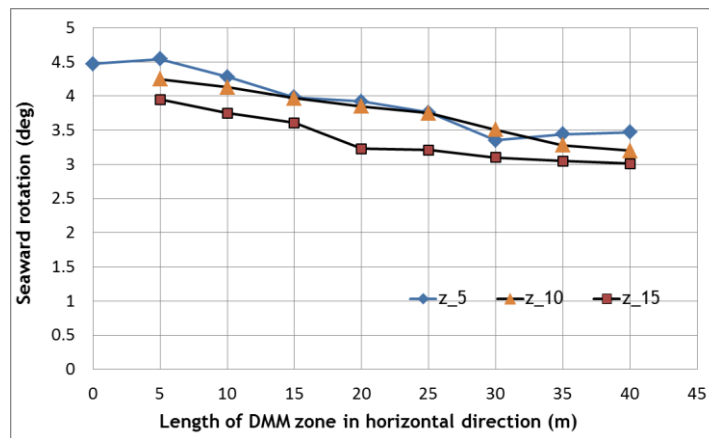
(c) **Quay wall's tilting angle by differing DMM improved zone length in backfill soil**

Figure 24. Computed deformation vs. various DMM improved zones in backfill soil

5.3.3 Scenario 3 – a single DMM improved zone in both foundation and backfill soil

The above analyses provide the possible efficient DMM improved zone configurations in the foundation soil and backfill soil, respectively, based on the evaluation of the two parameters - improved seismic deformation and efficiency. Two selected efficient DMM improved zone configurations in the foundation soil (Figure 21-(c)) and in the backfill soil (Figure 23) are further analyzed in this section, to obtain the optimum DMM improved zone configuration for the quay wall-soil system.

Table 15. Improved seismic results by Selected DMM Improved Zone Configuration

ID	DMM Improved zone dimensions (m)				Improved performance at the top seaward corner of caisson wall		
	Foundation soil (Scenario 1 - category 3)		Backfill soil (Scenario 2)		Improved deformation (m)	Reduction (%)	Efficiency
	Length	Depth	Length	Depth			
1	20	14	20	15	0.84	83	0.13
2	20	21	20	15	0.66	97	0.12
3	20	14	25	15	0.73	95	0.12
4	20	21	25	15	0.48	91	0.11

The configurations of the examined DMM improved zone and their corresponding improved deformation and efficiency results are listed in Table 15. The damage criteria generally in routine practice is shown in Table 16 (PIANC, 2001), and deformation criteria are calculated based on dimensions of improved caisson quay wall.

Table 16. Specified damage criteria for the improved quay wall (after PIANC, 2001)

Proposed damage criteria				
Level of Damage	Degree I	Degree II	Degree III	Degree IV
Residual deformation	< 0.5 m	0.5-1.0 m	1.0-1.8 m	> 1.8 m
Residual tilting	< 3 deg	3 – 5 deg	5 – 8 deg	> 8 deg
Specified performance grades				
Grade	Grade S	Grade A	Grade B	Grade C
Specification	Serviceable	Repairable	Near collapse	Collapse

Based on Table 16, remedial option 4 shows the lowest seismic deformation (0.48 m) and improvement efficiency (0.11) with the greatest improved zone volume ($20*21+25*15=795$ m^3 per unit width) among the four remedial options. As seen, the difference of the improvement efficiency for the four remedial options is insignificant; that is within 2%. Therefore, the improvement efficiency may not be the dominant consideration for this case. Table 16 provides the general damage criteria degrees I, II, III, VI for gravity caisson wall for various specified performance grades S, A, B, C, respectively (PIANC, 2001). Based on the simulation results herein, the remedial option 4 (shown in Table 15), the one requiring the largest improved zone as shown in Table 15, can ensure the performance-grade S and limit the seismic deformation of quay wall to be less than 0.5 m. Therefore, as indicated by PIANC (2001), only limited amount of restoration work is needed to fully restore the deformed quay wall after a similar strong earthquake. As an illustration example, the configuration of the DMM improved zone specified in remedial option no. 4 is presented in Figure 25.

The other three remedial cases (1, 2 and 3 in Table 15) can ensure the grade A (the deformed caisson wall have to be repaired before use, but the repairing/closing period is reasonably short) by limiting the improved deformation between 0.5 to 1.0 m, which would require a reasonable amount restoration work to fully restore the deformed caisson quay wall.
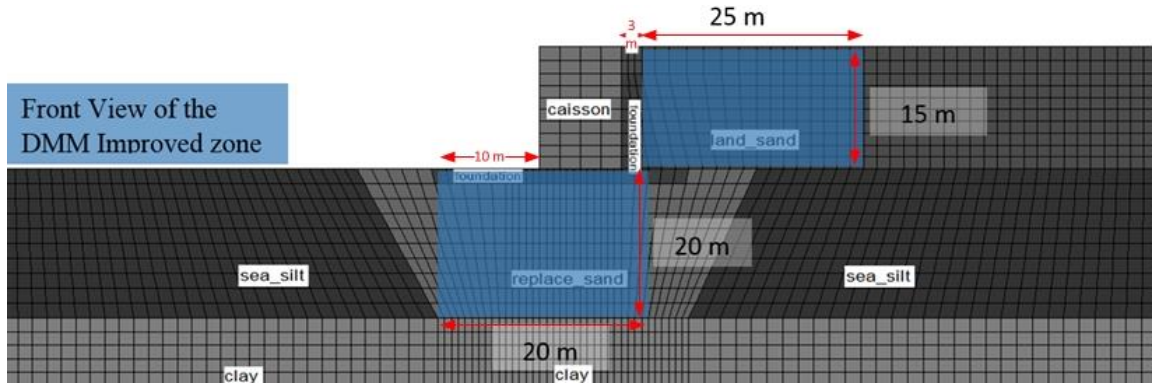
Figure 25. The configuration of the DMM improved zone specified in remedial case 4

5.3.4   Results summary of all three scenarios

Table 17 provides an overview of the improved performance-grade of all the remedial programs for scenario 1 and 2. As shown in the table 17, nearly all improved deformations by scenario 1 and 2 are significant, and the improved deformations are still unacceptable. Therefore, it is important to improve both foundation and backfill soil, as analyzed in scenario 3.

Ultimately, the final selection of utilized DMM remedial programs in an integrated consideration process which involves numerous parameters: the social importance of the constructed caisson quay wall, initial cost for caisson wall, DMM construction, and the predicted cost for restoration work, DMM construction and the predicted cost for the restoration work, which all can be site-specific.

5.4   Improvement Effectiveness and Efficiency Evaluation

The optimum DMM improved zone configuration would be the one that meets the specified performance grade with the smallest DMM improved zone, considering that the cost of installing the DMM improved zone is a function of the total improved volume. The improvement efficiency for each examined DMM improved zone in scenario 1 and 2 is presented in Table 17 and Figure 26. As shown in Figure 26, the improved deformation for the caisson wall-soil system decreases with the volume increase in applied DMM improved zone in terms of the length of DMM improved zone in horizontal direction. Meanwhile, the improvement efficiency also decreases with the increasing treatment length and depth.

Table 17. Improved results summaries by various configurations of DMM improved zones

(a) Results of Scenario 1

	Improved Deformation (m)	Efficiency	DMM Improved Zone Geometry		(PIANC,2001) Grade
			Length	Depth	
Scenario 1 – Category 1	3.55	0.42	5	7	C
	2.32	0.48	5	14	C
	2.39	0.34	5	21	C
	3.43	0.16	10	7	C
	2.19	0.17	10	14	C
	2.12	0.11	10	21	C
	3.46	0.13	15	7	C
	2.19	0.14	15	14	C
	2.12	0.16	15	21	C
	3.36	0.06	20	7	C
	2.28	0.10	20	14	C
	1.77	0.08	20	21	B
Scenario 1 – Category 2	2.16	0.91	5	7	C
	1.76	0.57	5	14	B
	1.72	0.42	5	21	B
	1.91	0.50	10	7	C
	1.74	0.28	10	14	B
	1.68	0.14	10	21	B
	1.89	0.33	15	7	C
	1.72	0.17	15	14	B
	1.64	1.60	15	21	B
	1.83	0.26	20	7	C
	1.71	0.33	20	14	B
	1.55	0.08	20	21	C
Scenario 1 – Category 3	1.43	0.39	10	7	B
	1.32	0.36	20	7	B
	1.29	0.38	30	7	B
	1.27	0.35	40	7	B
	1.37	0.35	10	14	B
	1.21	0.33	20	14	B
	1.18	0.20	30	14	B
	1.08	0.16	40	14	B
	1.26	0.33	10	21	B
	1.04	0.16	20	21	B
	1.05	0.10	30	21	B
	0.91	0.08	40	21	A

(b) Results of Scenario 2

|	Improved Deformation (m)	Efficiency	DMM Improved Zone Geometry		(PIANC, 2001) Grade
			Length	Depth	
	4.53	0.10	5	5	C
	4.50	0.12	10	5	C
	4.49	0.09	15	5	C
	4.17	0.14	20	5	C
	4.15	0.13	25	5	C
	4.10	0.11	30	5	C
	4.01	0.09	35	5	C
	3.84	0.13	40	5	C
Scenario 2	4.40	0.19	5	10	C
	4.19	0.15	10	10	C
	4.17	0.10	15	10	C
	4.14	0.08	20	10	C
	4.02	3.78	25	10	C
	3.78	0.08	30	10	C
	3.70	0.09	35	10	C
	3.71	0.07	40	10	C
	4.14	0.12	5	15	C
	4.02	0.15	10	15	C
	3.91	0.14	15	15	C
	3.21	0.14	20	15	C
	3.14	0.10	25	15	C
	3.11	0.08	30	15	C
	3.05	0.04	35	15	C
	3.04	0.03	40	15	C

For the improvement of backfill soil, the improvement efficiency in Figure 26-(b) decreases with the increasing of the length of DMM improved zone. However, the difference between the improved efficiency among various DMM improved zone configurations is not as significant as shown in scenario 1; the improvement efficiencies are constantly approximate from 0.1 to 0.3, which is approximate one-third to one-half of the efficiency by improving foundation soil, as shown in Figure 26-(a). This may indicate that improving foundation soil is potentially more effective in reducing the deformation of caisson wall than improving the backfill soil. This observation is also consistent with the results by Nakahara et al. (2007) that the effectiveness of improving the foundation soil can be two times more efficient than improving the backfill soil.

The efficiency becomes consistently low when DMM improved zone length exceeds 20 to 25 m in backfill soil.

Since the efficiencies among the various examined improved zone configurations are fairly small, the final decision of the utilized design will be primarily based on the comparison of improved deformation and specified performance grade, as discussed in scenario 3. The above analyses provide a basis for comparing the efficiency of different DMM improved zone configurations; they do not reflect the ability of the different configurations to achieve the specified performance grade. Select an optimum DMM improved zone would require considering both the specified performance and the efficiency based on the specific project characteristics.

Finally, within the framework of this case study, all four analyzed options in scenario 3 can be utilized to improve the gravity caisson quay wall as described in this study if the specified performance is grade S, which is commonly used in design of caisson wall in practice for earthquake motion with a probability of exceedance of 10 percent during life-span (PIANC, 2001). In practice, the final dimension of DMM improved zone should be confirmed by analyses to reflect the details of stratigraphy and system geometry.
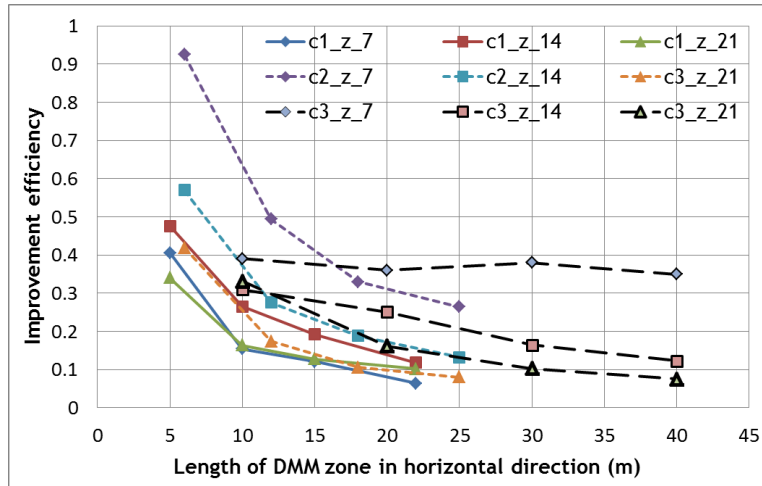
(a) Efficiency results of scenario 1
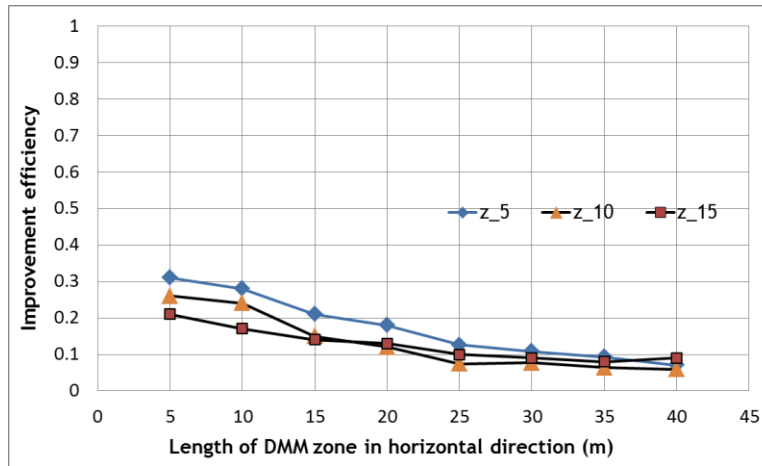
(b) Efficiency results of scenario 2

Figure 26. Improvement efficiency for multiple DMM improved zones in scenario 1 and 2

5.5   Conclusions

Within the framework of this case history, this study provides a procedure of obtaining the optimum DMM improved zone location and geometry for liquefaction mitigation of gravity caisson quay wall. This procedure may be used to optimize the liquefaction mitigation design of using other remedial schemes for similar type of quay wall prone to liquefaction damage. Two parameters, the improved deformation and efficiency are important. The numerical analyses identified the relative effectiveness of alternate DMM improved zones and provided insights on

how to optimize the DMM improved zone configuration in design. The following conclusions can be drawn based on this study:

1) All four remedial options analyzed in scenario 3 can be used to improve the caisson quay wall if the performance grade is "Serviceable" under an earthquake motion with probability of exceedance of 10% during life-span.

2) Remedial option 4 is recommended if the performance grade is "Repairable" under an earthquake motion with probability of exceedance of 10% during life-span.

3) For the improvement of foundation soil, the analyses show that placing a continuous DMM improved zone centered under the quay wall is more effective in reducing the seismic deformation other DMM improved zone configurations.

4) Extending the DMM improved zone to the bottom of foundation soil can prevent the propagation of failure surface and prevent the heave of foundation soil in front of the caisson wall.

5) The efficiency of placing a DMM improved zone immediate behind the caisson wall decreases with the increasing DMM improved zone length.

6) Improving the foundation soil can be approximately two times more efficient than improving backfill soil in reducing the seismic deformation of the quay wall.

7) The optimum DMM improved zone configuration should first meet the specified performance grade, and then obtain the satisfied efficiency among the other candidate configurations. The selection process may require a comprehensive parametric study.

CHAPTER 6. APPLICATION OF COMBINED STONE COLUMN AND DMM WALL

6.1   Introduction

Similar to Chapter 4 and 5, the objective of this chapter is to establish an easy-implemented remediation program using the combined stone column method and the wet DMM. To optimize remedial designs through quantitative evaluation, the improvement effectiveness of using combined methods is studied on a comparative basis by focusing on the improved seismic performances of the quay wall-soil system.

In this study, stone columns are installed in the foundation soil to increase the liquefaction resistance and to reduce the vertical settlement and loss of foundation soil strength when liquefaction occurs; DMM mixed walls are applied in the backfill soil to resist the lateral spreading displacement and the active dynamic earth pressure under shaking. In general, the types of improvement mechanisms (e.g., rapid drainage, densification or inducing stiffer elements in native soils) selected should be designed and applied depending on the failure mechanisms. In this study, there are two reasons of utilizing such a combination:

1) Liquefaction in the foundation soil and backfill soil contribute to the vertical and lateral deformation of caisson quay wall placed in liquefiable soil, respectively;

2) Stone columns and DMM been proved to be effective in reducing vertical and lateral deformation induced by liquefaction, respectively (Tanaka et al., 2000; Kogai et al., 2000; Yasuda et al., 2004; Mitchell 2008), for different type of structures prone to liquefaction-induced damage;

3) DMM walls as the underground barrier have been installed in the liquefiable backfill soil behind the quay wall to reduce the dynamic lateral earth pressure under seismic conditions (Kogai et al., 2000)

Therefore, the combination of stone column and DMM wall is expected to improve the seismic performance of the quay wall-soil system from two aspects:

1) Reducing the vertical settlement and loss of bearing capacity of foundation soil, which leads to a reduced deformation of its supported caisson quay wall;

2) Increasing the lateral deformation resistance of backfill soil by reducing/cutting EPWP generation and propagation, and dynamic active earth pressure in backfill soil.

The application of combined ground improvement methods for liquefaction mitigation of caisson quay wall structures is rarely discussed in previous studies. Herein, this study also provides initial insights of how to properly select more than one ground improvement method in one project to reduce the liquefaction potential of native soil and reduce the seismic damage of adjacent structures effectively.

In addition, due to the advantages of DMM, this study also quantitatively indicates the feasibility of improving backfill soil behind the existing quay wall structures, since the DMM is preferred in noise and vibration sensitive areas.

The improved performances of various remedial programs differ in the two design parameters: (1) the replacement ratio of stone columns in foundation soil and (2) number of DMM mixed walls in backfill soil. Then, multiple optimum remedial programs are proposed by optimizing these two parameters. The remediation is conducted within the well-calibrated case history (Inagak et al., 1996) following the philosophy of PBD (PIANC, 2001) that requires the assessment of seismic performance using deformation criteria, which should meet the specified performance grades (PIANC, 2001).

6.2 Application of the Combined Stone Column and DMM Wall

Stone columns and DMM are two widely used remedial measures for liquefaction mitigation (Mitchell, 2008). Stone columns are typically used in loose granular soils with insufficient strength properties (Elias et al., 2006). The main purposes of applying stone columns are (1) to increase the shear resistance of cohesive and non-cohesive soils (hence increasing bearing capacity); (2) to increase their stiffness (hence reducing settlements); and (3) increase the permeability of the soil mass, therefore reducing the liquefaction susceptibility of granular soils (Chu et al., 2009). This method can decrease the vertical settlement of the surrounded structure on the top if the installed stone columns can maintain good integrity even though the surrounding soils may become liquefied under shaking excitation.

For both DMM wall and sheet pile walls, the installed stiffer elements can perform as the underground barrier to minimize the lateral displacement of liquefied soils and ground motion transmissions and cut the migration path of EPWP. Therefore, the enclosed soil can remain relatively stable under strong shaking, and meanwhile the unenclosed soils adjacent to the improved zone may deform significantly. In contrast, with the stone column method, however, the DMM can minimize disturbance to the surrounding areas during installation process. Applying DMM mixed walls with alignment perpendicular to the direction of potential soil/slope movement is effective (Kogai et al., 2009; Yusada et al., 2004; Motamed et al., 2010). Therefore, in this study, DMM mixed walls are installed perpendicular to the alignment of quay wall in backfill soil, of which primary failure is lateral spreading displacement under earthquake loading (Iai and Sugano, 2000).

In general when more than one ground improvement method is applied, it is important to consider or optimize the combined remedial program by determining (at least qualitatively but

better quantitatively) the potential influences of the design parameters of each applied remedial method on the improved seismic deformations of the improved ground/structures.

6.2.1 Remedial program design parameters

6.2.1.1 Deep soil mixing method

The DMM as a popular ground improvement method for liquefaction mitigation was introduced in Chapter 5, and is not discussed further herein. The feasibility and effectiveness of DMM walls as underground barriers in liquefiable soils have been both experimentally and analytically evaluated (Tanaka et al., 2000; Motamed et al., 2010). Increasing the rigidity of embedded walls, in terms of increasing wall thickness or elastic modulus or bending stiffness, in liquefiable soil can reduce the deformation of liquefiable soil (Kogai et al., 2000). The wall stiffness, dimensions and installation layout of the DMM mixed walls are the main design parameters in liquefaction mitigation.

In this study, the wall thickness and depth is 1 m and the full thickness of the backfill soil layer (15 m), respectively. By restricting the rotation and displacement at the bottom of DMM mixed walls, the DMM mixed walls are "fixed" at the bottom of the backfill layer since the fixed-end wall has been proved to be more effective than the floating-type wall (Kogai et al., 2000; Motamed et al., 2010). The properties and stress-strain envelope of DMM-mixed materials are shown in Chapter 5, and are not repeated herein.

According to Tanaka et al. (2000), friction or shearing can be reasonably neglected between soil and the installed DMM-mixed walls because in this situation the dominant working mechanism between soil and DMM mixed walls is compression, since DMM walls are used to resist/reduce the dynamic earth pressure that is induced by the liquefiable backfill soil. This assumption is implemented by imposing the condition that displacements of the nodal points of

DMM mixed wall and the surrounding unimproved soil are the same with each other in the horizontal direction but can take independent values in the direction of vertical or perpendicular to the wall.

Three DMM wall installation layouts are examined. Based on the deformation of the unimproved quay wall-soil system presented in Chapter 2, the surficial deformation in backfill soil is almost negligible at or beyond the distance of approximate 60 m away from the caisson quay wall. Therefore, the DMM mixed walls are installed in backfill soil within the range of less than 60 m away from the caisson quay wall at the uniform distance of 30 m, 15 m and 10 m in wall_1, wall_3, and wall_5, respectively. Figure 28 shows the wall-soil system with installed DMM walls in backfill soil for illustration. The installed DMM walls in backfill soil are summarized below

- *wall_1*: install one single DMM wall at a distance of 30 m away from the quay wall;

- *wall_3*: install three DMM walls at the distance of about 13 m, 28 m and 45 m, respectively, away from the quay wall;

- *wall_5*: install five DMM walls at the distance of 10 m, 20 m, 30 m, 40 m and 50 m, respectively, away from the quay wall.
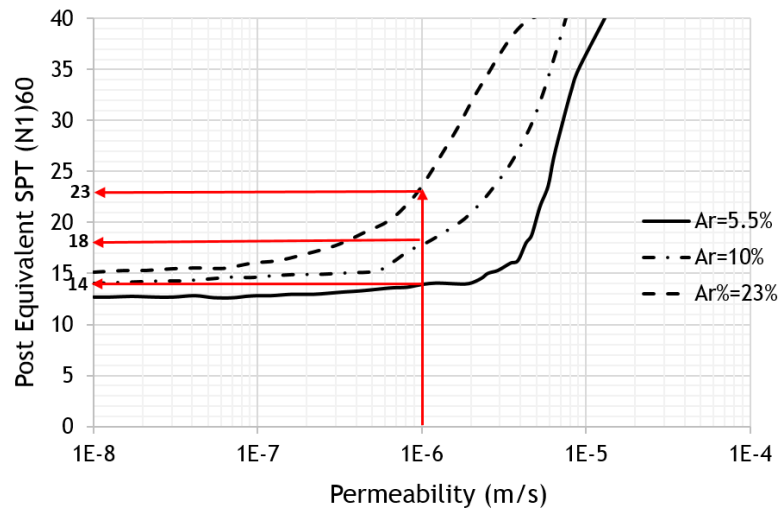
6.2.1.2 Stone column method

The stone column method design has been mainly empirical and led by contractor experience (Elias et al., 2006), which is similar to the vibro-compaction method presented in Chapter 4.

As presented in Chapter 2, the stone/aggregate columns can be represented by a group of sandy columnar structures with slightly higher stiffness and hydraulic conductivity than the surrounding untreated soils based on Yang et al. (2003). For simplification, stone columns were

successfully modeled using cylindrical meshes and were assumed follow Mohr-Column constitutive behavior (Arango, 2003). Motamed et al. (2010) suggested that the simulation results based on above idealizations being made in numerical analysis are normally reasonable.

Shenthan et al. (2004, 2006) proposed an analytical model of estimating the improved relative density $D_r\%$ of the soil among the installed stone columns based on the area replacement ratio ($A_r\%$) and the initial permeability of native soil prior to improvement.

Figure 27. Design chart for stone column method (After Shenthan et al., 2004, 2006)

With the reasonably estimated improved relative density $D_r\%$ based on the analytical model, this design method can aid in designing an appropriate stone column program without solely relying on expensive field trials. The design chart (in Figure 27) method proposed by Shenthan et al. (2004, 2006) is applied for the features of the stone column program in this study. Also in the same design method, the influence of interface properties between stone columns and surrounding improved soil is incorporated in its proposed design chart. With the input of permeability of native soil and design replacement ratio, the improved relative density or SPT blow count can be estimated based on Figure 27.

In this study, the simulations consider installing stone columns in the foundation soil zone vertically underneath the caisson quay wall. Three different area replacement ratios (A_r = 5.5%, 10% and 23%) were assumed, where A_r = (A_c/A_e)*100%, and A_c is circular area of the stone column, A_e is the tributary ($\frac{\pi*D_e^2}{4}$), and D_e = equivalent diameter of the tributary area = 1.05 times the center-to-center spacing between the stone columns installed in a rectangular pattern (Elias et al., 2006; Shenthan et al., 2004, 2006). The three analyzed A_r values correspond to center-to-center spacing of 4 diameters, 3 diameters and 2 diameters of the installed stone column, respectively. Details of the stone column program are listed as below and these specifications can be achieved by using a readily available vibratory probe (Elias et al., 2006) with power rating of at least 120 kW, frequency of 50 Hz and vibrator length of 3 m.

- The typically wet vibratory stone column equipment is utilized.

- Stone column diameter = 0.9 m

- Stone column length = 20 m (thickness of the foundation soil) for all three A_r values.

- Column spacing: 3.6 m for A_r = 5.5%; 2.7 m for A_r = 10%; 1.8 m for A_r = 23%

- A QC/QA program must be conducted to ensure the satisfaction of the above specifications (the minimum average SPT $(N_1)_{60}$ values in Figure 8) for the improved ground.

The permeability of native soil is assumed to be 1.0E-6 m/s for loose granular soil. Therefore, based on Figure 27, the corresponded post equivalent SPT blow count $(N_1)_{60}$ values can be determined to be 14, 18 and 23 for the replacement ratio of approximate 5.5% (*Ar_5*), 10% (*Ar_10*) and 23% (*Ar_23*), respectively. The post-improved soil properties and stone column properties are presented in Table 18. The majority of these simulated material properties are based on the published data or empirical correlations using SPT blow count $(N_1)_{60}$ values.

**Table 18. Improved soil and stone column properties used for simulation**

| Case_SC	Ini. SPT $(N_1)_{60}$	Ar %	Post. SPT $(N_1)_{60}$	Post Dr %	Density (kg/m^3)	Poisson	Shear M (Mpa)	Fric. (Deg)	Perm. (cm/s)
Properties of the Improved Soils by Stone Column Method									
1	10	5	14	60	1500	0.33	35	30	1.0E-3
2	10	10	18	65	1600	0.33	45	33	2.0E-4
3	10	23	23	75	1900	0.33	50	35	1.8E-4
Stone Column Material			25	80	2100	0.30	150	40	3.0E-2

6.2.1.3 Parametric study metrics

A comprehensive parametric study (Table 19) is proposed to evaluate the influence of the combined stone column and DMM method on the seismic stability of quay wall-soil system, and the behavior of liquefiable foundation and backfill soil by focusing on the generations of EPWP at the selected locations. Figure 28 shows the selected cases (*Ar_23_Wall_1, Ar_23_Wall_3, and Ar_23_Wall_5*) for illustration. Dimensions and properties of the quay wall-soul system model can be referred to Chapter 3, except for the installed stiffer elements that are the stone columns in foundation soil and DMM walls in backfill soil.

**Table 19. Conducted parametric study using the combined methods**

Remedial Case ID	0 DMM wall	1 DMM wall	3 DMM walls	5 DMM walls
SC_Ar = 0%	Ar_0_Wall_0 *(Unimproved)*	Ar_0_Wall_1 *(Case_1)*	Ar_0_Wall_3 *(Case_2)*	Ar_0_Wall_5 *(Case_3)*
SC_Ar = 5.5%	Ar_5_Wall_0 *(Case_4)*	Ar_5_Wall_1 *(Case_5)*	Ar_5_Wall_3 *(Case_6)*	Ar_5_Wall_5 *(Case_7)*
SC_Ar = 10%	Ar_10_Wall_0 *(Case_8)*	Ar_10_Wall_1 *(Case_9)*	Ar_10_Wall_3 *(Case_10)*	Ar_10_Wall_5 *(Case_11)*
SC_Ar = 23%	Ar_23_Wall_0 *(Case_12)*	Ar_23_Wall_1 *(Case_13)*	Ar_23_Wall_3 *(Case_14)*	Ar_23_Wall_5 *(Case_15)*
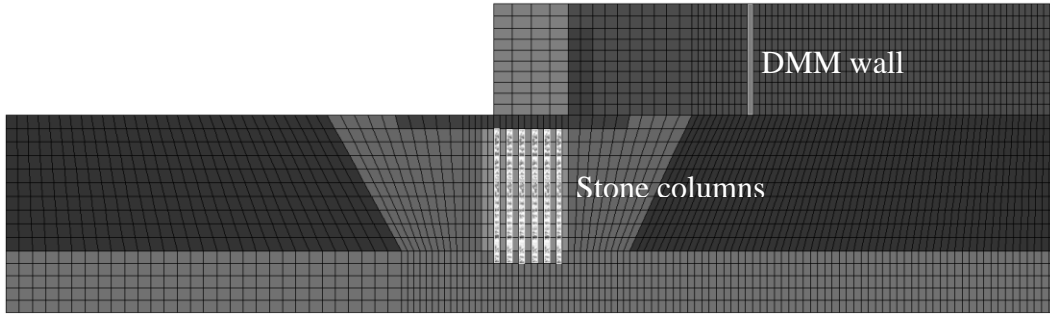
(a) Ar_23_Wall_1 (Case 13)
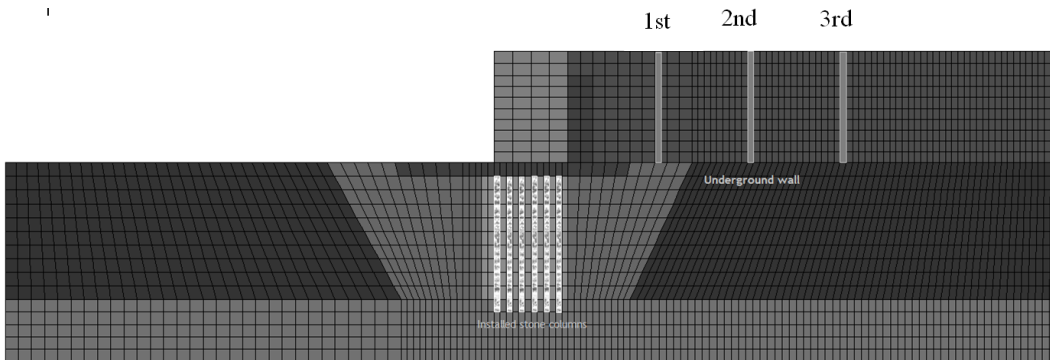
(b) Ar_23_Wall_3 (Case 14)
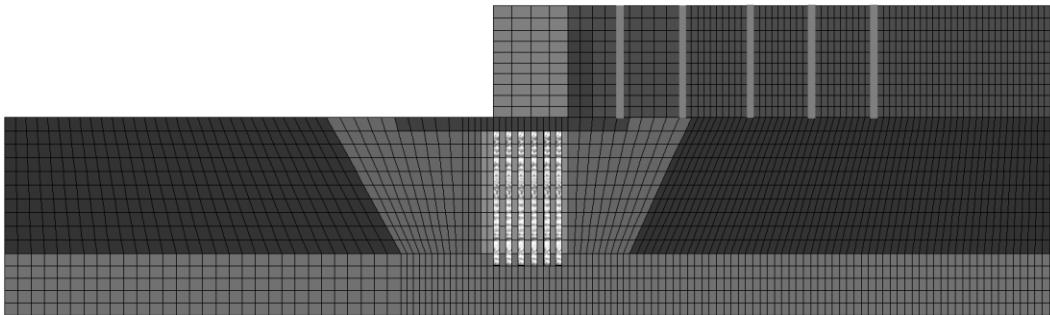
(c) Ar_23_Wall_5 (Case 15)

Figure 28. The improved models of selected remedial cases

6.3   Results and Discussions

Following the proposed parametric study metrics, a quantitative evaluation and comparisons of improvement effectiveness of the examined remedial cases are conducted. The deformation of the improved quay wall-soil system is analyzed as an indication of improvement effectiveness. Also, the time histories of EPWP at the selected locations in both foundation and

backfill soils are analyzed. With the results of the parametric study, the optimum remedial programs are proposed to achieve different objectives defined by various levels of damages and (restoration efforts and period of inoperative) (PIANC, 2001) in Table 20 of caisson quay wall-soil system under strong seismic events.

6.3.1   Improved deformation of quay wall

A summary of seismic residual deformations (total deformation, lateral and vertical deformations, where total deformation $= \sqrt{(vertical\ disp.)^2 + (hori.disp)^2}$ measured at the top seaward corner of the caisson quay wall is shown in Figure. Three black dashed lines in Figure indicate for the different specified performance grades. Three levels of damages defined in PBD (PIANC, 2001) can be expressed in terms of both structural and operational aspect.

Table 20. Acceptable level of damages in the PBD (PIANC, 2001)

| Level of Damage	Structural	Operational
Degree I: Serviceable	Minor or no damage	Little or no loss of serviceability
Degree II: Repairable	Controlled damage	Short-term loss of serviceability
Degree III: Near collapse	Extensive damage near collapse	Long-term loss of serviceability
Degree IV: Collapse	Complete loss of structure	Complete loss or serviceability

Figure 29 shows the improvement effectiveness of the various remedial efforts in terms of two evaluation criteria: improved displacement magnitude (unit: meter) and displacement reduction percentage at the top seaward corner of the quay wall. As shown, the majority of examined designs are very unlikely acceptable ("Repairable" or "Serviceable") from the point view of the quay wall structural damage and operational functionality with the application of seismic excitations. However, for the remedial case 6, 7, 9, 10, 11, 12 and 13 (in Table 19) can improve the quay wall to satisfy the specification of "Degree II - Repairable" by reducing improved deformation to be less than 10% of quay wall height (10% * 18 m = 1.8 m) but still greater than 5% of the quay wall height (5% * 18 m = 0.9 m). The best improved displacement is

approximately 0.7 m with over 85% reduction compared to the unimproved one by remedial case 14 and 15 in Figure 29-(a), which indicate that at least 3 DMM walls should be installed in backfill soil with uniform spacing behind the quay wall in addition to the improvement of foundation soil by stone columns with A_r% of 23%.

Therefore, the examined remedial cases can be classified into three categories based on their different improved performances: (1) improved performance is serviceable; (2) improved performance is repairable; (3) improved performance is unacceptable.

- Unacceptable level: Case 1, 2, 3, 4, 5, and 8;

- Repairable level: Case 6, 7, 9, 10, 11, 12 and 13;

- Serviceable level: Case 14 and 15;

Another interesting observation in Figure 29-(b) is that the reduction of horizontal displacement at the quay wall is influenced by the reduction of vertical displacement of the quay wall. In other words, a better improved foundation soil can increase the effectiveness of improving backfill soil for the analyzed caisson quay wall, or vice versa. In brief, the two efficiencies are positively correlated with each other. For example, comparing the results among cases 1, 5, 9 and 13 or 2, 6, 10 and 14, the comparisons indicate that with the increase of replacement ratio (Ar%) value from 5% to 23% of the installed stone columns in foundation soil, the lateral displacement reduction of quay wall also increase even though the number of installed DMM walls in backfill soil remains constant. Obviously, above results indicate the interactive influences of improving the backfill soil and foundation soil on the deformation of quay wall. The interactive influences should be considered in the liquefaction mitigation design by ground improvement.
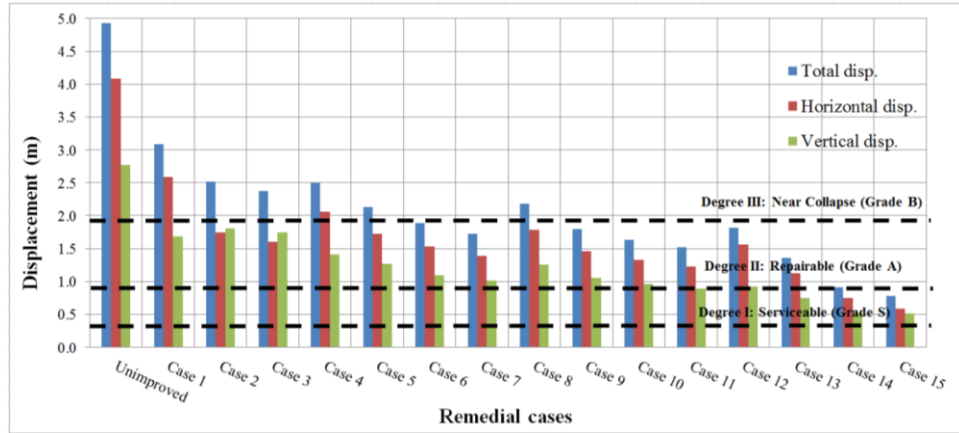
(a) Displacement magnitude
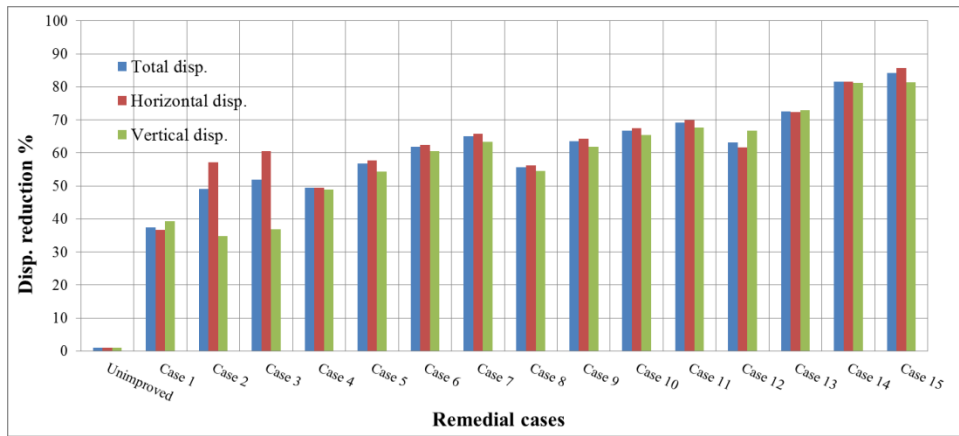
(b) Displacement reduction percentage

Figure 29. Computed residual deformations at the top seaward corner of quay wall

6.3.2 Improved deformations in backfill soil

In addition to the seismic performance of quay wall, the seismic deformation of backfill soil is also important for evaluating seismic stability and damage of foundations or structures located in backfill soil such as heavy cranes and many buried utilities. To address this issue, the deformations are measured at the selected locations on the surface of backfill soil starting from the inward edge of the quay wall with equal interval distance of 5 m toward inland direction (in Figure 30). The furthest location where only very small deformation occurs is about 80 meter away from the quay wall.

As observed in Figure 30, the critical deformation reduction on the surface of backfill soil is achieved in almost all the examined remedial cases. The improved deformation differences among cases 1, 2 and 3 are small as shown in Figure 30-(a), which indicate that the additional effort in improving backfill soil may not lead to an additional deformation reduction if the foundation soil remains unstable or unimproved.

Figure 30-(b), 30-(c) and 30-(d) also indicate that increasing the area replacement ratio $A_r\%$ (from 5.5% to 23%) of the stone columns in foundation soil can lead to a better improvement efficiency of backfill soil in terms of smaller displacement magnitude (greater than 1.5 m and less than 1.0 m at the distance of 0 m for cases 7 and 15, respectively) and the reduced area of seismically displaced region. The surface total displacement becomes generally small at a distance of 30 m and 40 m for cases 7 and 15, respectively. Comparing the results achieved by cases 12, 13, 14 and 15, it can be seen that if the $A_r\%$ value remains constant, increasing the number of installed DMM wall in backfill soil can obviously lead to a greater deformation reduction.

The same observations can also be made in Figure 31 by presenting the total displacement reduction percentage at the same locations as shown in Figure 30. When five DMM walls are installed at a uniform interval spacing of 10 m, the deformation reductions are more uniform and constantly higher than the cases with less DMM walls installed while the relative density $D_r\%$ in foundation soils remains constant. Therefore, the uniformly distributed DMM walls seem to be more effective in reducing the surficial displacement occurred in backfill soil. In addition, the deformation reduction values measured at the large distances of 60 m to 80 m in Figure 31 becomes more randomly distributed. This could be due to the small unimproved deformations or the improvement influences may become less affected in this region.

Therefore, the improved deformation of the quay wall as well as on the backfill soil both indicate that a combined method of stone column and DMM wall method is effective in reducing the seismic deformation of the analyzed quay wall-soil system. Increasing the area replacement ratio $A_r\%$ of the installed stone columns in foundation soil or number of DMM walls in backfill soil can lead to an improved seismic performance of both quay wall and liquefiable backfill soil.

Also, the effectiveness of improving the foundation soil and backfill soil is positively correlated with each other. Increasing the Ar % value of the stone column program in foundation soil can improve the improvement efficiency of backfill soil while keeping the number of DMM mixed wall constant, or vice versa.
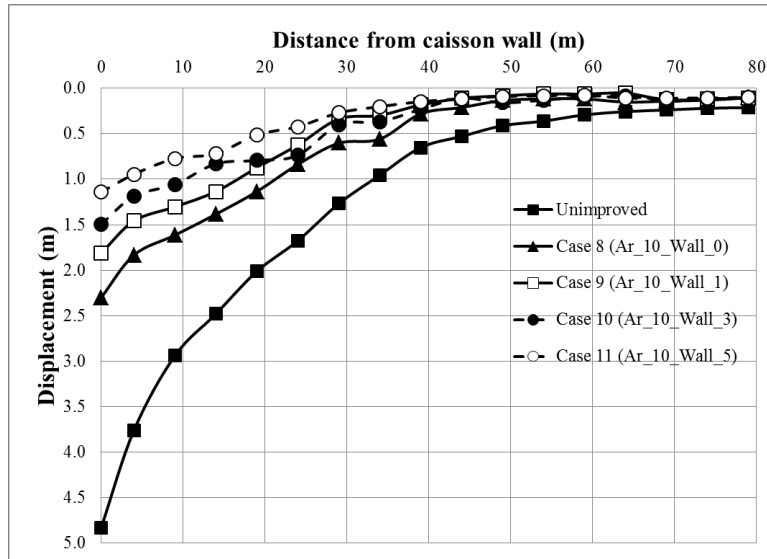
In following section, the generations of EPWP at the selected location in foundation soil and backfill soil are discussed and the influences of installed remedial elements on EPWP reductions are also evaluated.
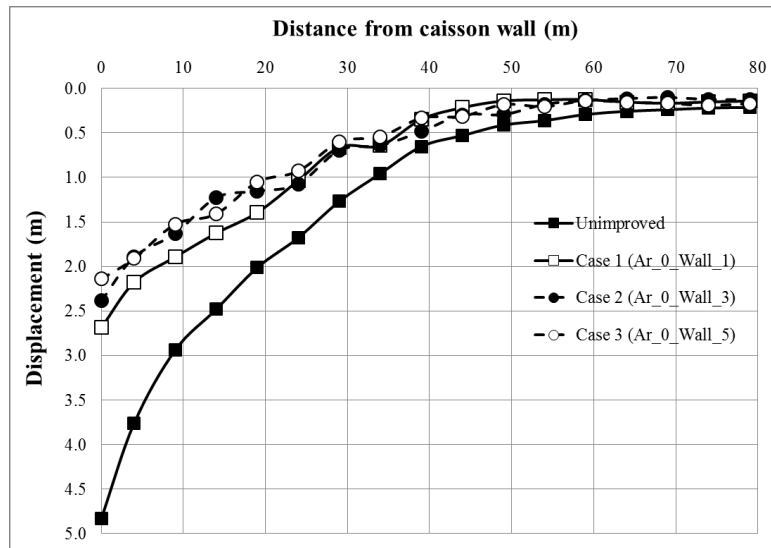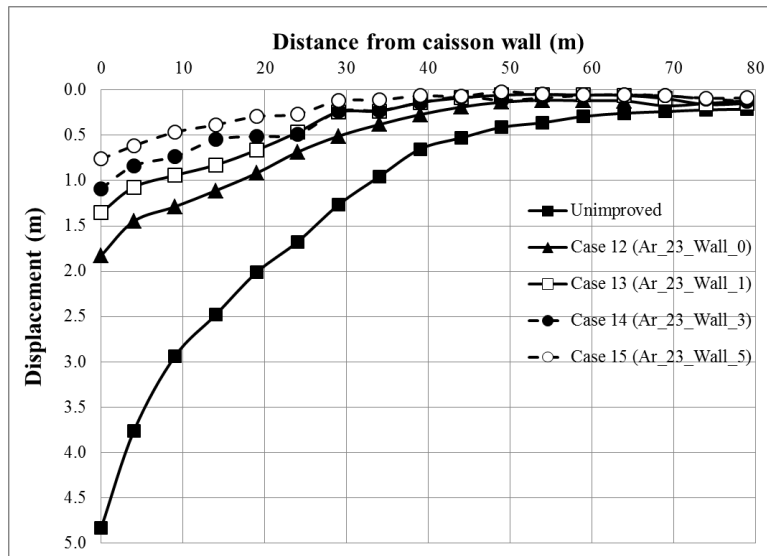
(a) No foundation improvement
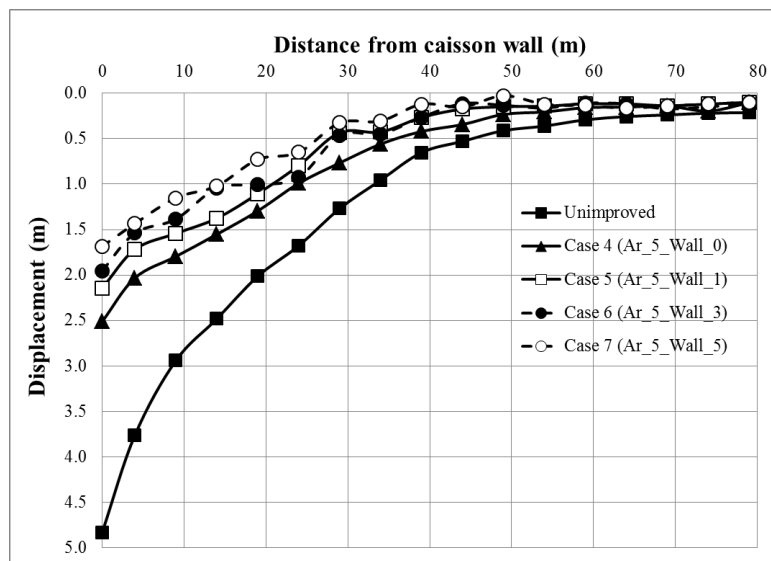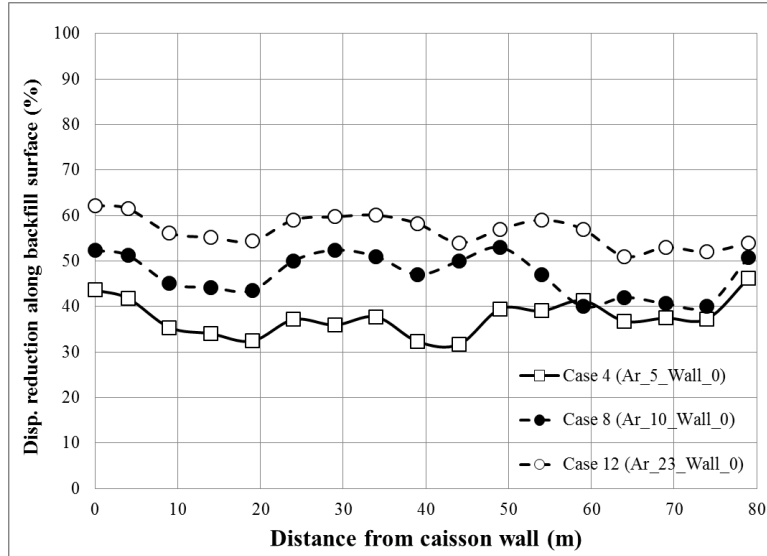

(b) Stone column method (Ar = 5%)

(c) Stone column method Ar = 10%

(d) Stone column Ar = 23%

Figure 30. Computed backfill soil surficial deformations

(a) No DMM walls installed
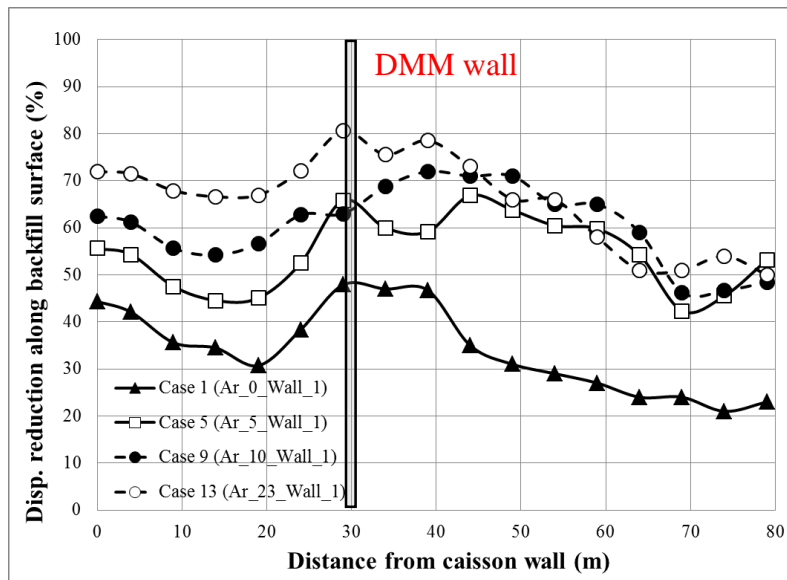
(b) One DMM mixed wall installed
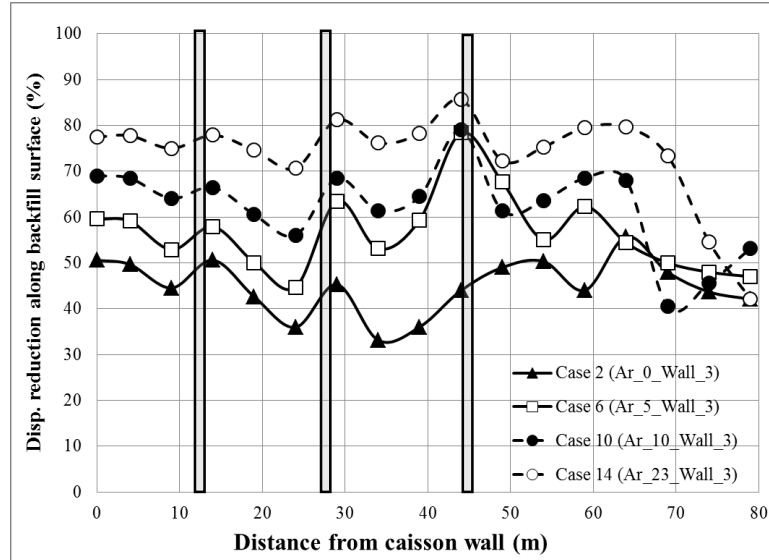
(c) Three DMM mixed walls installed
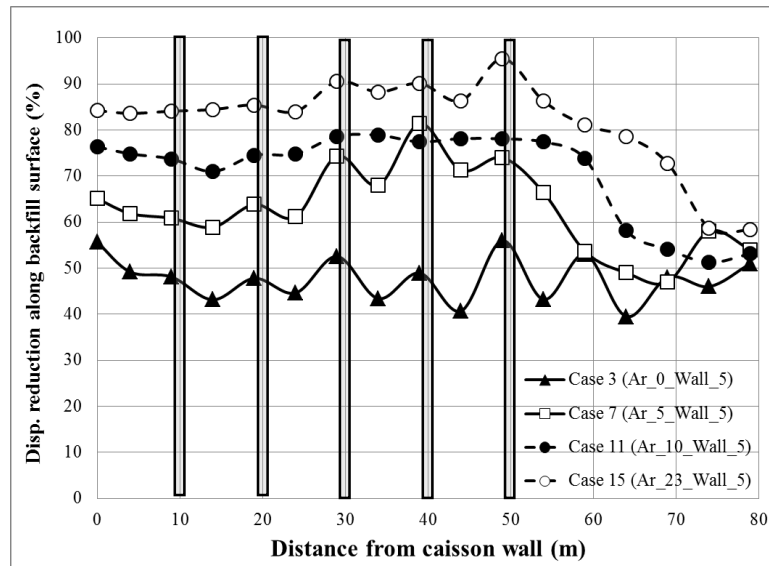
(d) Five DMM mixed walls installed

Figure 31. Computed backfill soil surficial deformation reduction percentage

6.3.3 EPWP ratio "r_u"

In addition to the improved displacement as an evaluation criterion to indicate the effectiveness of the combined remedial methods, the improved "r_u" value at the selected locations in the quay wall-soil system are also investigated on a comparative basis to evaluate the

influences of the installed stone columns and DMM walls. The "r_u" value computed from remedial cases 2, 6, 10 and 14 are presented to show the influences of stone columns in foundation soil with and without DMM walls in backfills. Also, the influences of DMM walls are on "r_u" value are evaluated by comparing the results from cases 1, 2 and 3 in which no stone columns installed in foundation soil.

Referring back Figure 12 in Chapter 3 for the relative location of Points A to H within the quay wall-soil system, points A, B and C are located within the backfill soil zone between the 1st and 2nd DMM wall based on their relative locations relative to the installed DMM walls. Points E and F are located in the unimproved foundation soil in front of the installed stone columns, and points G and H are located within the improved foundation soil zone. Within this study, the measured time histories of "r_u" value from the selected remedial cases at the following representative locations point B in backfill soil, point F in unimproved foundation soil and point H in improved foundation soils are presented.

At point B, while keeping three DMM walls installed in backfill soil, increasing the value of Ar% of installed stone columns in foundation soil from 0% to 23% can reduce the peak value of "r_u" value from 0.9 in the unimproved case to around 0.35 in case 14 (Figure 32). However, the residual "r_u" value still remains the greater or close to the value from unimproved case, which may still lead to a potential post-liquefaction deformation in the backfill soil. Therefore, an increased improvement in foundation soil also contributes the stability of backfill soil in terms of the reduced EPWP generation.

At point F, results in Figure 33 indicates that increasing A_r % of installed stone columns in foundation soil lead to a reduction of peak "r_u" value in the unimproved soil immediately adjacent to the improved zone. This is probably attributed to the increased stability of foundation

soils as compared to the unimproved cases. The unimproved peak value of "r_u" value is around 0.7, and the improved peak value is around 0.4 to 0.5 in the presented remedial cases. The residual "r_u" value only slightly decreases. Even though the foundation soil is not fully improved, the improved portion of foundation soil vertically underneath the quay wall can also contribute to the overall stability of foundation soil.

At point H, Figure 34 shows the influences of increasing foundation soil improvement by increasing the area replacement ratio of installed stone columns on generation of EPWP within the improved soils. The generation of EPWP at point H reduced significantly and approaches nearly to zero at the end of shaking due to the soil installation and rapid drainage provided by installation of stone columns. Figure 34 also highlights the increased stability of foundation soil by installing stone columns. As shown, a higher A_r% ratio can lead to less generation of EPWP, however, the benefits of additional stone columns when A_r% exceeds 10% tends to become less significant if comparing the results of case 10 and 14 in Figure 34.

Figure 32, 33 and 34 show the time histories of "r_u" value at points B, F and H, respectively. As the results shown, increasing the number of installed DMM mixed wall from one (in case 1) to five (in case 3) in backfill soil can reduce the peak and residual value of EPWP ratios at the selected locations, but the benefits are fairly limited due to the deformation of foundation soil. Based on discussion in earlier paragraphs, increasing improvement in foundation soils would increase the improvement efficiency in backfill soil. Therefore, above results also indicate the importance of foundation soil improvement.

As shown in Figure 35, by comparing the results of case 1 and 3 at point B, it can be seen that installing five DMM walls in case 3 is also more beneficial than installing one single DMM wall in backfill soil in reducing the generation of EPWP of the backfill soil closely adjacent to

the caisson quay wall in this study. Also in Figure 35, comparing the results of case 1 and case 3 at point G and H, the influence of installing one or five DMM walls in backfill soil on foundation soil can be highlighted. It may be concluded that a better improved backfill soil is also beneficial in reducing the development of EPWP in foundation soil.

(a) Case 2 (Ar_0_Wall_3)

(b) Case 6 (Ar_5_Wall_3)

(c) Case 10 (Ar_10_Wall_3)
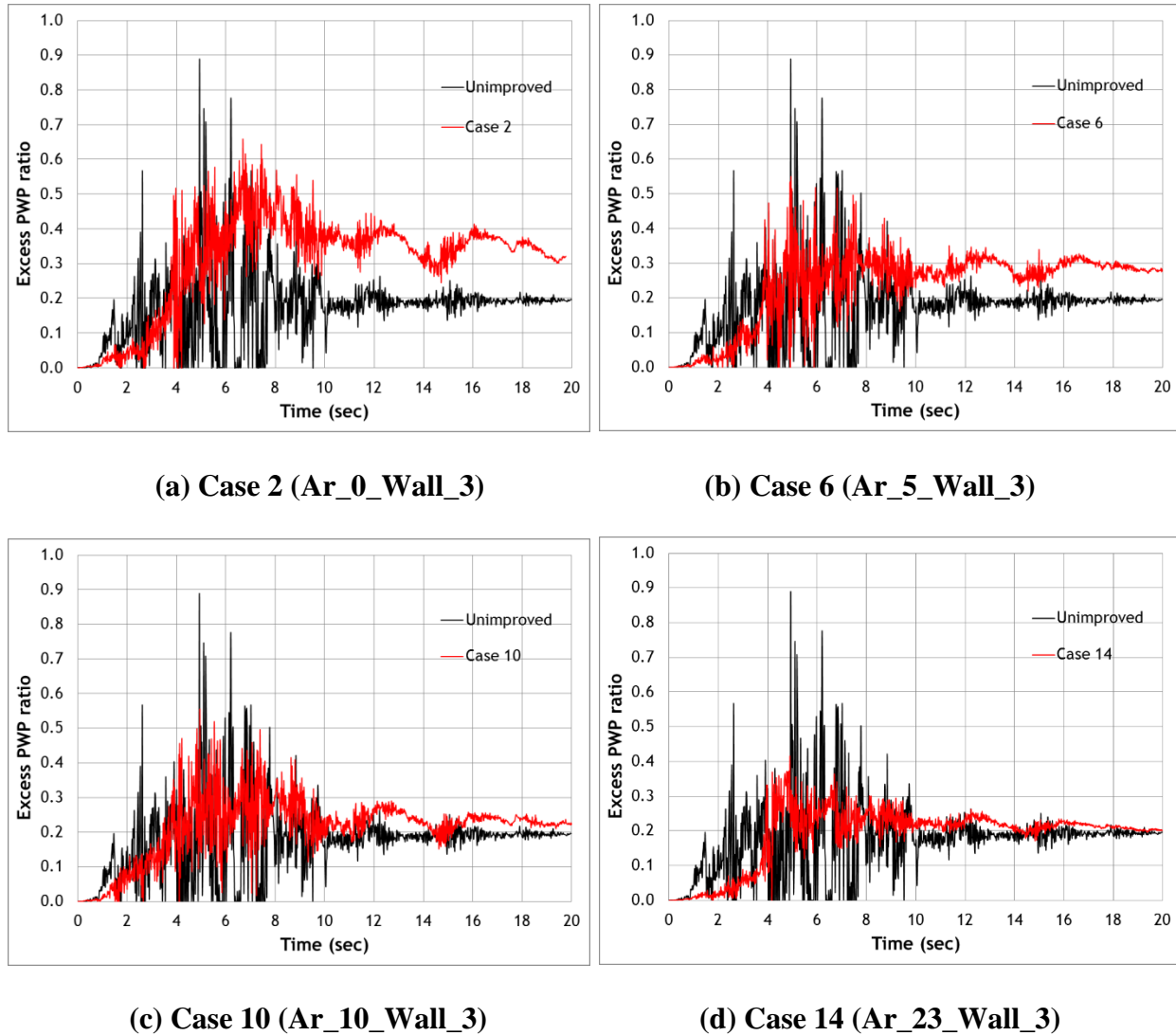
(d) Case 14 (Ar_23_Wall_3)

Figure 32. Time histories of "r_u" ratio at point B in backfill soil under various cases
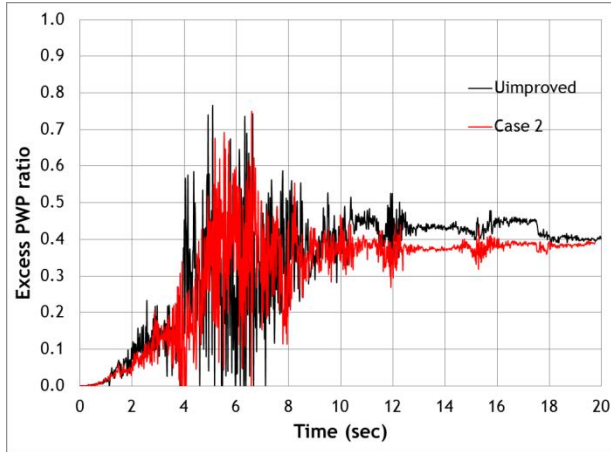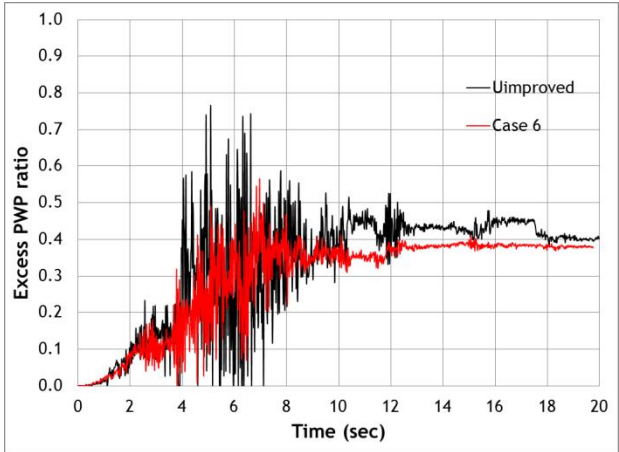
(a) Case 2 (Ar_0_Wall_3)
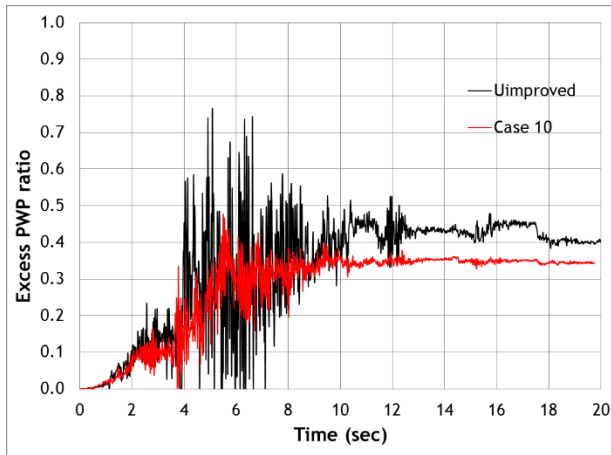
(b) Case 6 (Ar_5_Wall_3)
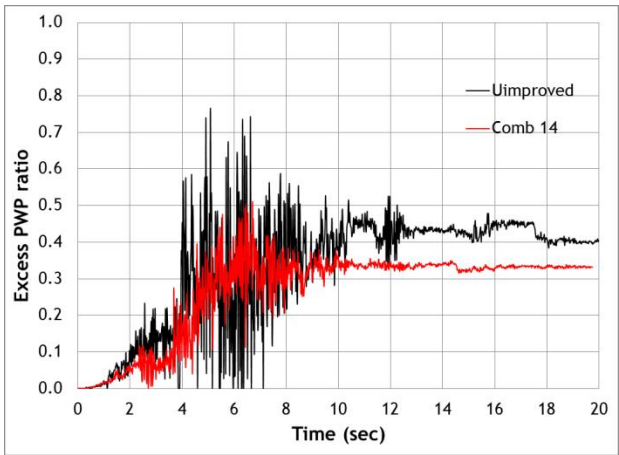
(c) Case 10 (Ar_10_Wall_3)

(d) Case 14 (Ar_23_Wall_3)

Figure 33. Time histories of "r_u" ratio at point F in backfill soil under various cases
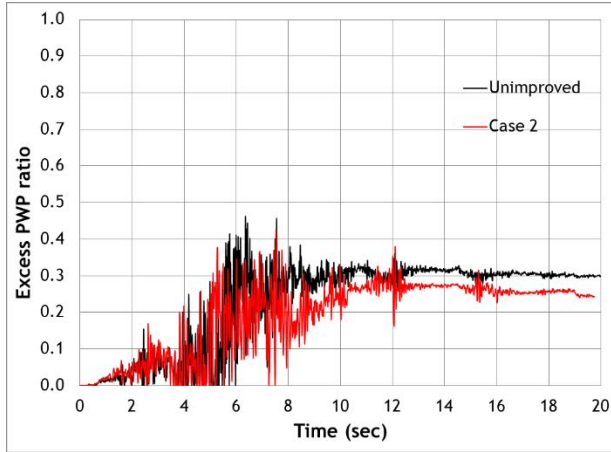
(a) Case 2 (Ar_0_Wall_3)
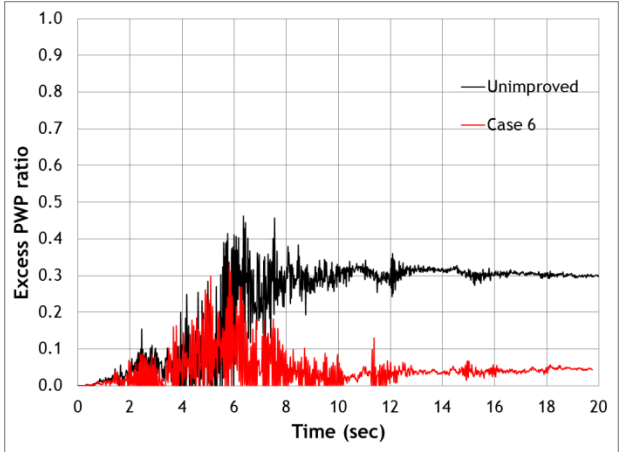
(b) Case 6 (Ar_5_Wall_3)
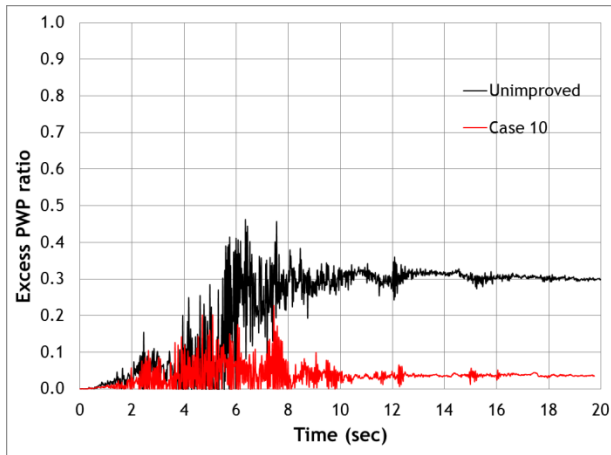
(c) Case 10 (Ar_10_Wall_3)
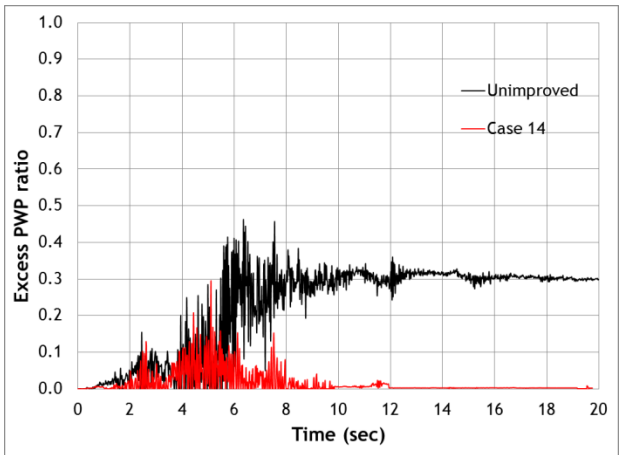
(d) Case 14 (Ar_23_Wall_3)

Figure 34. Time histories of "r_u" ratio at point H in foundation soil under various cases
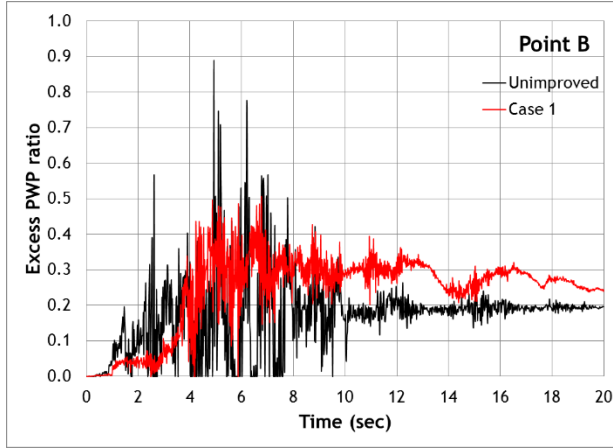
(a) Point B in Case 1 (Ar_0_Wall_1)
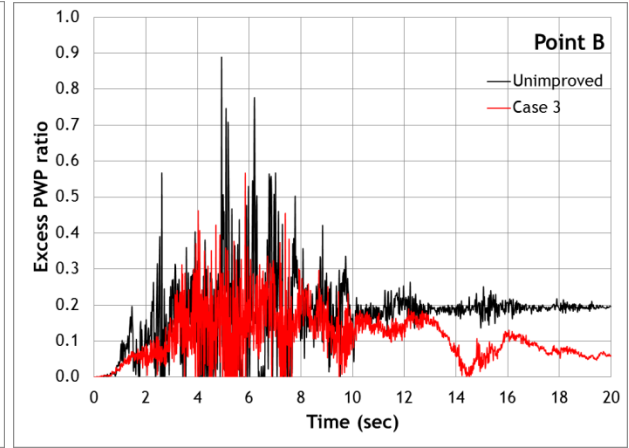
(b) Point B in Case 3 (Ar_0_Wall_5)
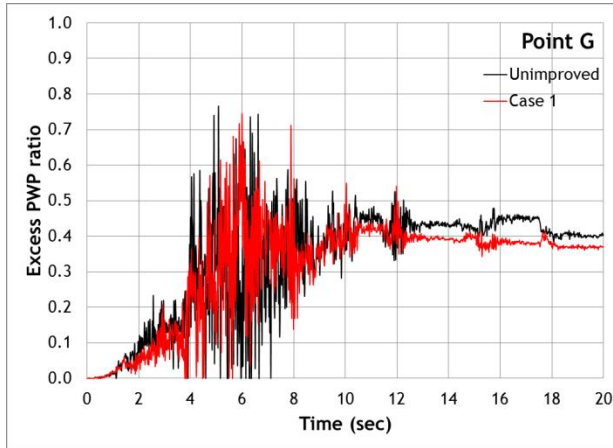
(c) Point G in Case 1 (Ar_0_Wall_1)
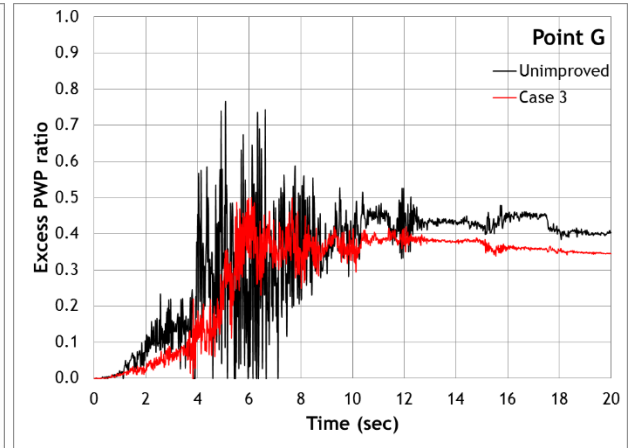
(d) Point G in Case 3 (Ar_0_Wall_5)
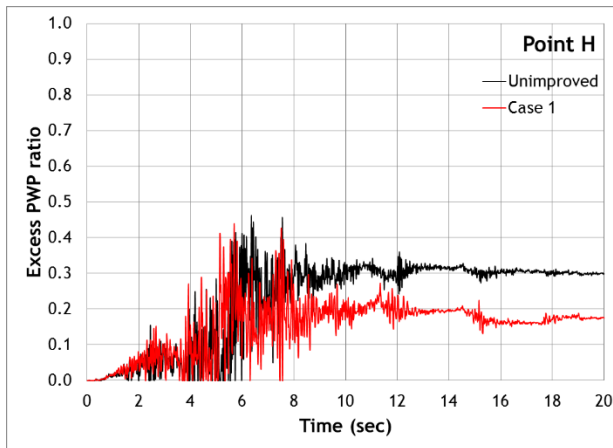
(e) Point H in Case 1 (Ar_0_Wall_1)
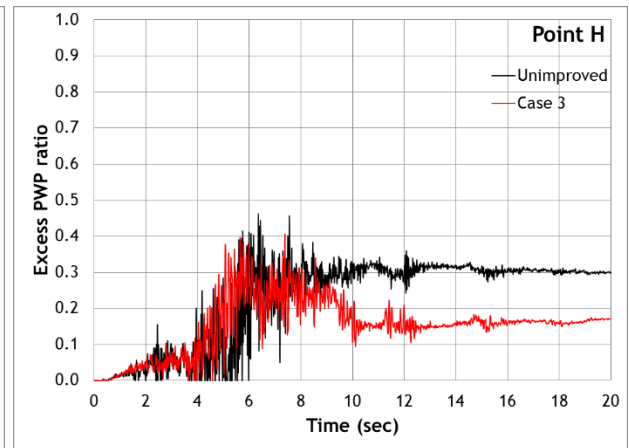
(f) Point H in Case 3 (Ar_0_Wall_5)

Figure 35. Time histories of "r_u" ratio at point B, G and H in case 1 and 3, respectively

Therefore, above results on "r_u" value at these highlighted locations generally agree well with the displacement observations of the caisson quay wall-soil system. It is concluded that a satisfactory remedial program should include both foundation soil and backfill soil, and the interactive influences should be considered in remedial design. The increased seismic stability of foundation soil can also be beneficial to the stability of backfill soil based on the above observations on the improved displacements and "r_u" value obtained from various remedial programs.

6.4   Conclusions

Combining the stone column and DMM wall methods, the improved seismic performance of caisson quay wall and generations of EPWP in liquefiable soils are evaluated in this study. The improved displacement at the tope seaward corner of the quay wall and the deformations on the surface of backfill land are the two primary evaluation parameters.

The observations on system deformation and time histories of EPWP ratios at several highlighted locations within the soil generally agree well. The following conclusions of this study can be drawn:

- The remedial program of combining both two methods is effective in reducing the seismic deformation of the quay wall in the case study.

- The proposed optimum remedial program/cases (refer to Table 19) to achieve the different specified performance grades based on PIANC (2001) are:

    o   Unacceptable Level: cases 1, 2, 3, 4, 5, 8.

    o   Repairable Level: cases 6, 7, 9, 10, 11, 12, 13;

    o   Serviceable Level: cases 14 and 15;

- The improvement efficiency in the foundation soil and backfill soil appears to be positively correlated based on the results of improved vertical and horizontal displacement of the quay wall and EPWP ratios at the selected locations. Additional research is recommended to further identify and quantitate this interactive influence under various remedial designs.

- As it is expected to advance the application of combined different remedial methods with different improvement mechanisms and advantages to address the practical construction constraints and improve the improvement efficiency.

CHAPTER 7. SEISMIC DISPLACEMENT EVALUATION CHARTS

7.1   Introduction

The application of densification methods to mitigate liquefaction risk is a widely used method in practice. To conduct remedial design using compaction methods, predicting the improved residual deformation of quay walls by considering the influence of in-situ soil liquefaction is a critical but difficult step in routine remedial programs for caisson quay wall structures due to the limits on time and cost. Previous field observations on damaged quay walls have indicated that the structural failures resulted from excessive deformation rather than catastrophic collapse (PIANC, 2001). The remedial method based on displacement is desirable over the conventional force based design methods for defining the comprehensive seismic performance of port structures. Therefore, it is desirable to establish a simple estimation technique for the improved seismic deformation of quay walls based on the recommendation of PBD (PIANC, 2001).

The applicability of effective stress analysis for improved seismic performance evaluation of gravity quay wall was verified based on the results presented in Chapter 2. Ichii et al. (2002) proposed a chart-method that can be used to predict the unimproved seismic deformation of gravity caisson quay wall based on the wall height and width, thickness of foundation soil and backfill, the liquefaction resistance (e.g., SPT or CPT) of backfill and foundation soil. However, there are few studies completed to provide a reasonable estimate of improved seismic deformation with the application of ground improvement to the in-situ liquefiable soil. The influences of various improvement features such as improved zone configurations and improved soil properties on seismic deformation of quay wall are rarely

discussed. The effectiveness of the ground improvement is also a function of level of improvement extent (densification or cementation) and the volume of improved soil.

To overcome this problem, an improved seismic displacement evaluation chart method is proposed based on the conducted parametric studies by varying remedial design parameters for the caisson quay wall subjected to various levels of seismic excitations. Based on the results of the conducted parametric study, a simple estimation technique for improved seismic deformation of quay walls placed on liquefiable soils can be established. The primary objective of this chapter is to document the development of such a simplified procedure for evaluating the order-of-magnitude of improved displacement for a gravity quay wall with the input of ground improvement design parameters. Since the details on the modeling verification and deformation estimation of the unimproved case history are presented in Chapter 2, only the procedure and results of the parametric study are presented in following sub-sections.

7.2   Analyzed Parameters of the Parametric Study

According to Ichii et al. (2002), the primary factors governing seismic deformation of a caisson quay wall include the wall dimensions, foundation and backfill soil dimensions, foundation and backfill soil dimensions and liquefaction resistance, and the design parameters of the utilized remedial program. Estimating the seismic performance of a caisson quay wall in liquefiable soil requires effective-stress analysis due to its complexity and high-demand on the user, the seismic effective stress analysis is typically applied in a deterministic fashion using a single scenario. A comprehensive parametric study is necessary to cover all of these factors and evaluate the net influence of each factor on residual deformation of quay wall. This is the value of this study.

Within this chapter, the key design parameters of the vibro-compaction program and level of excitation in terms of peak ground acceleration (PGA) are investigated. The dimensions and properties of the caisson quay wall, backfill soil and foundation soil remain unchanged as reported based on the in-situ recordings.

The major analyzed parameters of the improved zone configuration can be specified by the lateral length (L) of the improved zone in backfill soil and vertical depth (D) of the improved zone in foundation soil. Both parameters are normalized by a ratio with respect to wall height (H). The improved depth in backfill soil is equal to the full thickness of backfill soil profile. Therefore, the parameters used in this study were L/H = 0.5, 1.0, 1.5, 2.0, 2.5, and 3.0 (e.g. the ratio of 3.0 refers to 3.0*18 m = 54 m away from the inward side of the quay wall in backfill soil); D/H = 0.3, 0.6, 0.9 and 1.2 (e.g. the ratio of 1.2 refers to 1.2*18 = 22 m as the full thickness of the foundation soil profile under the quay wall). In this study, the quay wall height ("H") is 18 m and the wall width ("W") is 12 m, and both remain unchanged throughout this study. The parameters are selected within the range of interest for most port structures. Identical to the model analyzed in Chapter 3, the analyzed parameters D, L, W and H in this chapter are highlighted in the quay wall-soil system in Figure 36.
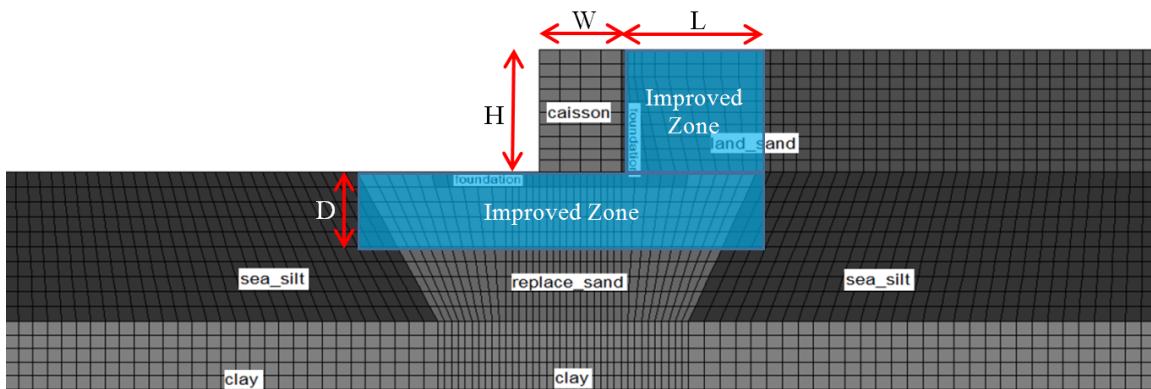
Figure 36. The quay wall-soil system to show the analyzed seismic design parameters

Similar to the design method used in Chapter 4, the improved D_r% is 60%, 70% and 80% with various probing distance of 2.3 m, 2.0 m and 1.7 m (Table 14 in Chapter 4), respectively, based on the empirical chart for preliminary design (Elias et al., 2006). The peak ground accelerations of the input seismic excitation assigned at the bottom node of the model are 0.4g, 0.6g, and 0.8g. Therefore, a comprehensive testing parametric study is shown in Table 21. In upper part (a) of Table 21, a total of 9 cases are shown by differing in the improved relative density D_r% and level of seismic input excitation (PGA); in the lower part (b) of Table 21, which is for each single case listed in part (a), total of 23 residual displacement displacements ("d" or normalized as "d/H" with respect to wall height H) are calculated by differing the densified zone configurations in terms of L/H and D/H ratios as presented above. Therefore, the total number of analyzed cases in this study is 24*9 = 216. The influences of other variables, such as caisson quay wall dimension and weight, seaward water depth, and other in-situ soil parameters, are not included. However, their influence on improved deformation estimation of quay wall can be studied by following the identical process as established herein.

Table 21. The conducted parametric study to establish the simplified chart method

(a)		Improved Dr %					
		60		70		80	
PGA (g)	0.4	Case_1		Case_2		Case_3	
	0.6	Case_4		Case_5		Case_6	
	0.8	Case_7		Case_8		Case_9	

(b)		L/H					
		0.5	1	1.5	2	2.5	3
D/H	0.3	$(d/H)_1$	$(d/H)_2$	$(d/H)_3$	$(d/H)_4$	$(d/H)_5$	$(d/H)_6$
	0.6	$(d/H)_7$	$(d/H)_8$	$(d/H)_9$	$(d/H)_{10}$	$(d/H)_{11}$	$(d/H)_{12}$
	0.9	$(d/H)_{13}$	$(d/H)_{14}$	$(d/H)_{15}$	$(d/H)_{16}$	$(d/H)_{17}$	$(d/H)_{18}$
	1.2	$(d/H)_{19}$	$(d/H)_{20}$	$(d/H)_{21}$	$(d/H)_{22}$	$(d/H)_{23}$	$(d/H)_{24}$

7.3   Parameter Sensibility on Improved Displacement of the Analyzed Quay Wall

The next challenge to overcome is to present the parametric study results from 216 numerical analyses in a meaningful way. A representative measure for the response of the quay wall is identified, i.e: a parameter termed as "Engineering Demand Parameters" or EDPs is needed to describe and quantify the structure response effectively and representatively. According PIANC (2001), the seismic performance of gravity caisson quay walls is typically evaluated by the seismic residual displacement at the seaward top corner of the walls. Therefore, the results of this conducted parametric study are summarized in terms of the residual displacement (d) at the seaward top corner of quay wall; then, the influence of the analyzed parameters can be evaluated on a comparative basis by quantifying their effects on the residual displacement (d).

First, based on the computed residual displacement (d) values, the optimum values of L/H and D/H for each of the 9 cases (shown in part (a) of Table 21) can be found with respect to different improved relative density D_r% and the peak ground acceleration value (PGA). Then, the effects of the major parameters are discussed with respect to the improved residual displacement magnitude (d) and the normalized residual displacement ratio (d/H). Therefore, the calculated displacement (d) or displacement to wall height ratio (d/H) are investigated against with the key design parameters (L/H and D/H) under the influences of various improved D_r % and seismic excitation levels (PGA) in following sections.

7.3.1   Optimum improvement zone configurations in terms of L/H and D/H values

The optimum L/H and D/H ratios for the 9 analyzed cases are shown in Table 22. The method of determining the critical L/H and D/H values are based on their improved displacement (d) values and the additional reductions in d with further increasing in L/H and D/H. For this

purpose, two evaluation criteria (1) improvement effectiveness expressed by the improved residual displacement (unit: m) and (2) improved efficiency (unitless) expressed by the ratio of displacement reduction over improvement effort indicated by the improved zone volume are used to evaluate a remedial plan. This is based on the assumption that remedial program cost primarily depends on the volume of improved soil. For illustration purposes, case 7 with improved D_r% = 60 % and PGA = 0.8 g is illustrated, and results of all the other cases are found similar to Case 7. In this study, the quay wall height is 18 m and the initial unimproved displacement at the top seaward corner of the caisson quay wall is computed to be 4.3 as presented in Chapter 3.

Table 22. The optimum values of D/H and L/H and the computed residual displacement (d)

Case ID	Improved D_r %	PGA (g)	L/H	D/H	d (m)	d/H
1	60	0.4	1.5	0.6	1.37	0.08
2	70	0.4	1.5	0.6	1.13	0.06
3	80	0.4	1.5	0.6	0.74	0.04
4	60	0.6	1.5	0.6	2.03	0.11
5	70	0.6	1.5	0.6	1.81	0.10
6	80	0.6	1.5	0.6	1.14	0.06
7	60	0.8	2.0	0.6	2.52	0.14
8	70	0.8	2.0	0.6	2.31	0.13
9	80	0.8	2.0	0.6	1.41	0.08

As can be seen in Figure 37, increasing L/H and D/H leads to a reduction in displacement (d) for all presented curves differing in D/H ratios. However, the magnitude of reduction in (d) or the additional benefit becomes less apparent when the value of L/H and D/H equals or exceeds to approximately 2.0 and 0.6, respectively. Therefore, the L/H value of 2.0 and D/H value of 0.6 is recommended as the optimum improved zone configuration under this specific condition. The reduced residual displacement is predicted to be 2.52 m and the achieved reduction percentage is approximate 62% (1-2.52/6.59=0.62 or 62%). This improved deformation may not be acceptable

since the improved displacement of 2.52 m is still larger than the repairable limit of near

complete collapse of less than 1.8 m under the strong earthquake motion for gravity caisson wall

(PIANC 2001). Therefore, specifying the improved D_r % of 80 % and the minimum L/H and

D/H value of 2.0 and 0.6 (36 m and 11 m in this case), respectively, is recommended to achieve

the improved displacement to be 1.41 m and the reduction percentage to be 80% (1-

1.41/6.59=0.8 or 80%).

(a) Computed displacement   (b) Computed *d/H* ratio
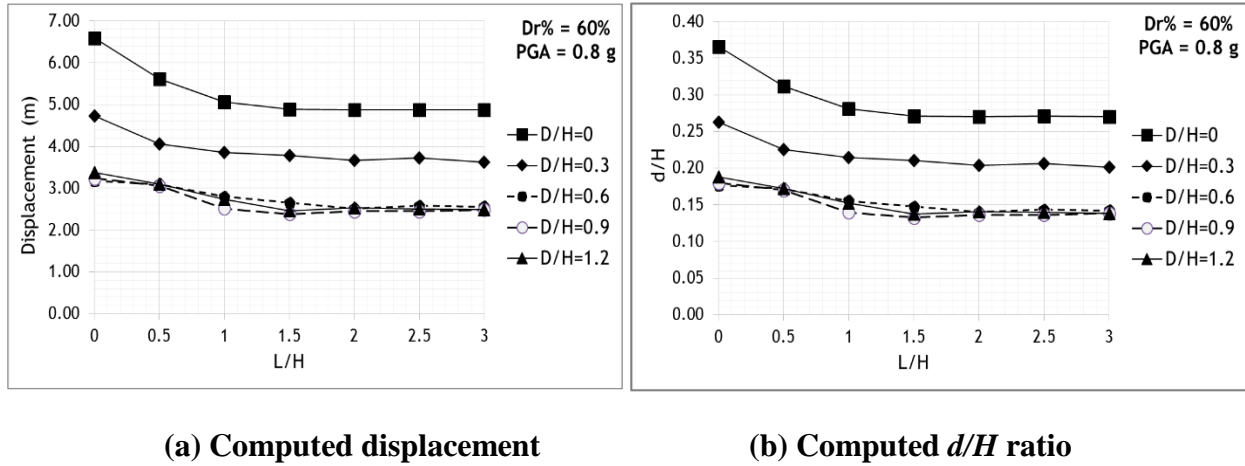
Figure 37. Calculated residual displacements with L/H and D/H ratio for case 7

7.3.2 Improvement zone length (L/H) in liquefiable backfill soil

The effects of lateral length of improvement zone to wall height ratio (L/H) on the

improved residual displacement are shown in Figure 38 (a-b for 0.4 g, c-d for 0.6 g and e-f for

0.8 g) for the improved relative density D_r% of 70% under three examined PGA values. For all

D/H values, increasing the improved zone length (L) in the backfill soil or the L/H values

exceeds 1.5 to 2.0, the influences of further increasing L/H or improving additional length of

backfill soil beyond this distance of 1.5 to 2.0 times of the quay wall height become less obvious

for the examined rang of D/H values.
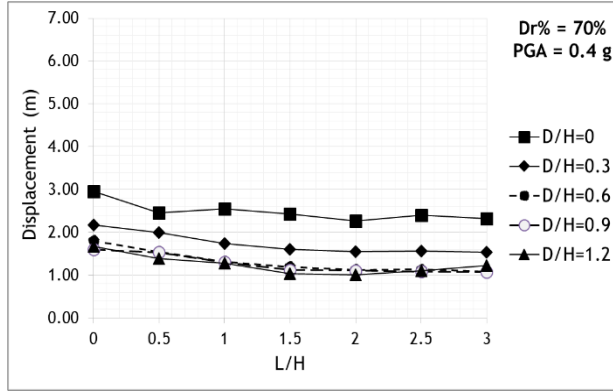
(a) **Displacement (PGA = 0.4 g)**
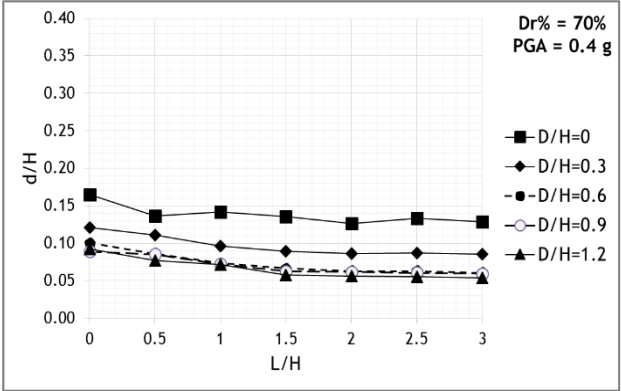
(b) *d*/H **ratio (PGA = 0.4 g)**
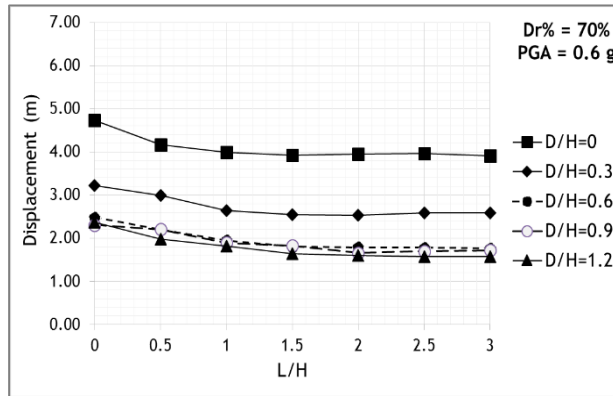
(c) **Displacement (PGA = 0.6 g)**
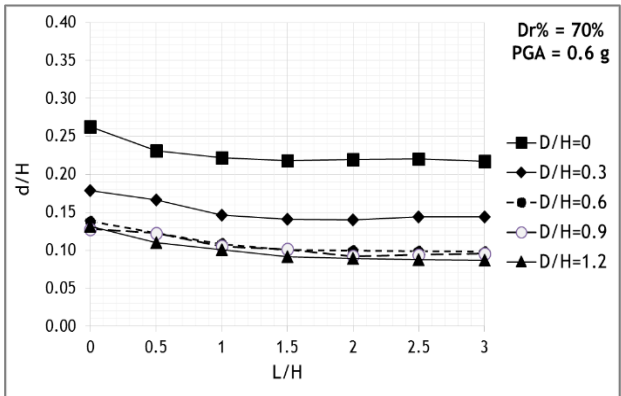
(d) *d*/H **ratio (PGA = 0.6 g)**
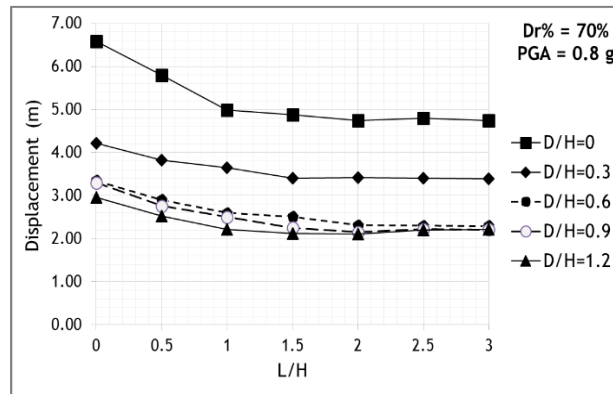
(e) **Displacement (PGA = 0.8 g)**
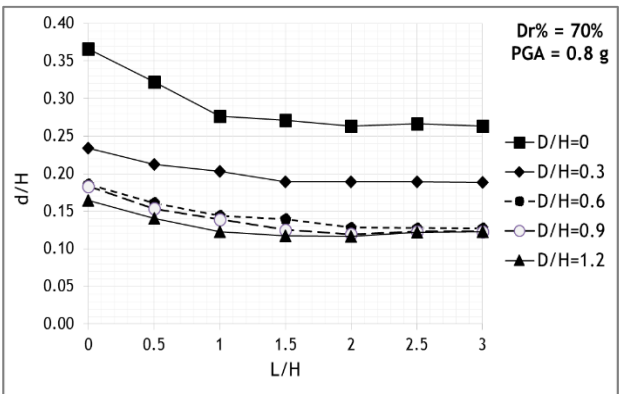
(f) *d*/H **ratio (PGA = 0.8 g)**

Figure 38. Effect of L/H ratio for three examined PGAs (D_r% = 70%)

7.3.3 Improvement zone depth (D/H) in liquefiable foundation soil

The effects of the improved zone vertical depth to wall height ratio (D/H) on the improved residual displacement are shown in Figure 39 for the improved D_r % of 70% under three examined PGA values. For all L/H values, increasing the improved zone depth (D) in the foundation soil or the D/H value can decrease the residual displacement of the quay wall, and the reduction magnitude also depends on the applied PGA and improved relative density D_r%. However, when D/H value exceeds 0.6, the influences of further increasing D/H becomes less significant for the examined range of L/H values.

7.3.4 Improved relative density (Dr %) and seismic excitation level (PGA)

Based on the optimum improvement zone configuration results presented in Table 22, these results are plotted against with their corresponding improved relative density D_r% under the various examined levels of excitation (PGA) in Figure 40, As seen within the typical range of improved relative density D_r% (from 60% to 80% analyzed in this study) for the vibro-compaction method (Elias et al., 2006), increasing the improved relative density D_r% or compacting with a closer probing distance would result in the reduced seismic deformation at a given level of excitation expressed by PGA. Also the higher level of excitation expressed by PGA would also lead to a larger improved residual displacement for a given improved relative density D_r% value.
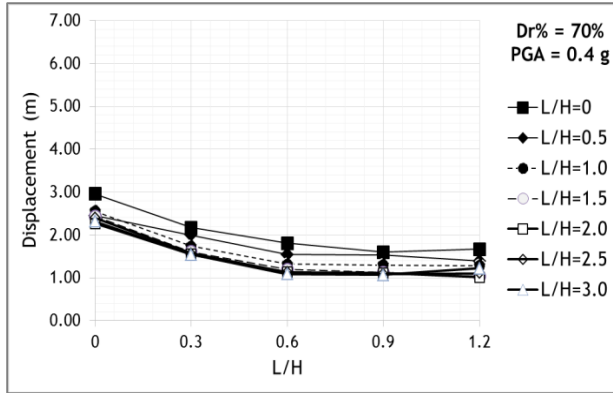
(a) Computed displacement
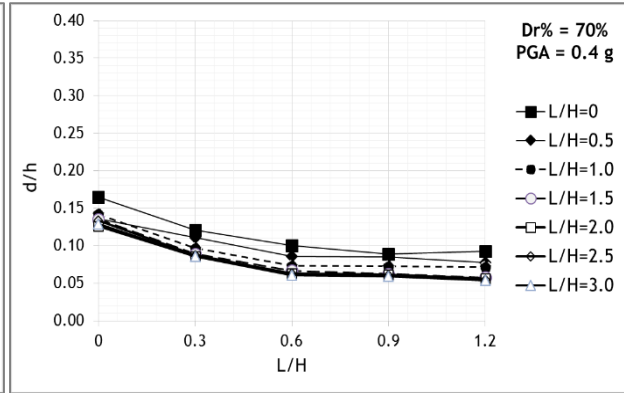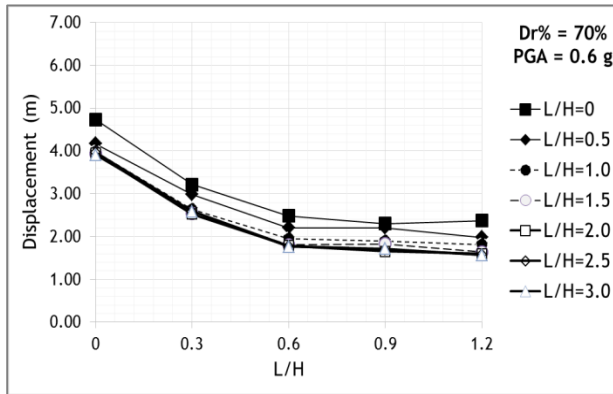
(b) Computed *d*/H ratio

(c) Computed displacement
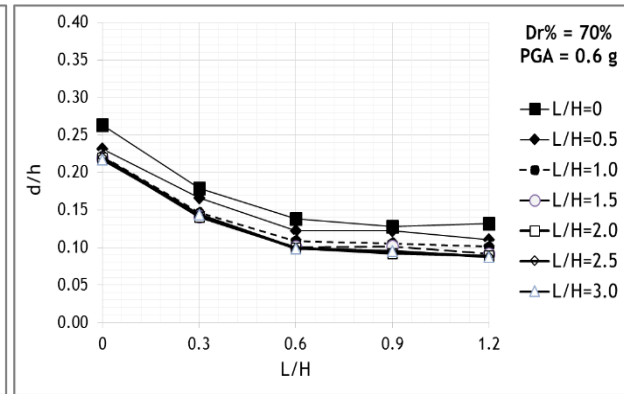
(d) Computed *d*/H ratio
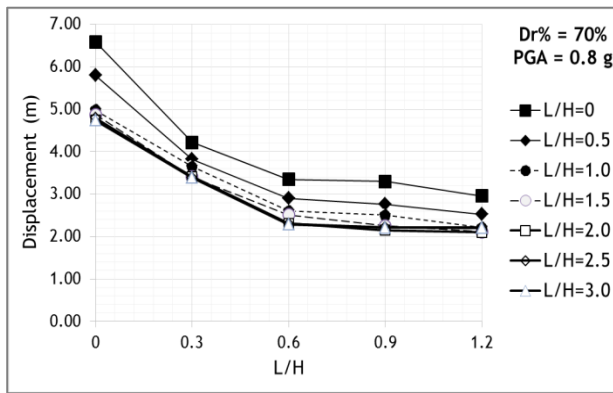
(e) Computed displacement
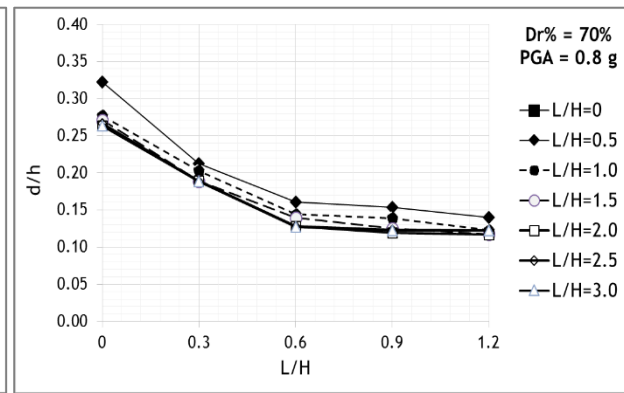
(f) Computed d/H ratio

Figure 39. Effect of D/H ratio for three examined PGAs (D$_r$% = 70%)
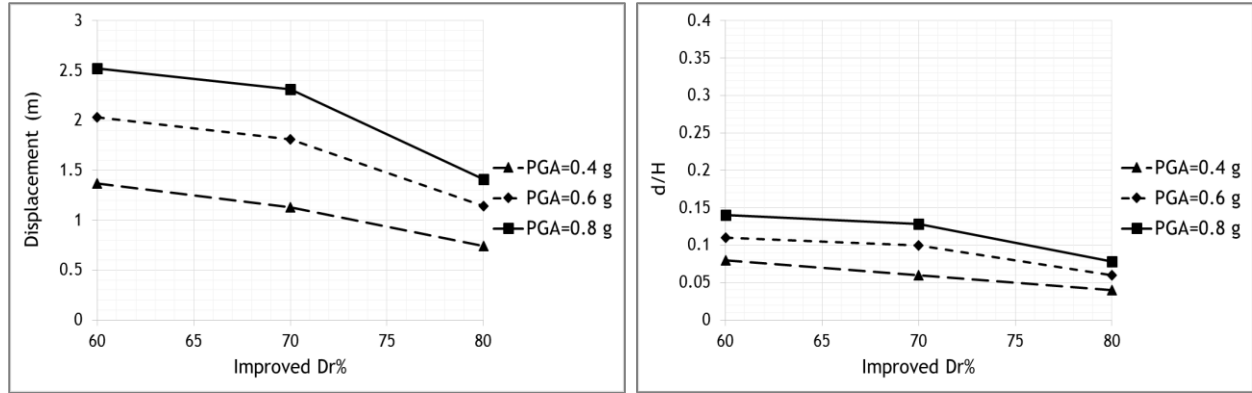
(a) Computed displacement   **(b) Computed *d*/H**

Figure 40. Effect of improved relative density D_r% for three examined PGAs

7.3.5 Overall parameter sensitivity

Among the analyzed parameters considered herein, the most sensitive remedial design parameters affecting the improved residual displacement of quay wall under a level of excitation is the improved zone configuration (expressed by D/H) in foundation soil, and the second is the improved zone configuration (expressed by L/H) in backfill soil. Especially under the intensive shaking (comparing Figure 38-(e) and (f) with Figure 39-(e) and (f), respectively), increasing D/H value is more beneficial than increasing L/H on the displacement reduction. This observation agrees well with the conclusion by Iai et al. (2000) that effect of improving foundation soil on the deformation of quay wall is approximately two times of that by improving backfill soil. The effect of improved relative density D_r% on improved deformation becomes slightly less obvious with increasing in excitation levels (Figure 40). The level of excitation also influences the improved displacement markedly (Figure 40). Therefore, specifying the designed earthquake motion is a critical step in remedial design to ensure that the improved performance satisfies the specified performance grade.

The parametric study above is for a caisson quay wall of H = 18 m and W = 12 m, and the soils in the model are following the description in Inagak et al. (1996), where both foundation

soil and backfill soil are liquefiable with initial SPT $(N_1)_{60}$ of 10 to 15. Furthermore, the above results under various scenarios with different wall height and width, in-situ soil properties and thickness, and frequency of excitations should be also studied by following a similar method as adopted in this study.

7.4   Procedure for Evaluating Improved Quay Wall Deformation

As mentioned earlier, the numerical analysis is particular useful for optimizing the remedial program using ground improvement based on PBD (PIANC, 2001). However, performing numerical analysis normally requires a high level of engineering and reasonable amount of effort. It is not always easy to apply for routine engineering practice. To overcome this problem, a simplified method is necessary for evaluating the improved seismic deformation with a given ground improvement remedial design features in routine design practice. A similar method has been proposed to quickly access the failure model and deformation magnitude of the caisson quay wall (Ichi et al., 2002). However, remediation effect was not incorporated in this method. The results of the above presented parametric study offer a basis to establish such a method incorporating the influence of soil improvement by the vibro-compaction method on improved seismic deformation prediction. Given the improved length and depth in liquefiable soil behind and below the quay wall and the specified relative density D_r% or SPT $(N_1)_{60}$, a simplified procedure can be developed for predicting the improved deformation of gravity wall that is similar to the wall described in Ichi et al. (2002). The flow chart for the simplified procedure is shown in Figure 41.
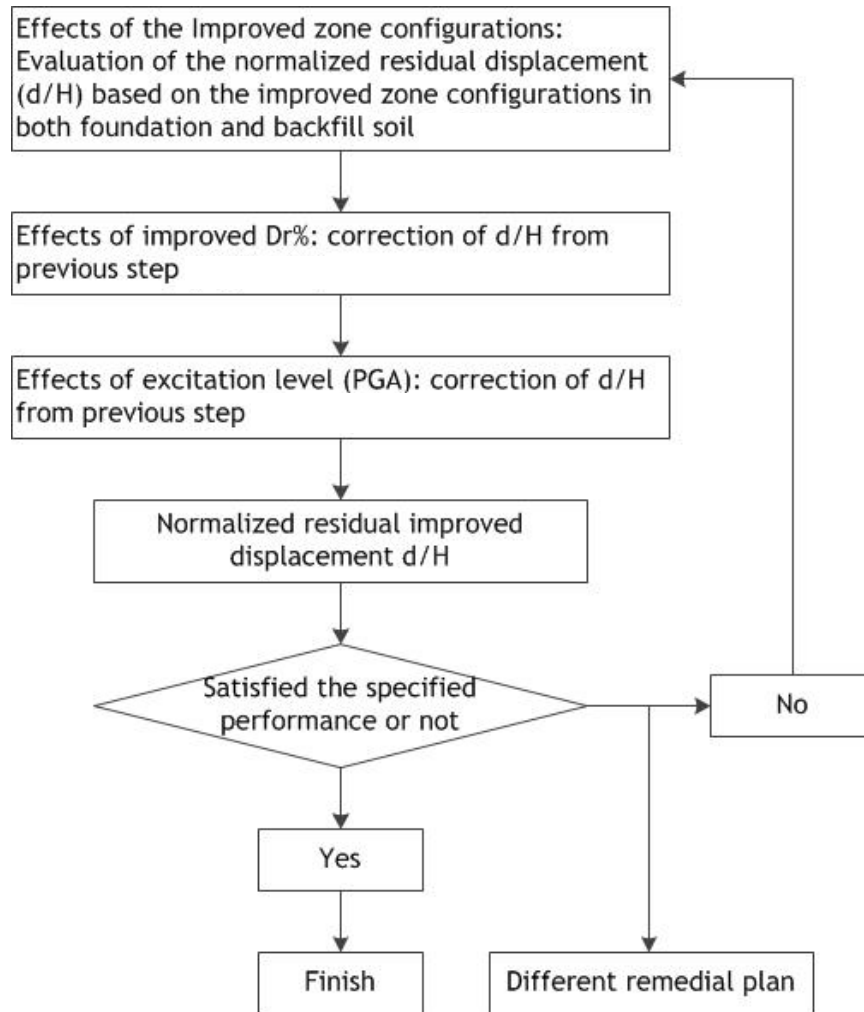
Figure 41. The proposed procedure to evaluate the improved quay wall displacement

In the proposed method, the improved residual displacement can be evaluated with respect to the above analyzed parameters in the order of its sensitivity to the improved deformation. As the first step, a rough estimation is made based on the improved zone configuration in Figure 38 and 39. Then, the correction for improved relative density $D_r\%$ and designated earthquake motion expressed by PGA is applied based in Figure 40.

7.5 Conclusions and Recommendations

The improved displacement of quay walls was investigated analytically within a framework of a well-calibrated case study through a comprehensive parametric study including

216 analyses by varying the improved zone configurations, improved relative density $D_r\%$ and level of excitation (PGA). A set of optimum designs in terms of improved zone configurations are found by differing improved relative density $D_r\%$ and level of excitations. The conclusions are applicable for typical caisson quay wall structures with wall height of 18 m and width of 12 m approximately, and the presented soil conditions described in Inagak et al. (1996).

The major conclusions from this study are: (1) the first sensitive parameter in the studied wall is the improved zone depth (D/H) in foundation soil, and a critical value of 1.5 to 2 for L/H is found to be most effective in reducing the residual deformation of the wall; (2) the influence of improved relative density $D_r\%$ becomes less under intensive shaking; (3) increasing the level of excitation in terms of PGA also markedly increase the improved deformation while all other parameters remain constant.

Based on the parametric study, a simple procedure of estimating the improved residual deformation of caisson quay wall is proposed in Figure 41. The applicability of the proposed procedure should be further confirmed by case history data. The other parameters including quay wall dimension and weight, in-situ liquefiable soil conditions and earthquake loading frequency should be further studied by following the similar method adopted in this study. The above analyses improve the understanding and prediction of the complex improved seismic behavior and enhance the engineering judgment in applying liquefaction mitigation to the gravity caisson quay wall on the liquefiable soil.

CHAPTER 8. A UNIFORM FRAMEWORK FOR EVALUATION AND COMPARISON OF IMPROVEMENT EFFECTIVENESS

8.1   Formulation of the Framework

The proposed uniform framework is established by adopting the philosophy of the PBD defined in PIANC (2001). The objective of seismic PBD is that the improved performance can satisfy the specified performance grades with allowance of limited liquefaction and seismic deformation. Therefore, the performance grades, in terms of structure deformations and economical loss used as the effectiveness evaluation and comparison criteria, are considered and compared among the various remedial programs. As indicated in Kramer (2008), the most complete evaluation a called "loss-level implementation," can also be implemented based on additional information on primary and secondary economical loss, which is usually case-specific and difficult to extrapolate to other scenarios. Therefore, only the deformation, improvement efficiency and performance grades (PIANC, 2001) are considered herein.

The analytical tool of using coupled effective-stress analysis is used to evaluate the improved performance of structure. Soil-foundation-structure interaction analyses, always a challenging task in geotechnical engineering, can be performed without prior constraints and pre-defined of failure mechanisms and without as a complete a characterization of nonlinear stress-strain behavior. Even though such analyses are far more time and effort-consuming than the conventional stress-based analysis, they can provide direct estimates of wide range of geotechnical and structural seismic response parameters without the constraints of a priori assumptions required by the simpler models. This allows the more comprehensive evaluation and comparison of the improvement performance and effectiveness. The flowchart in Figure 42 shows the process of the proposed uniform framework.
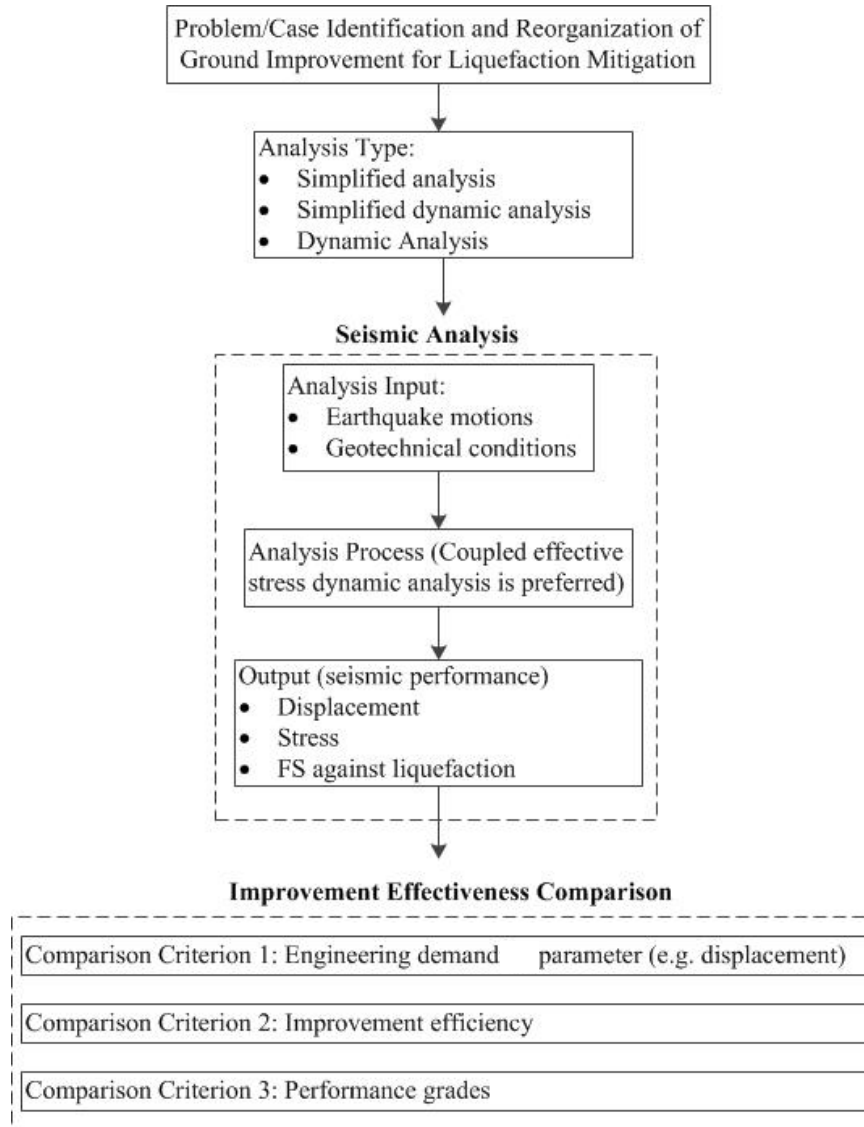
Figure 42. Flowchart of the framework for effectiveness evaluation and comparison

8.2   Improvement Effectiveness Evaluation and Comparison

The proposed framework is implemented within a well-calibrated case history, a damaged caisson quay wall placed in liquefiable soil reported in Kobe earthquake in 1995 (Inagak et al., 1996), and the details of unimproved failure mechanisms and improved performances by various analyzed countermeasures are presented in previous chapters. The improved performance is determined primarily by focusing on the seismic residual deformations of the quay wall-soil system. As shown in Figure 42 of the flowchart, the evaluation and

comparison criteria include three criteria: improved deformation (EDP) of the caisson quay wall, improvement efficiency and performance grades, which are discussed individually in following sub-sections.

The details of examined remedial cases, their corresponding case ID number and the associated features for each analyzed method can be found in previous chapters. For the convenience of this chapter, all of the examined remedial cases, case ID and their design features are provided in Table 23 for the following discussion. Similar to the previous expressions on the improvement zone dimensions, "D" and "L" in Table 23 represent for the improvement zone depth and lateral length in foundation soil and backfill soil, respectively. In Table 23, the remedial case ID numbers for all three analyzed methods are highlighted in gray, and the analyzed parameters in parametric study are written in color of red. The remedial cases ID in the three sub-tables of Table 23 are parallel to each other. In following figures, the improved effectiveness of each examined remedial cases for each remedial method are plotted, and the X-coordinate is the remedial case ID.

Table 23. Summary table of the remedial case IDs for three analyzed remedial methods

(a) Parametric study for the vibro-compaction method

Vibro-Compaction													
Vibro-compacted soil zone configurations													
Remedial Option ID		"L" in backfill soil (m)											
		0	5	10	15	20	25	30	40	50	60	70	80
"D" in foundation soil (m)	0	1	2	3	4	5	6	7	8	9	10	11	12
	3	13	14	15	16	17	18	19	20	21	22	23	24
	6	25	26	27	28	29	30	31	32	33	34	35	36
	9	37	38	39	40	41	42	43	44	45	46	47	48
	12	49	50	51	52	53	54	55	56	57	58	59	60
	15	61	62	63	64	65	66	67	68	69	70	71	72
	18	73	74	75	76	77	78	79	80	81	82	83	84
	21	85	86	87	88	89	90	91	92	93	94	95	96
	24	97	98	99	100	101	102	103	104	105	106	107	108

(b) Parametric study for the Deep soil mixing method

Deep Soil Mixing							
DMM improved zone volume configurations							
(Table 15 and 17 in Chapter 5)							
Remedial Case ID	"D"	"L"	Scenario / Category	Remedial Case ID	"D"	"L"	Scenario / Category
1	7	5	1 / 1	33	21	10	1 / 3
2	14	5	1 / 1	34	21	20	1 / 3
3	21	5	1 / 1	35	21	30	1 / 3
4	7	10	1 / 1	36	21	40	1 / 3
5	14	10	1 / 1	37	5	5	2 /
6	21	10	1 / 1	38	5	10	2 /
7	7	15	1 / 1	39	5	15	2 /
8	14	15	1 / 1	40	5	20	2 /
9	21	15	1 / 1	41	5	25	2 /
10	7	20	1 / 1	42	5	30	2 /
11	14	20	1 / 1	43	5	35	2 /
12	21	20	1 / 1	44	5	40	2 /
13	7	5	1 / 2	45	10	5	2 /
14	14	5	1 / 2	46	10	10	2 /
15	21	5	1 / 2	47	10	15	2 /
16	7	10	1 / 2	48	10	20	2 /
17	14	10	1 / 2	49	10	25	2 /
18	21	10	1 / 2	50	10	30	2 /
19	7	15	1 / 2	51	10	35	2 /
20	14	15	1 / 2	52	10	40	2 /
21	21	15	1 / 2	53	15	5	2 /
22	7	20	1 / 2	54	15	10	2 /
23	14	20	1 / 2	55	15	15	2 /
24	21	20	1 / 2	56	15	20	2 /
25	7	10	1 / 3	57	15	25	2 /
26	7	20	1 / 3	58	15	30	2 /
27	7	30	1 / 3	59	15	35	2 /
28	7	40	1 / 3	60	15	40	2 /
29	14	10	1 / 3	61	40	29	3 /
30	14	20	1 / 3	62	40	36	3 /
31	14	30	1 / 3	63	45	29	3 /
32	14	40	1 / 3	64	45	36	3 /

(c) Parametric study for the combined stone column and DMM wall method

Stone Column + DMM Wall Ar% of SC in foundation soil; No. of DMM wall in backfill soil (Table 19 in Chapter 6)		
Remedial Case ID	Ar% of SC	No. of DMM Wall
1	0	0
2	0	1
3	0	3
4	0	5
5	5.5	0
6	5.5	1
7	5.5	3
8	5.5	5
9	10	0
10	10	1
11	10	3
12	10	5
13	23	0
14	23	1
15	23	3
16	23	5

8.2.1   Comparison criterion 1: improved deformation

Seismic deformation is a particularly important consideration for geotechnical earthquake engineering. The quantitative determination of deformations provides direct and understandable information to evaluate and compare the effectiveness of ground improvement and adjust the remedial design. Figure 43 shows the effectiveness comparison expressed in terms of residual displacement of the top seaward corner of the quay wall. The improved vertical and lateral improved displacements by various remedial cases (differing in applied remedial method and design parameters) are plotted. The conducted parametric study for each method can be found in previous chapters. As shown, the improved displacements in both directions at the top corner of quay wall gradually decrease with the increasing remedial case ID for all three methods. This is

because of improved soil zone in backfill and/or foundation soils or improvement extents in each remedial case gradually increase with case ID.
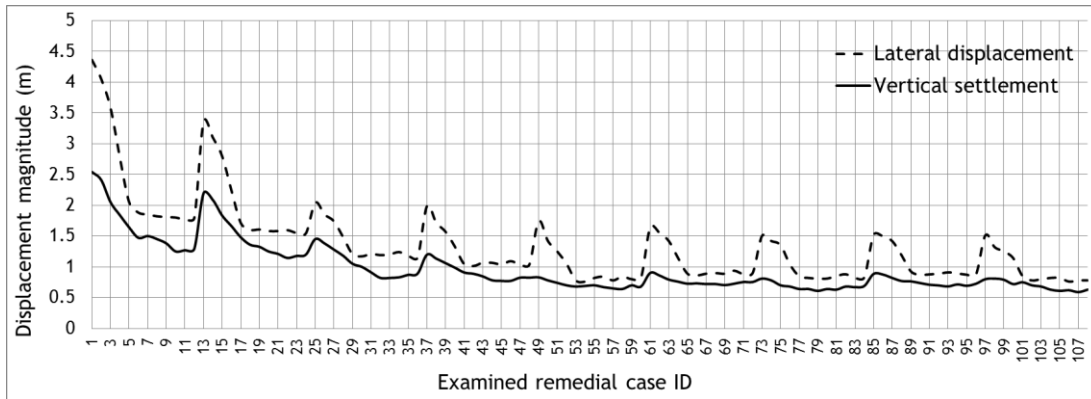
(a) Vibro-compaction method
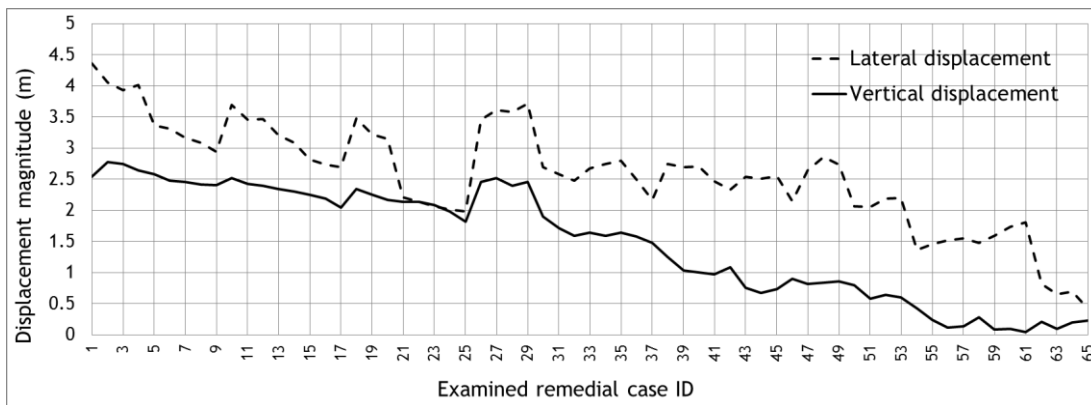
(b) Deep soil mixing method
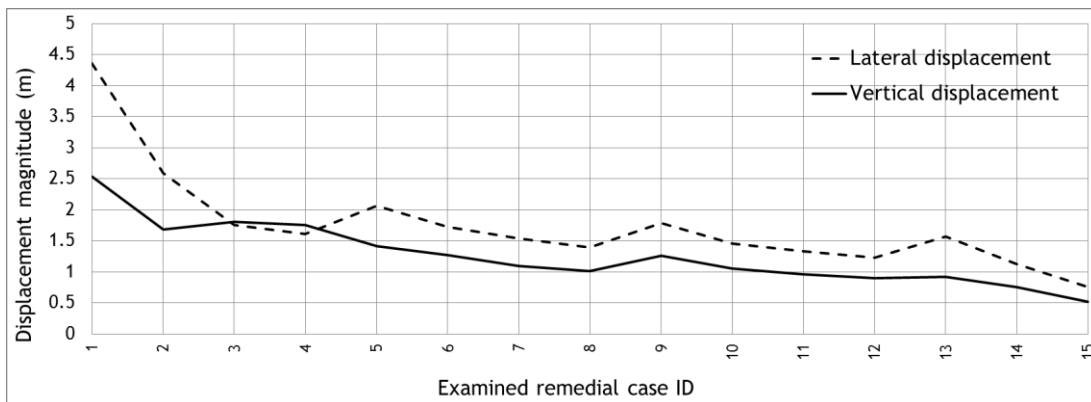
(c) The combined stone column and DMM wall method

Figure 43. Effectiveness comparisons based on the improved displacement magnitude (m)

8.2.2 Comparison criterion 2: improvement efficiency

Improvement efficiency or reduction factor is another comparison criterion, as recommended in Adams et al. (2011) and Motamed et al. (2010). Although the definition is slightly different by various researchers, the objective of defining this parameter is to highlight and compare the effectiveness by quantifying the difference of certain representative (EDPs) with and without for each specific remedial design differing in utilized remedial method and the remedial design parameters. The selected EDPs are always different for various structures or applied remedial methods. In general, improvement efficiency is regarded as a case-specific indicator of cost efficiency (Eq. 9) for a certain remedial program. The calculation formula of improvement efficiency is:

$$\text{Improvement efficiency}_{(i)} = \frac{\left(1 - \frac{\text{EDP}_{(i)} \text{ with mitigation}}{\text{EDP}_{(i)} \text{ without mitigation}}\right) \times 100}{\text{Total improved zone volumn}} \qquad \text{Equation 9}$$

The residual lateral displacement at the top seaward corner of quay wall is selected as the EDP for comparison of improvement efficiency. As shown in Figure 44, the improvement efficiencies of DMM method (as discussed in Chapter 5) are generally greater than that of vibro-compaction (as discussed in Chapter 4). The peak value of efficiency can reach 0.7 to 0.8 and 0.15 for DMM and vibro-compaction method, respectively. According, based on the results in Figure 44, for this specific quay wall-liquefiable soil system, the most efficient cases for each remedial method and associated design features including improved zone dimension and properties can be identified. The combined stone column and DMM wall method is not considered because of its different improving mechanisms.

It should be noted that neither comparison criterion 1 (EDP) nor 2 (improvement efficiency) is comprehensive enough for making the final decision of seeking a sufficient and economical remedial design. It is always important for a successful remedial design to satisfy the

specified deformation criteria with minimum cost, which indicates that both criteria 1 and 2 should be properly considered (Adams et al., 2011). By considering the residual operation and function of improved structures, it is necessary to conduct the comparison based on the specified performance grade. Also, another observation in Figures 43 and 44 is that both improved displacement and improvement efficiency roughly show a similar trend and all remains unchanged for certain remedial cases even through these cases differ in improved zone volume and improvement extent. Therefore, this observation can help to optimize the remedial features by determining the adequately minimum improved zone volume and improvement extent.
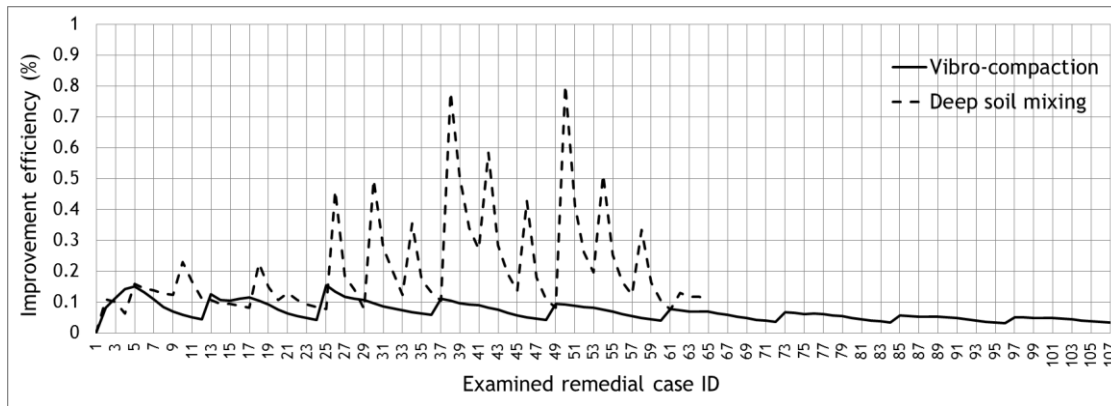
Figure 44. Effectiveness comparison based on improvement efficiency

8.2.3 Comparison criterion 3: specified performance grades

More emphasis has been placed, particularly in research, on response prediction (criterion 3) than on the prediction of physical damage (criterion 1). The response prediction is also more understandable to both engineering professionals and non-professionals. The concept of scenario-based design, i.e., based on the residual status of structures post-earthquakes have been presented in earlier documents (PHRI, 1998). According the specified performance grades recommended in PIANC (2001), the examined remedial cases for each method can be classified into three categories based on their improved status: serviceable, repairable and unacceptable. For caisson quay wall structure, the seismic residual functionality can be expressed using the

wall displacement together with the tilting angle and surface deformation in backfill soil (PIANC, 2001). The identifications of representative EDPs expressing the residual performance and functionality for various structures are still under development (Kramer, 2008).

Table 24. Specified performance grades by PIANC (2001)

Level of Damage	Structural	Operational
Degree I: Serviceable	Minor or no damage	Little or no loss of serviceability
Degree II: Repairable	Controlled damage	Short-term loss of serviceability
Degree III: Near collapse	Extensive damage in near collapse	Long-term loss of serviceability
Degree IV: Collapse	Complete loss of structure	Complete loss or serviceability

Table 25. Effectiveness comparison based on the improved performance grades

Remedial Methods	Examined Remedial Cases_ID		
	Specified performance grades (PIANC 2001)		
	Unacceptable	Repairable	Serviceable
Vibro-compaction	All of the rest examined cases	53 - 60, 77 - 84, 101 - 108	None
Deep soil mixing	All of the rest examined cases	62, 63, 64	65
The combined stone column and DMM wall	1, 2, 3, 4, 5, 8	6, 7, 9, 10, 11, 12, 13	14, 15

Based on the specified performance grades in terms of structural and operational damage in Table 24 and 25, the examined remedial cases of three methods can most likely to improve the quay wall to be the "Repairable level", only a few results in the "Serviceable" level, and the rest majority should be used due to the unacceptable improved performance.

Therefore, the improved quay wall may still be temporarily unavailable after strong earthquake loadings with a magnitude of 7.5 similar to the seismic input as used in this study. If the quay wall is critical and required to remain serviceable, using the deep soil mixing along or

the combined stone column and deep soil mixing are recommended by following the proposed remedial features in cases 14 65 and 15, respectively.

8.3   Improvement Effectiveness Comparison Summary

The proposed framework can be used to evaluate and compare the effectiveness of various different remedial methods for liquefaction mitigation based on the well-estimated dynamic response of structure-soil system. For better use of the estimation results, the dynamic response can be expressed by numerical EDPs or pre-specified performance grades as the evaluation criteria.

The results of this chapter indicate the majority of examined remedial cases using the three methods are not acceptable due to the excessive residual deformation. Under this particular examined earthquake motion recorded from Kobe earthquake in 1995, the vibro-compaction method can mostly likely to improve the caisson quay wall to be repairable; deep soil mixing and the combined stone column and deep mixing wall method can possibly improve the quay wall to be serviceable and repairable with significant but still minimally required amount of improvement effort to both foundation soil and backfill soil. The three performance grades "Unacceptable", "Repairable" and "Serviceable" are defined specifically for caisson quay wall structures.

CHAPTER 9. CONCLUSIONS AND RECOMMENDATIONS

Soil liquefaction always leads to severe damages in most types of civil infrastructures including caisson quay wall structures analyzed in this study. Various forms of mitigation including ground improvement have been used to reduce this damage. However, a uniform evaluation framework that is applicable to evaluate and compare the improvement effectiveness of different remedial geoconstruction methods for liquefaction mitigation has not been well established and applied to advance the current understanding on this issue. The lack of such a framework leads difficulty in the selection of remedial measures and mitigation design optimization.

This study covers various issues involved under the topic of liquefaction mitigation by ground improvement. These issues include: (1) the general consideration and selection of ground improvement methods for liquefaction mitigation (2) optimization of remedial designs, and (3) effectiveness evaluation and comparison of three commonly used countermeasures vibro-compaction, stone column and deep soil mixing method.

Issue (1) is addressed by establishing an interactive technology selection system based on a comprehensive review on suitability and constraints of ground improvement methods for liquefaction mitigation.

Issues (2) and (3) are completed within a well-calibrated case history through numerical analyses using FLAC^{3D} (Itasca, 2007). To address issues (2) and (3), a well-documented case study recorded in Kobe earthquake in 1995, an unimproved caisson quay wall damaged by liquefaction, is simulated and calibrated based on field observations and experimental measurements. In Chapters 3, 4, and 5 as the "remediation" chapters, multiple easily-executable remediation designs for each of the analyzed remedial methods are recommended based on the

improved performance and the specified performance grades obtained through numerical analyses. The recommended remedial designs are expected to be verified on similar gravity quay wall structures placed in liquefiable soil prone to earthquake loading. Eventually, by plotting all of the improved performance and effectiveness data together, a uniform framework is proposed to evaluate, compare and rank the various remedial ground improvement methods with different improvement mechanisms.

9.1   Results Summary

In Chapter 2, an appropriate selection of ground improvement methods based on site and project-specific characteristics is the first and critical step to achieve an adequate and economical liquefaction mitigation design. A comprehensive literature review on the applications of ground improvement for liquefaction mitigation was conducted and then used to develop the proposed technology selection system. Two examples are also provided to illustrate the implementation and how this selection system can benefit the routine practice. Keeping the selection system current with involving engineering criteria and improvement in technologies is important.

Starting from Chapter 3, the studies focus on issues (2) and (3). The details of the selected case history background, numerical modeling and calibration process are given in Chapter 3, which also provides the unimproved framework for the hypothetical application of remedial ground improvement methods in following chapters, and the soil zone that controls the stability of the caisson-type quay wall is determined for soil improvement using the three analyzed remedial methods.

In Chapter 4, it is found that by using the vibro-compaction method with a probing distance of 2.2 m, improving the first 25 m of backfill soil and top 12 m of foundation soil to a relative density of 65% can achieve the performance grade of "Repairable" as specified by

PIANC (2001). The improved quay wall would still be damaged by soil liquefaction after strong seismic events, but the restoration work is acceptable.

In Chapter 5, utilizing the wet DMM and following the similar analytical procedure as used in Chapter 4, it is found that a continuous DMM improved zone vertically under the caisson quay wall is more effective in reducing the seismic deformation than any other DMM improved zone configurations. Improving foundation soils can be approximately two times more efficient than improving backfill soil in reducing the seismic deformation of the caisson quay wall. The DMM improved zone is optimized to be the first 20 m of backfill soil and top 10 m of foundation soil based on two evaluation parameters: the satisfaction of improved deformation based on the specified performance grades by PIANC (2001) and acceptable improvement efficiency. Various remedial cases differ in different DMM improved zone locations and dimensions are classified into various categories based on their satisfied performance grades.

In Chapter 6, a combined stone column and DMM wall method is evaluated following the similar analytical procedure as used in Chapters 4 and 5. Numerous examined remedial designs, which differ in the replacement ratio of stone columns installed foundation soil and number of DMM wall installed in backfill soil, are categorized based on their improved performance grades. Based on the results, it is found that the combined improvement mechanisms can be effective in reducing the seismic deformation of the caisson quay wall constructed on liquefiable soil. Also, the interactive influences between the improvement efficiency in foundation soil and backfill soil are positive correlated based on the improved deformation of the quay wall and backfill soil, and the generation of excess pore water pressure in foundation and backfill soils. Therefore, it is further recommended to identify, quantitative and properly consider the interactive influences in remedial design.

With all above results, it is important to know that the conducted analyses, which requires proper calibration, can provide the important contributions to the assessment of seismic performance of the unimproved and improved caisson quay wall-soil system, and also model the characteristics of failure mechanisms, influences and effectiveness of improvements in a quantitative manner. Valuable insights in terms of optimum remedial design features such as improved zone configurations can be obtained.

As a stand-alone chapter, Chapter 7 proposes a simplified seismic displacement evaluation chart method based on the recommendations of Chapter 4. This proposed chart method could benefit routine practice especially when designing the compaction methods for liquefaction mitigation of caisson quay wall structures prone to liquefaction risk to achieve certain performance grades. This is a more rational design method than the latest applied conventional stress-based methods. The proposed procedure should be verified by more case history data or physical experimental data.

In Chapter 8, based on the improved performance results presented in Chapters 4, 5 and 6, the three analyzed remedial methods (1) vibro-compaction, (2) deep soil mixing, and (3) the combined stone column and deep soil mixing wall are compared and ranked in terms of the improvement effectiveness within the well-calibrated case history study. Depending on three different effectiveness evaluation and comparison criterions (improved deformation, improvement efficiency or specified performance grades), all of the examined remedial designs, regardless the use of remedial methods, improved zone properties and configurations, are categorized within the proposed uniform framework. As shown, the majority of examined remedial cases using the three methods are not acceptable due to the excessive residual deformation under this particular examined earthquake motion recorded from Kobe earthquake

in 1995. The vibro-compaction method can mostly likely to improve the quay wall to be repairable; deep soil mixing and the combined stone column and deep mixing wall method can possibly improve the quay wall to be serviceable and repairable with significant but still minimally required amount of improvement effort to both foundation soil and backfill soil. The proposed flow chart follows the philosophy of performance-based design (PIANC, 2001).

9.2   Recommendations for Future Study

As discussed in Chapter 2, the state-of-practice is perceived to be somewhat to highly non-uniform by the majority of geotechnical engineering committee in the U.S. (DFI, 2013; Seigel, 2013). This indicates the urgent need for continued studies to develop greater consensus within geotechnical engineering committee on the following but not limited to, issues in liquefaction mitigation by ground improvement:

1) The "combined" constitutive model reasonably capture the large deformation of the quay wall-soil system induced by liquefaction, and can be used as built-in soil model of FLAC^{3D} (Itasca, 2007) program, carrying out complex boundary condition and taking the liquefied deformation analysis between liquefied soil and structure, remedial stiffer element, etc;

2) Future development and refinement, validation and application of numerical analyses in advancing the liquefaction remedial design;

3) Application of performance-based design principles in remedial design and development of design criteria/level of design performances based on the tolerance(s) of various structures and design purposes;

4) Future efforts are needed to simplify and identify the representative response measures or engineering demand parameters (EDPs) and ground motion measures for optimizing remedial design by ground improvement;

5) Because ground improvement methods that apply drainage and/or reinforcement are not amenable to post-liquefaction verification, it is recommended to develop design and verification methods for routine engineering practice to verify the effectiveness of these methods;

6) Remediation costs including the transportation and operation of remediation equipment, materials, number of boreholes and other environmental and social considerations, etc, may be also used as effectiveness evaluation and comparison criteria among various remedial method candidates even though the determination of accurate remediation cost is highly case-specific;

7) For future study the seismic response of the improved caisson quay wall-soil system should be estimated covering all the dominant factors as well as their involved variability and uncertainties, such as improved zone locations and geometries, improved design parameters (area replacement ratio, improved soil strength), various earthquake motions;

8) To further advance seismic performance-based design methodology, it is still necessary to collect actual case history data as well as most test data and numerical simulation data, and feed them back to practice with appropriate interpretation.

Therefore, future research is recommended to conduct a verification, implementation, development and update of the proposed framework to advance the state-of-the-art of liquefaction mitigation design using ground improvement. With the growth of field data on improved performance post-earthquake, the remedial designs for all the widely used liquefaction

remedial methods are expected to be further advanced and standardized accordingly by following the similar presented process.

Many preliminary questions have been answered, and many more are still left. Only by continuing research and by identifying the most important areas for future research will be fully advancements. Implementation of performance-based design method and advanced numerical analysis tools is now becoming an essential tool for advancing and optimizing the liquefaction mitigation remedial design using ground improvement and will be even more so in the future. As commented by Samuel Butler (1612 - 1680): "Life is the art of drawing sufficient conclusions from insufficient premises." It is hoped that the research results presented in this dissertation can further advance the remedial design for liquefaction mitigation by ground improvement and reduce the life and economic loss caused by earthquakes.

REFERENCE

Andrus, R.D., Stokoe, K.H., (2000), "Liquefaction resistance of soils from shear-wave velocity test", *Journal of Geotechnical and Geoenvironmental Engineering*, ASCE 126 (11), 1015-1025.

Andrus, R.D., Stokoe, K.H., (2003), "Guidelines for Evaluating Liquefaction Response using Shear Wave Velocity Measurements and Simplified Procedures", *NIST GCR 03-854*, National Institute of Standards and Technology, Gaitherburg, MD.

Arango, I., (2003). "Mitigation of lateral ground displacement of liquefied soils with underground barriers, *Soil Dynamics and Earthquake Engineering,* 22 (2002), 1067-1033.

Adams, T., (2011), "Stability of Levees and Floodwalls Supported by Deep-Mixed Shear Walls: Five Case Studies in the New Orleans Area", *Ph.D Dissertation,* VT, Blackburg, VA.

Arablouei, A., Ghalandarzadeh, A., and Monstafagharabaghi, A.R., (2011), "A numerical study of liquefaction induced deformation on caisson-type quay wall using a partially coupled solution", Journal *of Offshore Mechanical Engineering,* 133, 021101-1.

Adalier, K., (1996), "Mitigation of earthquake induced liquefaction hazards", *Ph.D dissertation*, Rensselaer Polytechnic Institute, Troy, New York.

Alam, M.J., Towhata, I., and Wassan, T.H., (2005), "Seismic behavior of a quay wall without and with a damage mitigation measure". *GSP 133 Earthquake Engineering and Soil Dynamics*.

Alyami, M., Wilkison, S.M., Rouainia, M., Cai, F., (2007), "Simulation of seismic behavior of gravity quay wall using a generalized plasticity model", *Proceedings of 4th International Conference on Earthquake Geotechnical Engineering*, June 25 -28, 2007.

Alyami, M., Rouainia, M., Wilkison, S.M., (2009), "Numerical analysis of deformation behavior of quay walls under earthquake loading", *Soil Dynamics and Earthquake Engineering*, 29, pp 535-536.

Andresen, L., Jostad, H.P., Andresen, K., (2011), "Finite element analyses applied in design of foundations and anchors for offshore structures", *International Journal of Geomechchanics*, 11(6), 417-430.

Andrus, R.D. and Chung, R.M. (1995). "Liquefaction Remediation near Existing Lifeline Structures", *Proceedings of 6th Japan-U.S. Workshop on Earthquake Resistance Design of Lifeline Facilities and Countermeasures against Liquefaction*, June 11-13, 1996, Tokyo, Japan.

Broms, B.B. (2003). "Deep Soil Stabilization: Design and Construction of Lime and Lime/Cement Columns", Royal Institute of Technology, Stockholm, Sweden.

Bruce, M., Berg, R., Collin, J., Filz, G., Terashi, M., and Yang, D., (2013), "Federal Highway Administration Design Manual: Deep Mixing for Embankment and Foundation Support", *FHWA-HRT-13-016*, 10, 2013.

Boulanger, R.W. and Hayden, R.F. (1995). "Aspects of Compaction Grouting of Liquefaction Soils", *Journal of Geotechnical Engineering, Vol. 121, No. 12,* Dec. 1995.

Boulanger, R.W., (2012), "Shear reinforcement effects for liquefaction mitigation", DFI Liquefaction Forum: Consequences and Mitigation, St. Louis, MO.

Bryne, P., Park, S.S., Beaty, M., Sharp, M., Gonzalez, L., Abdoun, T. (2004). "Numerical modeling of liquefaction and comparison with centrifuge tests", *Canadian Geotechnical Journal*, 41: 193-211.

Bryne, P.M. (1991). "A cyclic shear-volume coupling and pore pressure model for sand", *Proceedings of the 2nd International Conference on Recent Advances in Geotechnical Earthquake Engineering and Soil Dynamics*, St. Louis., Mo., 11-15, March. 1, pp.47-55.

Bardet, J.P., Tobita, T., Mace, N., Hu, J., (2002), "Regional Modeling of Liquefaction Induced Ground Deformation", *Earthquake Spectra*, Vol. 18, No. 1, pp 19 – 46.

Baez, J.I., and Martin, G.R., (1995), "Permeability and shear wave velocity of vibro-replacement stone columns", Soil Improvement for Earthquake Hazard Mitigation, Edited by Roman D. Hryciw, ASCE, *GSP* No. 49, October, 1995.

Baez, J.I., (1995) "A design model for the reduction of soil liquefaction by vibro-stone columns", *Ph.D dissertation*, University of Southern California, Los Angeles, CA.

Charlie, W.A, Rwebyogo, M.F.J. and Doehring, D.O. (1992). "Time-dependent cone penetration resistance due to blasting", *Journal of Geotechnical Engineering*, 118(8), pp. 1200-1215.

Chen, Y.M., D.P. Xu. (2007). FLAC/FLAC3D Fundamentals and Examples. Waterpub, Inc., Beijing. (In Chinese).

Chu, J., Varaksin, S., Klotz, U., and Menge, P. (2009)."Construction Process", *Proceedings of the 17th International Conference on Soil Mechanics and Geotechnical Engineering*, Alexandria, Egypt, 5-9 Oct 2009.

Chameau, J.L., Santamarina, J.C. 1989). "Knowledge-based system for soil improvement", *Journal of Computing in Civil Engineering*, Vol. 3, No. 3, 253-267.

Cooke, H.G. and Mitchell, J.K. (1999). "Guide to Remedial Measures for Liquefaction Mitigation at Existing Highway Bridge Sites. *Technical Report MCEER-99-0015*, July.

Cooke, H.G. (2000). "Ground Improvement for Liquefaction Mitigation at Existing Highway Bridges"*, Ph.D Dissertation,* Virginia Tech, Blacksburg, VA.

Douglas, S.C., Schaefer, V.R., and Berg, R.R. (2012a). "Selection Assistance for the Evaluation of Geoconstruction Technologies for Transportation Applications", *Journal of Geotechnical and Geological Engineering*, Vol. 30, No. 5, 1231-1247.

Douglas, S.C., Schaefer, V.R., and Berg. R.R. (2012b). "Webs-based information and guidance system development report – SHRP2 project", *Report prepared for the Strategic High Research Program 2*, February. Dakoulas, p., Gazetas, G. (2008). "Insight into seismic earth and water pressures against caisson quay wall", *Geotechnique*, Vol. 58, No. 2, 95 -111.

Elias, V., Welsh, J., Wareen, J., Lukas, R., Collin, J., Berg, R. (2006). "Ground improvement methods: Reference Manual – Volume I". *NHI Course No. 13204*, FHA.

Finn, W.D., Bryne, P.M., Evans, .S, Law, T. (1996). "Some geotechnical aspects of Hyogo-ken Nanbu (Kobe) earthquake of January 17, 1995", *Canadian Journal of Civil Engineering*, 23: 778-796.

Filz, G.M. (2009). "Design of Deep Mixing Support for Embankment and Levees", *Proceedings International Symp. Deep Mixing & Admixture Stabilization*. Okinawa, Japan, May 19-21, 23.

Fast Lagrangian Analysis of Continua (FLAC). (2000). Itasca Consulting Group, Inc. Minneapolis.

Ground Improvement Committee of the Deep Foundation Institute, (2013). "Commentary on the Selection, Design and Specification of Ground Improvement for Mitigation of Earthquake-Induced Liquefaction". *DFI Journal*, Vol 7, No. 1.

Green, R.A., (2012), "Liquefaction risk mitigation by excess pore water pressure dissipation through compacted gravel piles", *DFI Liquefaction Forum*, Consequences and Mitigation, St. Louis, MO.

Hayden, R.F., and Baze, J.I., (1994), "State of Practice for Liquefaction Mitigation in North America", *Proceedings of U.S.-Japan Workshop on Soil Liquefaction: Remedial treatment of potentially liquefiable soils*, July 4-6, 1994.

Hamada, M., Towhata, I., Yasuda, S., Isoyama, R., (1987), "Study on permanent ground displacement induced by seismic liquefaction", *Computers and Geotechnics*, 4(1987) 197-120.

Hazarika, H., Kohama, E., Sugano, T. (2008). "Underwater shake table tests on waterfront structures protected with tire chips cushion", *Journal of Geotechnical and Geoenvironmental. Engr.*, 134 (12), 1706-1719.

Haulser, E.A. and Sitar, N. (2001). "Performance of Soil Improvement Technique in Earthquakes". *Journal of 4TH International Conference on Recent Advances in Geotechnical Earthquake Engineering and Soil Dynamics*. Finn, W.D. et al. (Eds.).

Haulser, E.A. (2002). "Influence of Ground Improvement on Settlement and Liquefaction: A study based on Field Case History Evidence and Dynamic Geotechnical Centrifuge Tests", *Ph.D Dissertation*, University of California, Berkeley.

Iai, S., (1988), "Large Scale Model Tests and Analysis of Gravel Drains", *Report of the Port and Harbor Research Institute Japan*, Vol 127, No. 3.

Iai, S., and Matsunaga, Y., (1990), "Soil improvement area against liquefaction", *Proceeding of 8th Japan Earthquake Engineering Symposium*, pp. 867-872.

Iai, S., and Sugano, T. (2000). "Shaking table testing on seismic performance of gravity quay walls", *Proceedings of 12th WCEE*, Aug 1-6.

Ichii, K., Sato, Y., Liu, H., (2002), "Seismic performance evaluation charts for gravity type quay walls", *Structural Engineering/Earthquake Engineering, JSCE*, Vol. 19, No. 1.

Iwasaki, Y., Tai, M. (1996). "Strong motion records at Kobe Port Island", *Soils Foundations (Special issue on geotechnical aspects of the January 17, 1995 Hoogoken-Nambu earthquake)*, 1, 29-40.

Inagak H, Iai S, Sugano T, Yamazaki H, Inatomi T.(1996). "Performance of caisson type quay walls at Kobe port", *Special Issue of Soils and Foundations* 1996; 119-136.

Ishihara, K. (1997). Terzaghi oration: Geotechnical aspects of the 1995 Kobe earthquake, *Proceedings 14th Conference Soil Mechanical Foundation Engineering*, Hamburg 4, 2047-2073.

Kogai, Y., Towhata, I., Aminoto, K., Putra, H.G., (2000), "Use of embedded walls for mitigation of liquefaction-induced displacement in slopes and embankments", *Soils and Foundations*, Vol. 40, No. 4, pp. 75 – 93.

Kramer, S., (2008). "Performance-Based Earthquake Engineering: Opportunities and Implications for Geotechnical Engineering Practice", *Geotechnical Earthquake Engineering and Soil Dynamics IV*, ASCE, GSP 181.

Kammerer, A.M., (2002), "Undrained Response of Monterey 0/30 Sand Under Multidirectional Cyclic Simple Shear Loading Conditions", *Ph.D Dissertation*, University of California, Berkeley.

Idriss, I.M., and Boulanger, R.W. (2008), "Soil Liquefaction during Earthquakes", Monograph MNO-12, Earthquake Engineering Research Institute.

Liu, L. and Dobry, R. (1997), "Seismic Response of Shallow Foundation on Liquefaction Sand", *Journal of Geotechnical and Geoenvironmental Engineering*, Vol. 123, No. 6, June.

Lee, C.J. (2005). "Centrifuge modeling of the behavior of caisson-type quay walls during earthquake loading", *Soil Dynamics and Earthquake Engineering*, 25, 117 – 131.

Look, B. (2007). Handbook of Geotechnical Investigation and Design Tables, Taylor & Francis, London, UK.

Martin, G.R., Finn, W.D.L., and Seed, H.B. (1975). Fundamentals of liquefaction under cyclic loading. *Journal of the Geotechnical Engineering Division*, ASCE, 101 (GT5): 423-438.

Mitchell, J.K., and Solymar, Z.V., (1984), "Time-dependent strength gain in freshly deposited or densified sand", *Journal of Geotechnical Engineering*, 110(11), pp. 1559 – 1576.

Mitchell, J.K., Baxter, C.D.P., and Munson, T.C. (1995). "Performance of improved ground during earthquakes", *Soil Improvement for Earthquake Hazard Mitigation*, ASCE GSP No. 49, pp. 1-36.

Mitchell, J.K. (2008), "Mitigation of liquefaction potential of silty sands", *From Research to Practice in Geotechnical Engineering Congress 2008*, pp 433 – 451.

Mitchell, James. K., (2013). Personal communication.

Martin, J.R., and Olgun, C.G. (2006), "Liquefaction mitigation using jet-grout columns – 1999 Kocaeli earthquake case history", *Ground Improvement and Seismic Mitigation*, ASCE GSP 152, pp. 349 – 358.

Motamed, R. and Towhata, I., (2010), "Shaking table model tests on pile groups behind quay walls subjected to lateral spreading", *Journal of Geotechnical and Geoenvironmental Engineering*, Vol. 136, No. 3, pp. 477 – 489.

National Research Council, (1985), "Liquefaction of Soils during Earthquakes", National Research Council, Committee on Earthquake Engineering, Washington, District of Columbia.

Moghadam, A.M., Ghalandarzadeh, A., Towhata, I., and Moradi, M. (2009). "Studying the effects of deformable panels on seismic displacement of gravity quay walls", *Ocean Engineering*, Vol. 36, 1129-1148.

Nishimura, S., Takahashi, H., and Morikawa, Y. (2012). "Observations of dynamic and non-dynamic interactions between a quay wall and partially stabilized backfill", *Soils and Foundations,* 52, 81–98.

Nguyen, T.V., Rayamajhi, D., Boulanger, R.W., Ashford, S.A., Lu,J., Elgamal, A., and Shao, L., (2012), "Effects of DSM grids on shear stress distribution in liquefiable soil", Proceedings GeoCongress 2012, *State of the Art and Practice in Geotechnical Engineering*, ASCE GSP 255, Oakland, CA, PP. 1948-1957.

Moss, R.E.S., Seed, R.B., Kayen, R.E., Stewart, J.P., (2006), "CPT-Based probabilistic and deterministic assessment of in-situ seismic soil liquefaction potential", *Journal of Geotechnical and Geoenvironmental Engineering*, ASCE 132(8), 1032-1051.

Navin, M., (2005). "Stability of Embankment Founded on Soft Improvement with Deep-Mixing-Method Columns", *Ph.D Dissertation*, VT, Blackburg, VA.

Namikawa, T., Koseki, J., Suzuki, Y. (2007). "Finite Element Analysis of Lattice-Shaped Ground Improvement by Cement-Mixing For Liquefaction Mitigation", *Soils and Foundations*, Vol. 47, No. 3, 559-576.

Olgun, C.G., and Martin, J.R., (2008), "Numerical modeling of the seismic response of columnar of reinforced ground", *Proceedings Geotechnical Earthquake Engineering and Soil Dynamics IV*, ASCE GSP 181, Sacramento, CA.

PIANC International Navigation Association, (2001), *Seismic Design Guidelines for Port Structures*, Balkema, 474.

Port and Harbor Research Institute (PHRI), (1997), *Handbook on Liquefaction Remediation of Reclaimed Land*, Balkema, 312 p.

Porbaha, A., Ghaheri, F., and Puppala, A.J. (2005), "Soil Cement Properties from Borehole Geophysical Correlated with Laboratory Tests", *Proceedings of Deep Mixing'05: International conference on deep mixing best practice and recent advances.*

Peck, R.B. (1979) "Liquefaction potential: science versus practice", *Journal of Geotechnical Engineering Division*, ASCE, 105 (gt3), PP. 393-398.

Rouke, T.D., and Goh, S.H., (1997), "Reduction of Liquefaction Hazards by Deep Soil Mixing", *Journal of Goetechnical and Geoenvironmental Engineering,* Vol 8, pp 87 – 105.

Rayamajhi, D., Nguyen, T.V., Ashford, S.A., Boulanger, R.W., Lu., J., Elgamal, A., and Shao, L. (2012), "Effect of discrete columns on shear stress distribution in liquefiable soil", Proceedings GeoCongress 2012, *State of the Art and Practice in Geotechnical Engineering,* ASCE GSP 255, Oakland, CA, pp. 1918-1927.

Pestana, J.M., Hunt, C.E. and Goughnour, R.R., (1997), "FEQDrain: A Finite Element Computer for the Analysis of the Earthquake Generation and Dissipation of Pore Water Pressure in Layered Sand Deposits with Vertical Drains", *Report No. UCB/EERC-97/15*, University of California, Berkeley, 88 p.

Robertson, P.K., and Wride, C.E., (1998), "Evaluating cyclic liquefaction potential using the cone penetration test", *Canadian Geotechnical Journal*, 35(3), 442-459.

Shenthan, T., Thevanayagam, S., Martin, G.R., (2004), "Densification of saturated silty soils using composite stone column for liquefaction mitigation", *Proceedings of 13th WCEE*, Canada, 2004.

Shenthan, T., Thevanayagam, S., Martin, G.R., (2006), "Numerical simulation of soil densification using vibro-stone columns", *Proceedings of GeoCongress* 2006.

Sugawa, N., Y. Ito, and M. Kawai. (1996). "New core sampler with planet gear for investigating the cement-mixed ground", *Grouting and Deep Mixing, Proceeding of IS-Tokyo' 96*, Tokyo, May 14-17, pp. 635-658.

Seed, H.B. and Lee, K.L. (1966) "Liquefaction of Saturated Sands during Cyclic Loading", *Journal of Soil Mechanics and Foundation Division*, ASCE, Vol. 92, No. SM6, PP. 105 - 134.

Seed, H.B. and Idriss, I.M. (1967), "Analysis of Soil Liquefaction: Niigata Earthquake", *Journal Soil Mechanics and Foundation Division*, ASCE, Vol. 93, No. SM3, pp. 83 - 108.

Seed, H.B. and Idriss, I.M. (1971), "Simplified Procedure for Evaluating Soil Liquefaction Potential", *Journal Soil Mechanics and Foundation Division*, ASCE, Vol. 97, No.9.

Seed, H.B. and Booker, J.R. (1977). "Stability of Potentially Liquefiable Sand Deposits Using Gravel Drains", *Journal of the soil Mechanics and Foundations Division*, ASCE, Vol. 103, No. GT7, PP. 757-768.

Seed, H.B., Idriss. I.M., and Arango, I. (1983) "Evaluation of Liquefaction potential using field performance data", *Journal of Geotechnical Engineering*, 109(3), pp. 458-482.

Seed, R.B., Cetin, K.O., Moss, R.E., Kammerer, A., Wu, J., Pestana, K., Reimer, M., (2001), "Recent advances in soil liquefaction engineering and seismic site response evaluation", *Proceedings of 4th International Conference and Symposium on Recent Advances in Geotechnical Earthquake Engineering and Soil Dynamics*, University of Missouri, Rolla, MO, Paper SPL-2.

Seed, R.B., Cetin, K.O., Moss, R.E., Kammerer, A., Wu, J., Pestana, K., Reimer, M., Sancio, R.B., Bray, J.D., Karen, R.E., and Faris, A., (2003), "Recent Advances in Soil Liquefaction Engineering: A Unified and Consistent Framework", Keynote presentation, 26th Annual ASCE Los Angeles Geotechnical Spring Seminar, Long Beach, CA.

Siegel, T., (2013). "Liquefaction Mitigation Synthesis Report", *DFI Journal*, Vol.7, No.1.

Tanaka, H., Murata, H., Kita, H., Okamoto, M., "Study of sheet pile wall method as a remediation against liquefaction", *Proceedings of 12th WCEE*, 2000.

Towhata, I. (2008), *Geotechnical Earthquake Engineering, Springer Series in Geomechanics and Geoengineering*.

Taiyab, M., Alam, M., Zbedin, M. (2012). "Dynamic Soil-Structure of Gravity Quay Wall and Effect of Densification in Liquefiable Sites", *International Journal of Geomechnaics*. (In Press).

Takahashi, H., Hayano, K. (2009). "Dynamic model tests in centrifuge on lattice-shaped DMM ground improvement for retraining displacement of quay wall," *Performance-Based Design in Earthquake Geotechnical Engineering – Kohusho, Tsukamoto & Yoshimini (eds)*, Taylor & Francis Group, Landon, UK.

Terashi, M. (2003). "The state of practice in deep mixing methods", *Proceedings of 3rd International Conference Grouting and Ground Treatment*, New Orleans, 25-49.

Tokimatsu, K., Asaka, Y., (1998), "Effects of Liquefaction-Induced Ground Displacements on Pile Performance in the 1995 Hyogoken-Nambu Earthquake", *Special Issues of Soils and Foundations*, 163-177, 1998.

Yasuda, S., Ogasawara, M., (2004), "Studies of Several Countermeasures against Liquefaction – Induced Flow and an Application of A Measure to Existing Bridges in Tokyo*", Journal of Japan Association for Earthquake Engineering,* Vol. 4, No. 3 (Special Issue), 2004.

Youd, T.L., Perkins, D.M., (1987), "Mapping of Liquefaction Severity Index", *Journal of Geotechnical Engineering*, Vol. 113, No. 11, paper No. 21981.

Yang, Z., Elgamal, A., Adalier, K., Sharp, M.K. (2003). "Earth dam on liquefiable foundation and remediation: numerical simulation of centrifuge experiments", *Journal of Engineering Mechanics*. 130 (10).

Youd, T.L., Idriss, I.M., Andrus, R.D., Arango, I., G., Christian, J.T., Dobery, R., Finn, W.D.L., Harder, L.F., Jr., Hynes, M.e., Ishihara, K., Koester, J.P., Liao, S.S.C., Marcuson, W.F., Martin, (2001), "Liquefaction resistance of soils: Summary report from the 1996 NCEER/NSF workshop on evaluation of liquefaction resistance of soils", *Journal of Geotechnical and Geoenvironmental Engineering*, 127(10), pp. 817-833.

Youd, T.L., Hansen, C.M., Bartlett, S.F., (2002), "Revised Multilinear Regression Equations for Prediction of Lateral Spread Displacement", *Journal of Geotechnical and Geoenvironmental Engineering*, Vol. 128, No. 12, December 1, 2002.

Youd, T.L., Deden, D.W., Bray, J.D., Sancio, R., Cetin, K.O., Gerber, T.M., (2009), "Zero-Displacement Lateral Spreads, 1999 Kocaeli, Turkey, Earthquake", *Journal of Geotechnical and Geoenvironmental Engineering,* Vol. 135, No. 1, pp 46 – 61.

Youd, T.L., Bartlett, S.F., (1995), "Empirical Prediction of Liquefaction-Induced Lateral Spread", *Journal of Geotechnical Engineering*, Vol. 121, No. 4, Pager No. 7247.

Yasuda, S., Ishihara, K., Harada, K., and Shinkawa, N., (1996), "Effect of improvement on ground subsidence due to liquefaction", *Soils and Foundations*, JSSMFE, Special Issue, January, pp. 99-107.

Zhang, G., Robertson, P.K., Brachman, R.W.I., (2004), "Estimating Liquefaction-Induced Lateral Displacements Using the Standard Penetration Test or Cone Penetration Test", *Journal of Geotechnical and Geoenvironmental Engineering*, Vol. 130, No. 8. Pp 861 - 871.